



Aalto University
School of Engineering

Jan Sher Akmal

Digital Unique Component Manufacturing through Direct and Indirect Additive Manufacturing

Master's thesis submitted for examination of the degree in
Master of Science (Technology)

Espoo 11.09.2017

Supervisor: Professor Jouni Partanen

Advisor: Mika Salmi



Author Jan Sher Akmal

Title of thesis Digital Unique Component Manufacturing through Direct and Indirect Additive Manufacturing

Degree program Master of Science in Mechanical Engineering

Major/minor Digital Design and Manufacturing

Code IA3027

Thesis supervisor Prof. Dr. Dir. Principle Scientist Jouni Partanen

Thesis advisor(s) Dr. Research Dir. Staff Scientist Mika Salmi

Date 11.09.2017

Number of pages 132 + 31

Language English

Abstract

The objective of this study is to define an optimum additive manufacturing process which incorporates not only low volume production and short delivery time but also missing, or defective documentation of the industrial components. This inevitably requires the integration of digitization through reverse engineering and state of the art direct and indirect additive manufacturing methods as these are built upon the fundamentals of lead time and cost efficiency which complement business potentials.

The work was commissioned by Outotec (Finland) Oy and Aalto University. The data of exemplary components was provided by Outotec (Finland) Oy. The digitization measures and the ISO/ASTM standard additive manufacturing methods were explored and an integrated screening and design process was developed. Cost and lead time analyses were performed in correspondence to exemplary components and their relative business advantages against conventional manufacturing methods were discovered. In addition, performance of two exemplary components was evaluated via additive manufacturing enabled optimization studies. In order to validate and verify the suitability of the manufactured materials according to the predefined standards of Outotec (Finland) Oy, corrosion tests and tensile tests were performed.

As a result of this thesis, an additive manufacturing integrated screening algorithm and design process is developed through which costs and lead times of 15 industrial components are evaluated and are utilized for good advantage. In addition, design for additive manufacturing is used to enhance the performance of two industrial components and prototypes are manufactured in order to provide proof of concept. Finally, it is discovered that additively manufactured Stainless Steel 316L is not as corrosion resistant compared to wrought alloys of EN 1.4404 and EN 1.4432 in very aggressive corrosion environments and it has an ultimate tensile strength of approximately 595 MPa with 13% anisotropy in favour of horizontal print orientation. Whereas, additively manufactured Titanium Ti64 is corrosion resistant with respect to its bulk material with an ultimate tensile strength of approximately 1100 MPa containing 5% anisotropy in favour of horizontal print orientation. Overall, this study provided a fundamental workflow for implementation of industrial additive manufacturing for higher production efficiency.

Keywords Direct and indirect additive manufacturing, 3D printing, 3D modelling, reverse engineering, design for additive manufacturing, screening algorithm, topology optimization, cost analysis, lead time analysis, corrosion testing, tensile testing

Tekijä Jan Sher Akmal

Työn nimi Digital Unique Component Manufacturing through Direct and Indirect Additive Manufacturing

Koulutusohjelma Diplomi-insinööri

Pää-/sivuaine Konetekniikka**Koodi** IA3027

Työn valvoja Prof. Dr. Dir. Principle Scientist Jouni Partanen

Työn ohjaaja(t) Dr. Research Dir. Staff Scientist Mika Salmi

Päivämäärä 11.09.2017**Sivumäärä** 132 + 31**Kieli** Englantia

Tiivistelmä

The objective of this study is to define an optimum additive manufacturing process which incorporates not only low volume production and short delivery time but also missing, or defective documentation of the industrial components. This inevitably requires the integration of digitization through reverse engineering and state of the art direct and indirect additive manufacturing methods as these are built upon the fundamentals of lead time and cost efficiency which complement business potentials.

The work was commissioned by Outotec (Finland) Oy and Aalto University. The data of exemplary components was provided by Outotec (Finland) Oy. The digitization measures and the ISO/ASTM standard additive manufacturing methods were explored and an integrated screening and design process was developed. Cost and lead time analyses were performed in correspondence to exemplary components and their relative business advantages against conventional manufacturing methods were discovered. In addition, performance of two exemplary components was evaluated via additive manufacturing enabled optimization studies. In order to validate and verify the suitability of the manufactured materials according to the predefined standards of Outotec (Finland) Oy, corrosion tests and tensile tests were performed.

As a result of this thesis, an additive manufacturing integrated screening algorithm and design process is developed through which costs and lead times of 15 industrial components are evaluated and are utilized for good advantage. In addition, design for additive manufacturing is used to enhance the performance of two industrial components and prototypes are manufactured in order to provide proof of concept. Finally, it is discovered that additively manufactured Stainless Steel 316L is not as corrosion resistant compared to wrought alloys of EN 1.4404 and EN 1.4432 in very aggressive corrosion environments and it has an ultimate tensile strength of approximately 595 MPa with 13% anisotropy in favour of horizontal print orientation. Whereas, additively manufactured Titanium Ti64 is corrosion resistant with respect to its bulk material with an ultimate tensile strength of approximately 1100 MPa containing 5% anisotropy in favour of horizontal print orientation. Overall, this study provided a fundamental workflow for implementation of industrial additive manufacturing for higher production efficiency.

Avainsanat Direct and indirect additive manufacturing, 3D printing, 3D modelling, reverse engineering, design for additive manufacturing, screening algorithm, topology optimization, cost analysis, lead time analysis, corrosion testing, tensile testing

Acknowledgement

This master's thesis study is conducted under the umbrella of FIN3D, Finnish Industry New Age 3D project which focuses on state of the art digital technologies involving industrial internet and additive manufacturing for end use products. The research motive of this study has been the implementation of additive manufacturing as a spare parts service in collaboration with Outotec (Finland) Oy. The work is funded by TEKES (Finnish Funding Agency for Innovation), Aalto University and the participating companies.

First and foremost, I would like to extend my deepest acknowledgment to my advisors Dr. Mika Salmi and Mr. Roy Björkstrand for their professional and unconditional guidance, support, trust and motivation throughout this study. In addition, I would like to express my gratitude to my supervisor Professor Jouni Partanen for entrusting me with this responsibility and sharing his pioneering wisdom throughout this thesis work.

I would also like to state the fact that this thesis work would not have been possible without the collaboration and support of Outotec (Finland) Oy. To this end, I would like to express my great appreciation to Mr. Juha Koivuniemi, Mr. Tuomas Hirsi and Dr. Mari Lindgren for providing a professional platform with rapid support for this thesis work. I strongly hope that the literature studied, processes developed and the outcomes discussed in this work will be used to Outotec (Finland) Oy's good advantage.

My Special thanks are extended to Dr. Mari Lindgren for overseeing the corrosion testing at Outotec Research Center, to Mr. Mika Salmikivi for assisting with loading and boundary conditions of spare parts at Outotec (Finland) Oy, to Doctoral Candidate Mr. Kalle Jalava for assisting with casting mould design at Aalto University, to Laboratory Specialist Mr. Kim Widell for assisting with tensile testing at Aalto University and to my Advanced Manufacturing team for assisting with the practicalities of this work.

Finally, I would like to thank my family, friends and all those who have supported me directly and/or indirectly throughout this quest of learning and making the world a better place.

Espoo 11.09.2017

Jan Sher Akmal

Table of Content

Title	
Abstract	
Acknowledgement	
Table of Content	1
Abbreviations	3
1 Introduction.....	4
1.1 Background	4
1.2 Research Problem	4
1.3 Objective	4
1.4 Scope.....	5
2 Theory and State of the Art	6
2.1 Additive Manufacturing.....	6
2.1.1 Direct VS Indirect.....	6
2.1.2 Binder Jetting	7
2.1.3 Directed Energy Deposition	8
2.1.4 Material Extrusion	9
2.1.5 Material Jetting.....	10
2.1.6 Powder Bed Fusion.....	11
2.1.7 Sheet Lamination.....	12
2.1.8 Vat Photopolymerization	13
2.2 Design for Additive Manufacturing.....	14
2.2.1 Shape Complexity.....	14
2.2.2 Hierarchical Complexity.....	16
2.2.3 Material Complexity.....	16
2.2.4 Functional Complexity.....	17
2.2.5 Optimization Methods	17
2.3 Business Aspects and Potentials.....	17
2.3.1 Agile Manufacturing.....	17
2.3.2 Lean Manufacturing.....	18
2.3.3 Implementation.....	19
3 Spare Parts	23
3.1 Screening Process Algorithm	23
3.2 Results of Screening Process.....	25
4 Computer Aided Design	27
5 Cost and Lead Time Analysis.....	33
5.1 Results of Injection Moulding Parts	34
5.1.1 Anode Hangbar.....	34
5.1.2 Positioning Cone	39
5.1.3 Summary of Injection Moulding Parts.....	42
5.2 Results of Subtractive Machining Parts.....	42
5.2.1 Turbine Blade Housing	42
5.2.2 Upper Shank	45
5.2.3 Chain Wheel.....	47
5.2.4 Cutting Blade.....	49
5.2.5 Guide Frame	51
5.2.6 Roll Support	53
5.2.7 Sliding Bush	55

5.2.8	Rail Fastener.....	57
5.2.9	Fork Bar	59
5.2.10	Stopper Flange Assembly	61
5.2.11	Adjustable Mounting Plate.....	63
5.2.12	Bush	65
5.2.13	Brake Flange	67
5.2.14	Summary of Subtractive Manufacturing Parts	69
6	Performance	70
6.1	Shape Optimization: Chain Wheel	70
6.1.1	Objective	70
6.1.2	Load Calculations	71
6.1.3	Mode of Failure	74
6.1.4	Materials.....	74
6.1.5	Static Analysis	75
6.1.6	Optimization Study.....	78
6.1.7	Conclusion.....	84
6.2	Topology Optimization: Upper Shank.....	86
6.2.1	Objective	86
6.2.2	Load Calculations	86
6.2.3	Mode of Failure	87
6.2.4	Static Analysis: Preliminary Baseline.....	88
6.2.5	Topology Optimization Preliminary Iteration.....	90
6.2.6	Preliminary Cost and Lead Time Analysis	94
6.2.7	Static Analysis: Final Baseline.....	96
6.2.8	Topology Optimization Final Iteration	98
6.2.9	Conclusion.....	102
6.2.10	Final Cost and Lead Time Analysis	102
7	Verification	105
7.1	Corrosion Testing	106
7.1.1	Uniform Corrosion	107
7.1.2	Localized Corrosion.....	109
7.2	Tensile Testing	111
8	Discussion.....	114
8.1	Results.....	114
8.2	Challenges	114
8.3	Future Development	115
9	Conclusion	117
10	References	119
	Appendices	124
	Appendix 1. Spare Parts Screening Process	
	Appendix 2. Spare Parts Further Analysis	
	Appendix 3A. Uniform Corrosion Testing Results	
	Appendix 3B. Localized Corrosion Testing Results	

Abbreviations

AM	Additive Manufacturing
ASTM	American Society of Testing and Materials
BJ	Binder Jetting
CAD	Computer Aided Design
CNC	Computer Numerical Control
DED	Directed Energy Deposition
DMD	Direct Metal Deposition
DMLS	Direct Metal Laser Sintering
EBDM	Electron Beam Direct Manufacturing
EBM	Electron Beam Melting
FDM	Fused Deposition Modelling
FOS	Factor of Safety
IFF	Ion Fusion Formation
IM	Injection Moulding
ISO	The International Organization for Standardization
LENS	Laser Engineered Net Shaping
ME	Material Extrusion
MJ	Material Jetting
mm	Millimetre
NPJ	NanoParticle Jetting
PA	Polyamide
PLA	Polylactide
PBF	Powder Bed Fusion
SL	Sheet Lamination
SLM	Selective Laser Melting
SLS	Selective Laser Sintering
SM	Subtractive Manufacturing
SP	Service Provider
VP	Vat Photopolymerization

1 Introduction

Manufacturing has evolved throughout the centuries starting from craftsmanship, to industrialization, to mass production, to mass customization and finally to the era of eManufacturing which consists of the most challenging market demands including variable volume, consistent quality, statistical process control, compatibility and complete customization incorporating lean manufacturing and agile manufacturing. Consequently, the development of new technologies pushes existing technologies to adapt to such demands to keep up with the dynamics of growing competition. The aim of this study is to define digital unique component manufacturing through direct and indirect additive manufacturing to meet such challenging demands.

1.1 Background

The topic of this study is formed on the basis of creating solutions and manufacturing process for service components of old installation bases of Outotec (Finland) Oy. These installations are located globally and their documentation can be missing, defective or in a format which is not supported for modern digital engineering tools. The system resembles to an outdated spare part service leading to low volume production, short delivery time and unreliable information regarding the components. Hence, reverse engineering methods capable of digitization and modern digital manufacturing methods capable of unique, lean and agile manufacturing are taken into consideration. Since there are numerous new digital manufacturing methods each representing different costs, lead time and technical properties, this study focuses on additive manufacturing including both direct and indirect methods. The decisive factors defining the optimum manufacturing process are cost and relative business advantages achieved by it. The additive manufacturing capable optimization methods are discovered with an emphasis on shape optimization and topology optimization where determination of shape profile and distribution of materials are explored for minimizing mass and volume, respectively thus, promoting lean and agile manufacturing. The working environment, under which the service components are to be operated is evaluated with respect to the standards of Outotec (Finland) Oy and verification experiments are conducted. Ultimately, an integrated workflow design process is developed with selected data tools for unique component manufacturing.

1.2 Research Problem

The research problem concerning this study is digitization of components due to lack of sufficient documentations and defining a suitable manufacturing process which promotes low volume production and short delivery time by overcoming logistics constraints while still being cost effective and offering various business advantages such as effective lead time. Additionally, the suitability and the constraints of the selected approach with state of the art technologies is taken into consideration including its development in the future. The research question for this research problem is formulated as following:

When is additive manufacturing cost effective with convenient lead time for unique components of spare parts with, without or limited digital data?

1.3 Objective

The main objective of this study is *to discover cost effectiveness of additive manufacturing of exemplary components provided by Outotec (Finland) Oy which overcomes the*

current constraints concerning speed in terms of the whole process, logistics, low volume production and limited documentation. Other objectives include verifying the selected manufacturing process through verification methods for manufactured material properties in context with Outotec (Finland) Oy's standards.

1.4 Scope

The scope of this thesis is delimited to direct and indirect additive manufacturing methods of metals and polymers since there are various new digital manufacturing methods with different costs, lead time and technical properties. At this point, it is well understood beyond doubt that additive manufacturing offers a state of the art method for fulfilling the defined research problem however, it requires the need of depth research and analysis to define the most cost effective and suitable AM process. The exemplary components to be manufactured are restricted to mainly metals and few polymers as per requirement of Outotec (Finland) Oy. Hence, the selection process is looked upon from a perspective of direct and indirect AM methods of metals and polymers. The direct method is defined as a primary process which manufactures end use product(s) fulfilling its fundamental physical properties. Whereas, the indirect method involves additional process(s) to primary process in order to comply with the end use product's fundamental physical properties. Furthermore, AM can act as an accelerator or a catalyst for producing the end use rapid tooling directly such as dies, patterns and moulds through which an end use product(s) can be manufactured via conventional manufacturing. Verification methods are delimited to additively manufactured samples of Stainless Steel and Titanium. The corrosion resistance is verified via uniform corrosion and localized corrosion testing. Finally, the mechanical verification is delimited to tensile testing for measuring the ultimate tensile strength of the printed materials.

2 Theory and State of the Art

2.1 Additive Manufacturing

AM is a process which involves adding and joining of materials to make parts using digital data of a 3D model, typically layer by layer, contrary to subtractive manufacturing and formative manufacturing methodologies (ISO/TC 261, 2015). The concept was originated in the early 1980s (Gibson, et al., 2015) and it is widely used in broad range of industries including military, aerospace, automotive, biomedical and energy fields (Guo & Leu, 2013). The thickness of the layers and tessellation of geometry in AM is inversely proportional to the resolution, detail of the part in terms of how close it is to the original 3D model. Hence, higher resolution leads to longer build time. According to ISO/ASTM 52900:2015(en) standard, it contains seven process categories which include binder jetting, directed energy deposition, material extrusion, material jetting, powder bed fusion, sheet lamination and vat photopolymerization. These processes mainly differ in the techniques that they use in terms of their compatibility of the materials followed by creating and joining of the layers. These are explained in the subsequent text.

2.1.1 Direct VS Indirect

A vast amount of literature exists classifying metallic additive manufacturing in terms of material (Gu, 2015), material feed stock (Frazier, 2014), energy source (Herzog, 2016), bonding mechanism (Vayre, et al., 2012) and manufacturer (Herderick, 2011). A brief classification is adopted from a combination of these sources to present a basic understanding of direct and indirect metallic additive manufacturing classification as shown in Figure 1. The direct method is defined as a primary process which manufactures end use product(s) fulfilling its fundamental physical properties. Whereas, the indirect method involves additional process(s) to primary process in order to comply with the end use product's fundamental physical properties. The indirect metal ME and SL methods are mainly used for research and development purposes (Gibson, et al., 2015) and indirect PBF method has become obsolete since the introduction of direct PBF method.

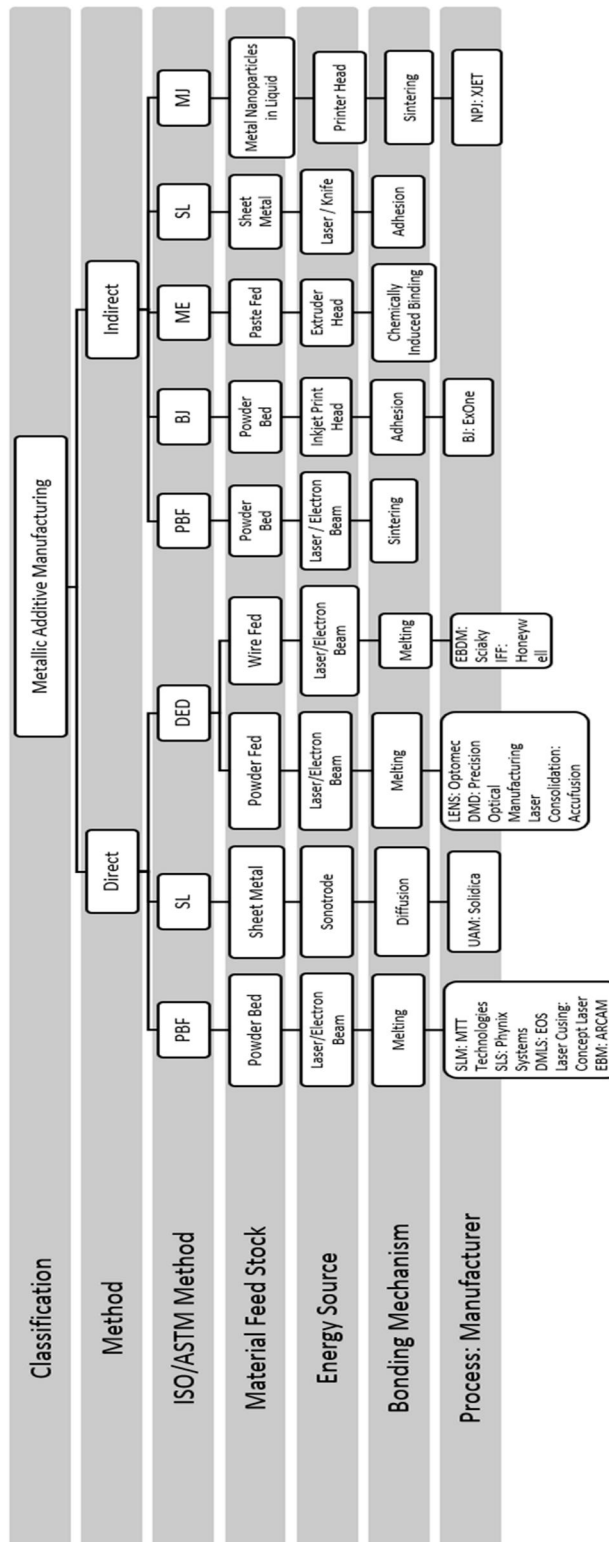


Figure 1. Classification of Metallic Additive Manufacturing.

2.1.2 Binder Jetting

Binder jetting, BJ originally known as Three-Dimensional Printing (3DP), invented at MIT (Gibson, et al., 2015), is an AM process in which powder materials are joined by selectively depositing a liquid bonding agent (ISO/TC 261, 2015). A schematic of the process can be seen in Figure 2. It offers scalable colour printer nozzles, leading to high deposition rate at comparatively low cost due to the fact that it doesn't require relatively

high power source for bonding. On the other hand, direct BJ manufactured parts typically have weaker material properties which are dependent on the bonding agent compared to other AM processes. The process doesn't require support structures for the parts since these are supported by the powder bed.

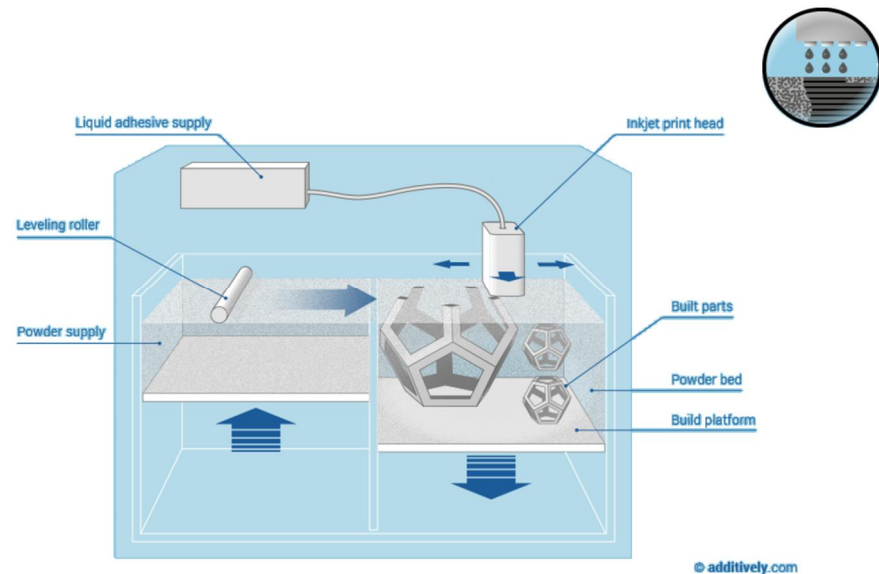


Figure 2: Schematic of Binder Jetting Process (Additively Ltd. , 2017)

BJ offers both direct and indirect printing of parts with various range of materials including but not limited to polymers, metals and ceramics. Since the material properties of BJ manufactured parts are relatively poor, the directly printed parts are mainly used for prototyping purposes other than moulds and cores for sand casting which are categorized as rapid tooling. Material properties can be improved by infiltration leading to indirect printing methods. These include patterns for investment and sand casting where polymer powders and wax-based infiltrates are used (Gibson, et al., 2015). Metals and composites can be manufactured using polymer binders leading to formation of 'green' part after binding process. This is followed by debinding, sintering and reimpregnation/infiltration to manufacture a reasonably dense part (K.P. Karunakaran, 2012). Companies such as 3D systems (3D Systems Inc., 2017), Voxeljet (Voxeljet AG, 2017) and ExOne (ExOne GmbH, 2017) offer on demand manufacturing and supply commercially available machines as well as materials.

2.1.3 Directed Energy Deposition

Directed energy deposition, DED often referred to as "metal deposition" technology (Gibson, et al., 2015), is an AM process in which materials are fused together by melting via focused thermal energy as they are being deposited (ISO/TC 261, 2015). A schematic of the process can be seen in Figure 3. The energy source is typically a laser or an electron beam. Since the process involves melting, the microstructure of the built part can be selectively controlled by varying the cooling rates and material complexity. On the other hand, its limitations include poor resolution, poor surface finish and in case of powder fed system a low deposition rate leading to slow build speed. The process requires support structures in case of complex three dimensional geometry unless it's equipped with a multi-axis deposition head (Gibson, et al., 2015).

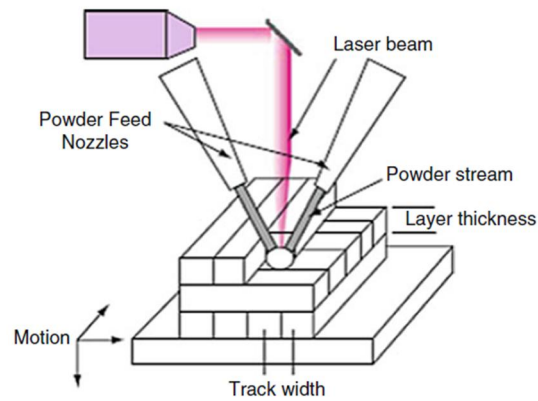


Figure 3: Schematic of DED process with a laser energy source (Gibson, et al., 2015)

DED offers direct additive manufacturing of parts with materials in form of powder or wire consisting of mainly metals however, these can also include but are not limited to polymers, ceramics and metal composites. This process can be used to add additional features directly to the existing parts including coating to enhance performance and/or it can be used for repairing purposes. This can result in prolonged life of die casting and injection moulding dies by deposition of wear-resistance alloys in critical locations (Gibson, et al., 2015). Companies such as Optomec (Optomec Inc., 2017) and DM3D Technology (DM3D Technology LLC, 2017) offer DED services as well as supply commercially available machines and materials.

2.1.4 Material Extrusion

Material Extrusion, ME currently the most popular on the market (Gibson, et al., 2015), is an AM process in which material is selectively extruded through a nozzle or orifice (ISO/TC 261, 2015). A schematic of the process can be seen in Figure 4. Typically, a thermal process controls the state of the material while extrusion although it can also be a chemical process. It offers one of the most effective mechanical properties of the parts built by polymer based AM process starting from low to high costs (Gibson, et al., 2015). It's limited in terms of build speed, accuracy, and material density as these are dependent on acceleration and deceleration of the plotting head, nozzle and viscoelasticity of the material respectively. The process requires supports for complex geometry that can be removed mechanically which is viable for similar and/or secondary material and chemically which is viable only for dissolvable secondary material.

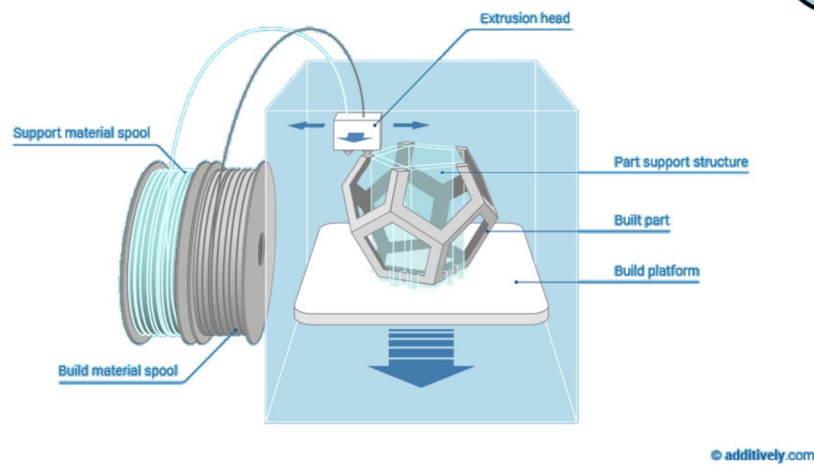


Figure 4: Schematic of ME process (Additively Ltd., 2017)

ME offers direct printing of the parts with a wide range of polymers preferably amorphous. These have reasonable mechanical properties at low costs which increase with higher-end machines. The process is also used for direct bio-extrusion of gels and bio-compatible polymers for cell growth and tissue engineering (Gibson, et al., 2015). To widen its approach, it can be used for manufacturing polymer based patterns for sand casting of metals as well. Furthermore, it offers indirect manufacturing of parts made up of ceramics and/or ceramic composites. Companies such as Stratasys (Stratasys Ltd., 2017) and 3D Systems (3D Systems Inc., 2017) offer ME services on demand as well as supply commercially available machines and materials.

2.1.5 Material Jetting

Material Jetting, MJ first demonstrated in 1980s as Ballistic Particle Manufacturing (Gibson, et al., 2015) is an AM process which selectively deposits droplets of build materials (ISO/TC 261, 2015). A schematic of the process can be seen in Figure 5. The process can be categorized into two droplet formation technologies controlling the frequency of the formation of drops including continuous stream and drop on demand. The continuous stream includes binary deflection, multiple deflection, hertz and microdot techniques whereas drop on demand includes thermal, piezoelectric, electrostatic and acoustic droplet actuating designs (Hue, 1998). In terms of scalability, the process offers scalable colour print heads up to thousands of nozzles at relatively low costs compared to other processes that use high power sources. This can lead to high speed and ease of material integrated manufacturing. It requires supports for complex geometries which can be integrated into print nozzle(s) of different material that can easily be removed by hand, water and/or solution bath (Stratasys Ltd., 2017).

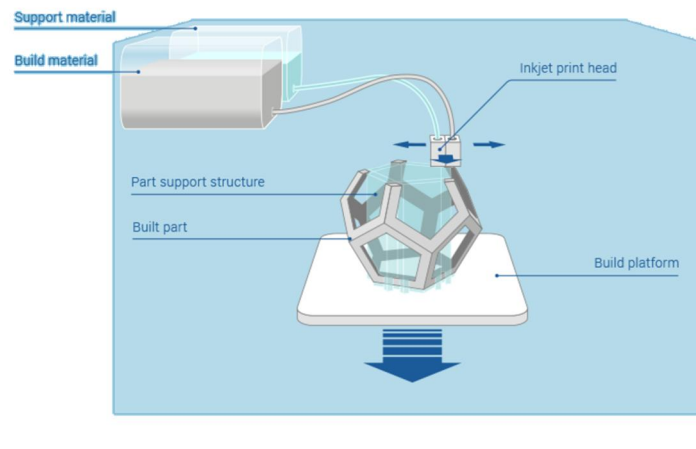


Figure 5. Schematic of MJ process (Additively Ltd., 2017)

MJ process is capable of manufacturing part(s) directly with materials including waxes, polymers, ceramics and metals. The process can be used for manufacturing wax based investment casting patterns for various industries including jewellery, dentistry and metal. Until the year 2016, only waxes and polymers were commercially available while ceramics and metals were mainly printed on a research and development basis with a preference of materials with low melting point. Recently, XJET (XJET Ltd., 2016) changed the dynamics of MJ and made a breakthrough by introducing NanoParticle Jetting, NPJ of ceramic and metal to the world. NPJ additively manufactures parts indirectly through heat treatment. The machines and materials of XJET are expected to be commercially available by the last quarter of 2017. Companies such as Stratasys (Stratasys Ltd., 2017) and 3D Systems (3D Systems Inc., 2017) supply commercially available machines and materials including services on demand.

2.1.6 Powder Bed Fusion

Powder Bed Fusion, PBF is one of the first commercialized and widely used AM process (Gibson, et al., 2015) in which powder bed regions are selectively fused using thermal energy (ISO/TC 261, 2015). The source of thermal energy is typically a laser such as CO₂ or fiber laser or it is an electron beam which is limited to metals due to the need of electron conductivity. Powder fusion mechanisms include solid state sintering, chemically induced binding, liquid phase sintering and full melting. A schematic of the process can be seen in Figure 6. Since the powder material is vulnerable to oxidation and degradation from the ambient atmosphere, the process occurs in a controlled, nitrogen, argon or a shielding gas filled enclosed chamber. It uses infrared and/or resistive heaters to minimize the required laser power and to avoid curling distortion caused by large thermal gradients. Material properties of PBF manufactured part(s) are comparable to those of the engineering grade materials, competing with injection moulding and other polymer manufacturing methods (Gibson, et al., 2015). The process offers the ability to increase productivity via nesting multiple parts in one build as the powder bed eliminates the need for support structures for polymers. For metals and alloys, the supports attached to a substrate plate are mandatory in order to assist heat conduction and prevent curling distortion.

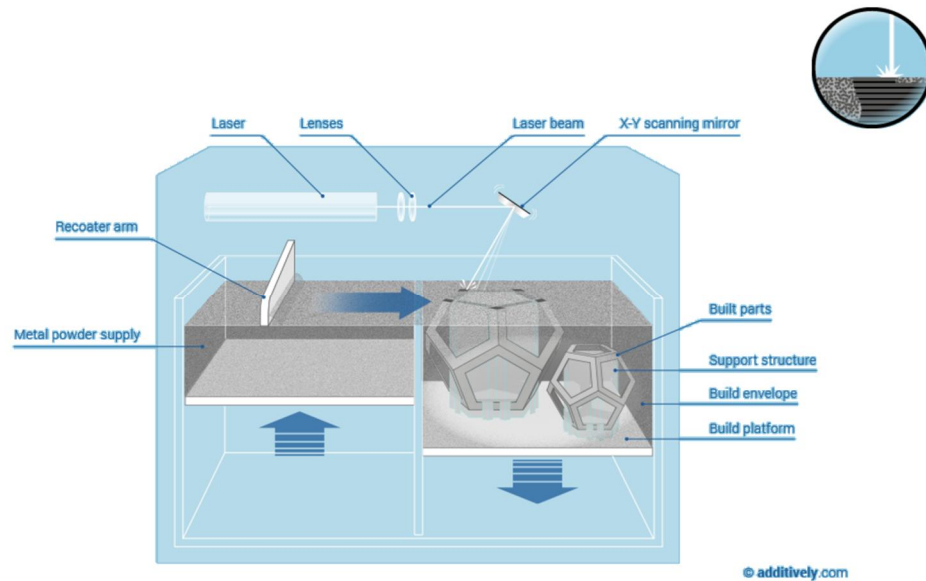
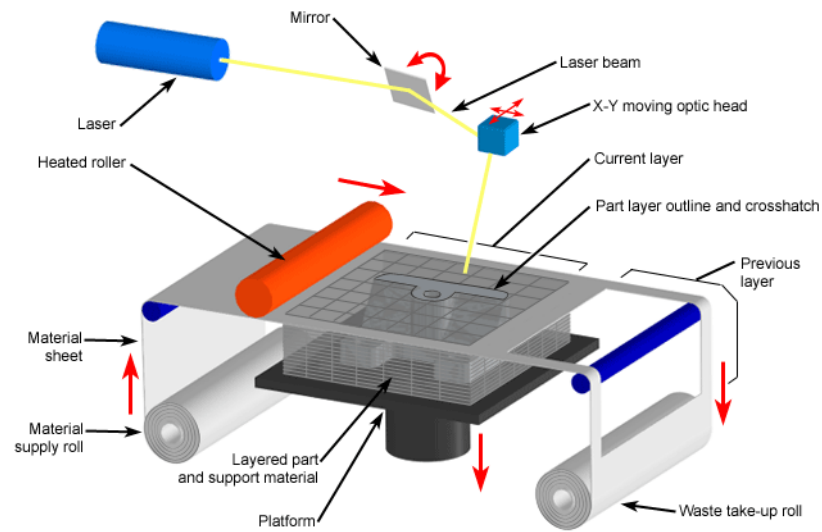


Figure 6. Schematic of PBF: Selective laser melting Process (Additively Ltd., 2017)

PBF process offers the ability to manufacture parts directly as well as indirectly using a wide range of materials in contrast to other AM processes. PBF compatible materials include polymers preferably semi-crystalline, metals preferably weldable, waxes, ceramics and composites of the aforementioned materials. Even though there is a growing number of terminologies marketed by many AM companies, Selective Laser Sintering (SLS) is typically used for direct manufacturing of polymers as well as waxes. SLS was also used for indirect manufacturing of metals and ceramics through formation of ‘green’ part followed by debinding, sintering and reimpregnation/infiltration methods which has become obsolete due to the introduction of direct methods. Selective Laser Melting (SLM) is typically used for direct manufacturing of polymers and metals. The process can be used to directly manufacture polystyrene and wax based patterns for investment casting and thermosetting binder based moulds, cores and inserts for sand casting (Gibson, et al., 2015). Companies such as 3D systems (3D Systems Inc., 2017) and EOS (EOS GmbH, 2017) provide commercially available machines and materials along with services on demand.

2.1.7 Sheet Lamination

Sheet Lamination, SL is one of the first commercialized AM process known as Laminated Object Manufacturing, LOM (Gibson, et al., 2015) in which a part is formed by bonding sheets of material (ISO/TC 261, 2015). The formation of the part is assisted with a laser or a mechanical cutter which cuts the outer contours of the sheets on layer by layer basis. The bonding mechanisms of the sheets can include adhesion, heating, clamping and/or ultrasonic welding. A schematic of the process can be seen in Figure 7. The order of forming and bonding mechanisms plays a critical role in defining the capabilities of the process. For instance, internal features or channels are difficult or impossible to manufacture with bond-then-form order due to inability of material removal from the internal features of the part (Gibson, et al., 2015). However, the opposite order, form-then-bond can overcome this constraint but at the cost of external supports which are not needed in bond-then-form order. The process allows colour printing and exhibits faster build rates for certain machines than other AM processes since only the outer contours of the layers forming the part are cut. The unused material of the part layer is sliced into a cross hatched pattern to assist support removal called decubing (Liao, 2001).



Copyright © 2008 CustomPartNet

Figure 7. Schematic of SL: Laminated Object Manufacturing (CustomPartNet., 2017)

SL consists of the ability to manufacture parts directly with a wide range of materials including but not limited to paper, polymers and metals. Ceramics can be manufactured indirectly via thermal post processing. This process can assist sand casting by manufacturing paper and/or polymer based patterns. SL variant, Ultrasonic Additive Manufacturing can be used to create parts with complex internal features, multifunctionality, multiple materials and integrated components such as wiring, fiber optics, sensors and instruments (Gibson, et al., 2015). Companies such as Mcor Technologies (Mcor Technologies Ltd., 2015) and Wuhan Binhu (Wuhan Binhu Mechanical & Electrical Co. Ltd., 2014) provide machines as well as provide services on demand.

2.1.8 Vat Photopolymerization

Vat Photopolymerization, VP, discovered by Charles W. Hull in the mid-1980s (Gibson, et al., 2015) is an AM process in which light-activated polymerization is used to selectively cure liquid photopolymers in a vat (ISO/TC 261, 2015). The activation medium can simply be visible light or it can be UV rays, X-rays, gamma rays or electron beams. When VP is equipped with one or more lasers for curing process, the general term is then referred to Stereolithography, SLA (ASTM International, 2013). A schematic of SLA, VP process is shown in Figure 8. The process configurations may include vector scan in which point wise approach is used, mask projection in which layer wise approach is used, two-photon in which point by point approach is used at nano-scale or another configuration in which a line-wise approach is used (Gibson, et al., 2015). The magnitude of curing, hence, printing in terms of speed increases in a subsequent order from two-photon, to vector scan, line-wise approach and mask projection for obvious reasons. The process offers relatively better accuracy and surface finish of the printed parts with respect to other AM processes, however, at the cost of lower mechanical properties. It requires support structures to hold the part onto build platform as it is built (Gibson, et al., 2015).

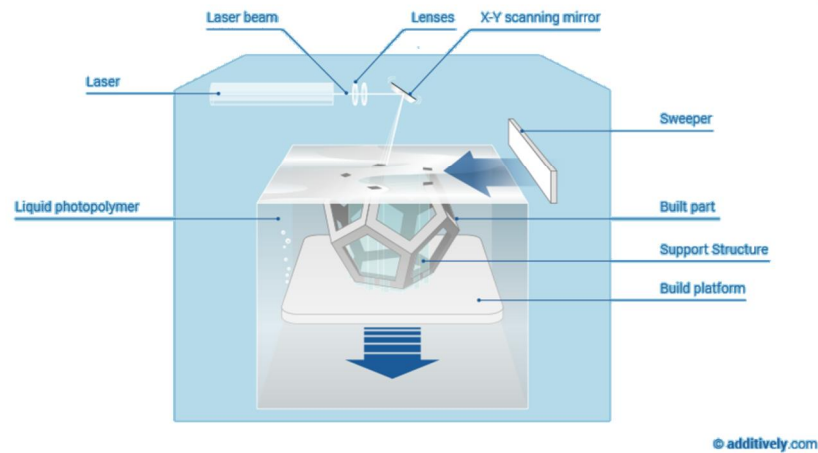


Figure 8. Schematic of VP: Stereolithography (Additively Ltd., 2017)

VP process offers the ability to directly print the parts with photopolymer materials including acrylate, epoxy, vinyl ether and/or a combination of these depending on the desired mechanical and metallurgical properties. Due to the limited mechanical properties offered by the process, the printed parts are mainly used as functional prototypes or in some cases end use products due to their high finishing properties. The process can also assist sand casting and investment casting by directly manufacturing relative patterns. The mechanical properties of the parts can be enhanced by post curing or post heat treatment leading to indirect methods. Companies such as 3D Systems (3D Systems Inc., 2017), Envisiontec (EnvisionTEC, 2017) and Formlabs (Formlabs, 2017) supply machines and materials whereas, 3D Systems also provides services on demand.

2.2 Design for Additive Manufacturing

As opposed to design for manufacturing which involves a vast range of expertise in limited potentialities of conventional processes of joining, shaping and finishing in quest of lean and agile manufacturing, the design for additive manufacturing offers optimization of this quest by synthesis of very broad shape complexity, hierarchical complexity, material complexity and functional complexity. These unique AM capabilities are described in the subsequent text.

2.2.1 Shape Complexity

AM offers shape complexity for free, it is possible to build virtually any shape possible even if it is impossible to manufacture through conventional machining processes which are limited by tool movement such as under drafts, over hangs, undercuts and internal features. Hence, parts that have complex shape form and are cumbersome as well as laborious to make through conventional machining processes take advantage of AM. However, there are limitations of AM such as part size, production duration, surface finish, resolution and accuracy.

The size of the part is directly dependent on the build chamber of the machine. Relatively large sizes of build chambers for three different metal additive manufacturing feed stocks are 400mm x 400mm x 400mm (EOS: M 400-4), 900mm x 1500mm x 900mm (Optomec:

LENS 850-R) and 610mm x 610mm x 5182mm (MER: plasma transferred arc) for powder bed, powder feed and wire feed respectively. Larger build chambers are also available for instance 4000mm x 2000mm x 1000mm of VX4000 which to date, Voxeljet claims to be the world's biggest industrial 3D printing system for sand casting to create metal parts (Voxeljet AG, 2017).

Production duration of the part is influenced by the deposition rate, which in fact depends on multiple factors according to the technology under consideration such as laser/electron beam spot size, nozzle size and scan speed. Lower laser/electron beam spot size, nozzle size and scan speed lead to longer production duration. The deposition rate can range from 25g/h to 9kg/h for different technologies (Nycz, et al., 2016; Gibson, et al., 2015). Furthermore, as per Salmi, et al. (2016), the production duration per part depends critically on geometry, orientation, printing process and number of parts manufactured per build cycle.

The surface finish of AM depends on the orientation of the part, top surface parallel to the energy source exhibits approximately 2 to 3 times better surface roughness than side surface perpendicular to the energy source for DMLS and EBM (Frazier, 2014). Furthermore, top surface perpendicular to the energy source exhibits approximately 5% rougher surface than the parallel one and the side surface perpendicular to the energy source exhibits approximately 3% larger surface roughness than the parallel one for DMD (Koch & Mazumder, 2000). Other factors which effect the surface roughness include a compromise of power source, scan speed, deposition rate and/or fusion mechanisms with respect to material properties, bed temperature and type of AM technology. The average surface roughness, R_a of $9\mu\text{m}$ can be achieved by selective laser melting of metal parts (Gu, et al., 2012; Stratasys Direct, Inc., 2017) and less than $1.7\mu\text{m}$ can be achieved by micro selective laser melting using low scan speeds (Eberhard & Kniepkamp, 2015). It can range from poor to excellent depending on the technology under consideration. Salmi, et al. (2017) recorded R_a value of $5.66\mu\text{m}$ for direct metal AM of EOS Cobalt Chrome SP2 powder which as a result of post processing was decreased to $0.18\mu\text{m}$ via ultrasonic burishing while the performance of the component was increased by approximately 47% in terms of hardness.

Accuracy of AM is typically dependent on the bonding energy source in terms of melt pool or droplet size, material properties in terms of granular size, viscosity, shrinkage and residual stress induced distortion, thermodynamics of the build chamber in terms of curling distortion and the speed of the scan or build. According to Hofmeister, et al. (2001), AM featured parts via DED of LENS technology, contain anisotropic properties with microstructural scale being the most sensitive to variation in z-axis in terms of layer height than fluctuations in laser power and scan speed due to the fact that heat conduction is predominant on cooling rate and resultant structure. According to the data sheet of Stainless Steel 316L of Stratasys Direct, Inc. (2017), the nature of anisotropy of its metal PBF process exhibits 19.15% less yield strength in the Z axis. Generally, large melt pool or droplet size, large build volumes, large thermal gradients and fast build/scan speeds lead to lower accuracies. The accuracy can range from submicron to 1000s of microns tolerances depending on aforementioned parameters and type of technology. According to Stratasys Direct, Inc. (2017), the metal printed parts have a general tolerance of $\pm 0.127\text{mm}$ for the first 25.4mm and here onwards a tolerance of $\pm 0.051\text{mm}$ per 25.4mm which is approximately ($\pm 0.2\%$). The resolution of AM depends on build mechanisms such as galvanometers in case of laser source and gearboxes as well as motors for other

build mechanisms. Both, accuracy and resolution increase with higher end machines. (Gibson, et al., 2015; Horn & Harrysson, 2012)

In conclusion, even though AM offers the freedom of shape of the part, it is delimited by geometric finishing parameters. High surface finish, accuracy, resolution and low production duration can be achieved by AM at the cost of trade-offs of lower deposition rate or melt pool, lower scan speed, relatively smaller size and volume of the part as well as the use of high-end machines. However, in order to meet the finishing standards of CNC machining in terms of the aforementioned parameters, the design for AM can be equipped so that it can subsequently be followed by conventional subtractive finishing methods including but not limited to hand finishing, tumbling, vibratory finishing, abrasive flow machining, shot peening, milling, honing and/or lapping. This approach can also be applied to additively manufactured polymer parts of consumer or professional grades to improve the dimensional stability of the parts as explained by Ituarte, et al. (2015).

2.2.2 Hierarchical Complexity

AM possesses the capability of selectively managing the hierarchical complexity of a part leading to variability in its lattice structure scaling from macrostructure, to mesostructure, to microstructure and even to the scale of nanostructure. It can provide a revolutionizing approach to create new materials such as nanophase, amorphous, functionally gradient and porous materials for specific applications by changing process parameters (Gu, et al., 2012). This tailorability is achievable in AM processes such as ME, MJ, VP, SL and especially in DED which also consists of the capability of developing equiaxed, columnar, directionally solidified and single crystal grain structures (Gibson, et al., 2015). According to Wohlers Associates Inc. (2017), the scanning pattern of energy beam can create customizable microstructures that have never been seen before leading to metallic AM parts having material properties approaching those of forged parts and exceeding those of cast parts due to rapid solidification and microstructure relative uniformity. However, due to complex mutual interactions of materials and process parameters including the non-equilibrium conditions of power sources, the uncontrollability and/or unpredictability of the phase and lattice formation, AM is still quite ambiguous and requires further research in physical and chemical metallurgical phenomena on a case by case basis (Gu, et al., 2012).

2.2.3 Material Complexity

As AM involves the addition of material(s) on a layer-by-layer basis or material incremental manufacturing, it offers the possibility of depositing different materials at different locations of the part leading to formation of location specific properties throughout the part. The unique integration of homogenous materials and heterogeneous materials changing material composition, abruptly or gradually can offer a ground-breaking methodology in creating parts with properties and functions that are currently non-existence (Gu, et al., 2012). This unique capability of AM can be used via several AM processes preferably DED, MJ, ME and/or hybrid systems (Vaezi, et al., 2013). However, manufacturing suitable parts considering the compatibility of different materials can be challenging and requires intensive research on case specific scenarios. In addition, different AM methods require unique properties of materials for their processability for instance, polymer based methods require amorphous characteristics and powder based methods require high flowability hence, leading to limited availability of materials.

2.2.4 Functional Complexity

The fundamentals of AM enable functional complexity within the part, which can lead to static and/or dynamic part consolidation involving operational mechanisms. These mechanisms can consist of several kinematic joints such as revolute, cylindrical, spherical, universal, vertical and/or horizontal joints in one build (Gibson, et al., 2015). In addition, AM offers the possibility of manufacturing in situ assemblies which involve the fabrication of assemblies around already made component(s). This level of functional complexity can reduce or even eliminate the amount of parts to be assembled, amount of handling time and tooling of part(s) and/or assemblies (Atzeni & Salmi, 2012). AM processes involving powder based systems can easily take advantage of this capability as powder can easily be removed from the provided clearance between assemblies. In addition, it is also practised for ME based systems where solvable support structures are used.

2.2.5 Optimization Methods

The unique aforementioned capabilities of AM give rise to optimization methods that cross the limitations of conventional manufacturing constraints. These can include size optimization where stresses and/or strains are maximized for certain loading and boundary conditions by minimizing dimension(s) of the part, shape optimization where stresses and/or strains are maximized for certain loading and boundary conditions by fluctuating the surface profile(s) of the part, and topology optimization where the stresses and/or strains for certain loading and boundary conditions are maximized by distributing the material of the part in terms of either truss based design and/or volume based design. Several Computer Aided Engineering softwares such as Abaqus, Ansys and SolidThinking are commercially available for such optimizations where finite element analysis can be performed in terms of displacement analysis, vibrational analysis, stability analysis, non-linear analysis and/or thermo-elastic analysis.

2.3 Business Aspects and Potentials

The final part production or end use part production through direct and indirect additive manufacturing is also known as direct digital manufacturing (DDM) (Gibson, et al., 2015). Its predecessor rapid prototyping is an application of AM intended for reduction of lead times of prototypes (ISO/TC 261, 2015). The end use part production has grown to 60.6% with an estimated 3.66 billion USD of the total product and service revenue of AM worldwide which is estimated to be 6.063 billion USD according to the recent Wohlers report (Wohlers Associates Inc., 2017). The same report emphasizes high gains in metal AM dedicated to end use production of ideally high value, low volume and complex parts in industries such as aerospace, medical and automotive. By observing the growth rate since 2003, presented in the report, this type of production can easily be anticipated to grow at an exponential rate over the next several years. The cause of such growth becomes apparent when key drivers of AM convince manufacturers to adapt to such technological gains as cost effectiveness and faster lead times with mass customization. These key drivers can be categorized in terms of agile and lean manufacturing which are presented in the subsequent text.

2.3.1 Agile Manufacturing

Agile manufacturing is responsiveness to customer needs and market fluctuations whilst still having a control of costs and quality (Wang & Koh, 2010). AM serves as a responsive

manufacturing tool to fulfil these criteria as it offers economical mass customization of parts. It can virtually build each digital part with different geometries in one build cycle leading to supply of parts on a variable demand including lot sizes of one since no tooling is required. This enables major cost reductions since no CNC machine programmer or operator is needed and in terms of tool related setbacks such as tool maintenance, repair, storage and eventual production delays. In addition, it promotes faster innovation time followed by faster lead times of spare parts and fast turnaround of the designs which might even fail validation and/or verification tests. Medical applications of AM including manufacturing of preoperative anatomical models can provide a vast range of possibilities and can effectively be used in surgery and dentistry since each patient has a unique geometrical profile (Salmi, 2013; Salmi, 2016). Moulds from Align Technology (Align Technology Inc., 2017) and hearing aids from Siemens AG (Siemens AG, 2017) provide an excellent example where patient specific geometries are produced via AM. Salmi, et al. (2013) provide a proof of concept of additively manufactured occlusal splints via a clinical pilot study which might reduce costs and working time in future.

2.3.2 Lean Manufacturing

Lean manufacturing is about doing more with less by eliminating waste in terms of reducing inventories, lot sizes, supplier base and elimination of paperwork (Wang & Koh, 2010). As opposed to conventional subtractive methodologies which involve design limitations and scrap, AM consists of the ability to manufacture digital parts with complex geometries using precisely the material that is needed leading to digital decentralized manufacturing, part consolidation, higher performance, long term sustainability, elimination of paperwork and physical inventories by giving birth to digital record and electronic (e) inventories.

Digital decentralized manufacturing can provide a physical replica of the digital model through a single AM machine hence, eliminating the need of large centralized factories and promoting localized manufacturing around the globe. Part consolidation reduces the number of parts in assemblies leading to reduced documentation, quality control, process management, assembly lines and labour. GE Aviation managed to reduce the number of parts for its Advanced Turboprop engine from 855 parts to 12 parts and the number of parts for its bearing support and sump from 80 parts to a single part with AM enabled design and manufacturing (Wohlers Associates Inc., 2017). Higher performance may include designs proven to be more efficient in terms of weight, deformation, fluid dynamics, thermodynamics and/or stress distribution. Kuhn-Stoff in collaboration with EOS reduced the weight of a mechanical gripper by 86% and consolidated the number of parts from 21 to two while surpassing verification tests leading to reduction in manufacturing costs up to 50% and reduction in lead time up to 75% (EOS GmbH, 2017). Sustainability includes lower CO₂ foot print. Digital records and e-inventories enable local manufacturing at a global level and reduce paperwork, logistic constraints, on/off site storages and the costs related to these. Holmström, et al. (2009) propose conceptual designs for deploying AM in the spare parts supply chain in terms of improved service and reduced inventories. According to Autodesk Inc. (2017), Airbus in collaboration with Autodesk Inc. reduced the weight of a bionic partition of Airbus A320 by 45 % using AM leading to 3180 kg of fuel savings per year. This reduction would in turn cut down 166 metric tons of CO₂ emissions per aircraft annually and when applied to thousands of new orders of the plane, it could literally save up to hundreds of thousands of metric tons of CO₂ emissions per year. Furthermore, Caterpillar, a heavy equipment manufacturer generally associated with

construction and mining equipment opened their additive manufacturing factory in December 2015 (Caterpillar, 2017) through which they have been taking advantage of design for additive manufacturing by redesigning their diesel engine fuel chambers for higher performance (Zelinski, 2017). Caterpillar is also taking advantage of AM via production of parts for its dozers, excavators and other equipment in addition to gages, display and scale models, assembly fixtures, hand tools, moulds, and functional models leading up to hundreds of thousands of savings in cost (Gardner Business Media, Inc., 2015).

2.3.3 Implementation

In order for AM to be introduced and eventually implemented in an organization as a suitable manufacturing method, it requires the need of evaluating the supply chain in terms of cost; how effective it is compared to status quo, lead time; how fast is the product produced, and verification; do the product's properties comply with certain standards and specifications. Table 1, Table 2 and Table 3 present the cost parameters of injection moulding (IM), subtractive manufacturing (SM) and additive manufacturing (AM) respectively. Subtractive manufacturing refers to the conventional manufacturing where the material is removed from stock profile(s) to manufacture the component. In brief, main cost parameters of each manufacturing process consists of material cost, labour cost and machine cost however, due to the differences in each manufacturing method these main parameters are subdivided into further categories as seen from the presented tables. It should also be taken into account that injection moulding and subtractive manufacturing also include cost per part of mould and tooling respectively, in addition to the aforementioned main parameters. AM, on the other hand, does not require tooling for different geometries or parts.

Table 1. Injection Moulding Cost Parameters adapted from (Atzeni, et al., 2010).

Injection Moulding Cost Parameters	
Parameter	Unit
Production Volume	[pcs]
Machine Cost per hour	[EUR/h]
Cycle time	[h]
Number of Cavities	[-]
Machine cost per part	[EUR]
Machine operator cost per hour	[EUR/h]
Percentage of operator time	[%]
Machine operator cost per part	[EUR]
Material cost per kg	[EUR/kg]
Part weight	[kg]
Material cost per part	[EUR]
Mould cost	[EUR]
Mould cost per part	[EUR]
Total Cost per part	[EUR]

Table 2. Subtractive Manufacturing Cost Parameters.

Subtractive Manufacturing Cost Parameters	
Parameter	Unit
Production Volume	[pcs]
Machine Cost per hour	[EUR/h]
Energy	[EUR/h]
Cycle time	[h]
Machine cost per part	[EUR]
NC programmer cost per hour	[EUR/h]
Percentage of programmer time	[%]
Machine operator cost per hour	[EUR/h]
Percentage of operator time	[%]
Labour cost per part	[EUR]
Material cost per kg	[EUR/kg]
Part weight	[kg]
Material cost per part	[EUR]
Tooling cost	[EUR]
Tooling cost per part	[EUR]
Total Cost per part	[EUR]

Table 3. Additive Manufacturing Cost Parameters adapted from (Atzeni & Salmi, 2012).

Additive Manufacturing Cost Parameters	
Parameter	Unit
Number of parts produced per job	[-]
Material cost per kg	[EUR/kg]
Part volume	[mm ³]
Density of the sintered material	[g/mm ³]
Mass of material per part	[kg]
Material cost per part	[EUR]
Machine operator cost per hour	[EUR/h]
Set-up time per build	[h]
Pre-processing cost per part	[EUR]
Depreciation cost per year	[EUR/year]
Hours per year	[h/year]
Machine cost per hour	[EUR/h]
Build time	[h]
Machine cost per build	[EUR]
Machine Processing cost per part	[EUR]
Machine operator cost per hour	[EUR/h]
Post-processing time per build	[h]
Heat treatment cost per build	[EUR]
Post-processing cost per part	[EUR]
Total Cost per part	[EUR]

These parameters can be used to calculate the cost per part of any component manufactured through these methods with respect to its production volume. Hence, it can provide a very clear scientific approach of comparing the cost effectiveness of each method. For instance, the following Equation 1 can be used to evaluate the number of breakeven parts

of IM with respect to AM according to the fundamentals of economics. Breakeven points serve as crossovers between two or more manufacturing methods, before which either one is economical than the other and after which it is vice versa. The same equation can also be used to calculate the number of breakeven parts for SM and AM.

$$Cost_{AM} = Cost_{IM} + \frac{C_T}{N} \quad (1)$$

$$N = \frac{C_T}{Cost_{AM} - Cost_{OM}} \quad (2)$$

Where: $Cost_{AM}$ = Additive Manufacturing cost per part [EUR]
 $Cost_{IM}$ = Injection Moulding cost per part [EUR]
 C_T = Cost of Tooling [EUR]
 N = Number of Breakeven parts [-]

In addition, the duration of manufacturing the part, lead time can also be calculated according to these parameters which plays a crucial role in defining the responsiveness to market demand. Finally, the manufactured product should be verified in terms of requirements testing in order to evaluate whether or not it complies with the standards, regulations, requirements, specifications and/or imposed conditions. Furthermore, it should also be validated in terms of field testing to assure it meets the needs of the customers and/or involved stakeholders.

Senvol (Senvol LLC, 2017) has outlined seven AM cost effective supply chain scenarios based on their history of quantitative AM analyses. It claims that if a component falls under one or more of the categorized scenarios, then it maybe be cost effective through AM. Table 4 lists and describes these scenarios.

Table 4. Seven Supply Chain Scenarios which may be cost effective (Senvol LLC, 2017).

Supply Chain Scenario	Description
Expensive to Manufacture	Do you have parts that are high cost because they have complex geometries, high fixed costs (e.g. tooling), or are produced in low volumes? AM may be more cost-efficient.
Long Lead-Times	Does it take too long to obtain certain parts? Are your downtime costs extremely high? Do you want to increase speed-to-market? Through AM, you can often get parts more quickly.
High Inventory Costs	Do you overstock or understock? Do you struggle with long-tail or obsolete parts? AM can allow for on-demand production, thus reducing the need for inventory.
Sole-Sourced from Suppliers	Are any of your critical parts sole-sourced? This poses a supply chain risk. By qualifying a part for AM, you will no longer be completely reliant on your current supplier.
Remote Locations	Do you operate in remote locations where it is difficult, time consuming, or expensive to ship parts to? AM may allow you to manufacture certain parts on-site.
High Import / Export Costs	Do you pay substantial import/export costs on parts simply because of the location of your business unit and/or your supplier? On-site production via AM can eliminate these costs.
Improved Functionality	AM can enable a part to be redesigned such that its performance is improved beyond what was previously possible.

Senvol also provides a free to access database (Senvol LLC, 2017) of over 1400 machines and materials which it claims to be the first and most comprehensive database.

3 Spare Parts

3.1 Screening Process Algorithm

A process for differentiating the suitability of AM methods to that of conventional subtractive manufacturing methods is developed in context of a logical flowchart to evaluate and to screen the provided spare parts as shown in Figure 9. Table 5 presents a summary of the provided spare parts consisting of either 2-dimensional or 3-dimensional data format which are analysed as part of this study. In principle, this flowchart can be used as an algorithm to evaluate any desired number of spare parts.

Table 5. Summary of provided spare parts.

Summary of Provided Spare Parts	
Entity	No.
Individual Parts	16
Assemblies	7
Total Parts	36

The starting point and ending points are presented by a rounded rectangular shape and a circular shape respectively. The diamond shape is used to illustrate a decision block with an output of yes or no. A rectangular shape is used to show a process. The direction of flow from one decision or process to the next one is represented by an arrow headed line segment. The wavy clouds next to the decision block outputs explain the properties associated with that decision. Most decision blocks are labelled with a level of priority. Level 1 represents the highest priority as a part cannot be built through AM if it doesn't satisfy this condition. The availability of desired material for AM, the availability of build space for desired size and availability of AM compatible 3D data are given first priority. Quality indicators such as tolerance and surface roughness of the final part are given second priority since the part can be printed and the desired level of tolerance and surface roughness may be achieved with post processing. The third priority is given to the optional optimization capabilities of AM which can be used to increase the performance of the part.

The post processing for direct and indirect metal AM are represented by conventional machining since direct metal AM requires the need of machining for separating the built part from the support structures connected to the substrate plate and indirect metal AM requires heat treatment and infiltration methods to the green part in order to build the end use product.

The final decision block leading to AM process evaluates the level of design complexity of the part to that of manufacturability of AM. Even though AM possess the capability of virtually manufacturing any level of complex geometry, there are few anomalies concerning the design. For instance, certain overhang geometries require support structures in order to overcome creep caused by gravitational forces and curling distortion caused by large thermal gradients during bonding of layers. In case this geometry is placed inside another completely enclosed geometry, the support structures are impossible to remove whether these are created or whether the part is supported by the powder bed. In addition, thin holes beyond a minimum value are also restricted depending on the dimensions of the part, shrinkage of material and the AM method. One must take these anomalies into consideration before designing complex geometries within the part such as conformal

channels, gating systems and/or runners to make sure that there is a possibility of removing supports and that the part is able to maintain its functional loads after the part has been manufactured through AM.

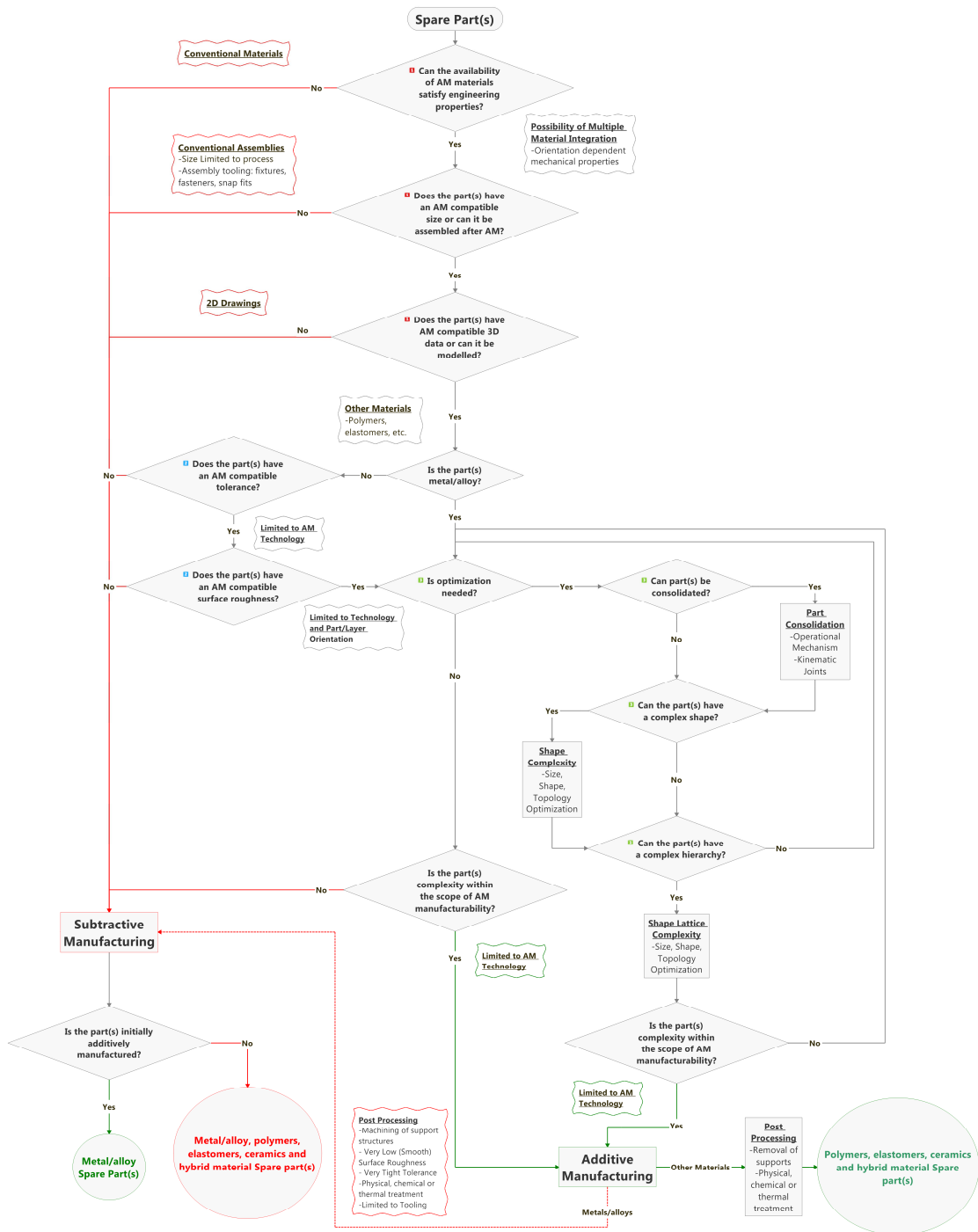


Figure 9. Spare Parts Additive and Subtractive Manufacturing Flowchart Algorithm.

3.2 Results of Screening Process

The algorithm presented in Figure 9 shows whether a specific spare part can be manufactured using AM however, just because it can be manufactured through AM, it doesn't inevitably mean that it should be. For the purpose of this study, spare parts which can be produced through AM are analysed with a generic point of view with regards to the cost effectiveness, lead time and the possibility of eventual increase in performance. An AM manufactured part always effects these factors in either a positive or a negative manner. The selected components are then further analysed by means of quantitative methods. Table 6 shows the list of attributes that are extracted from the provided spare parts data to conduct this screening analysis.

Table 6. Spare parts screening attributes.

Spare parts Screening Attributes	
Part Number	
Preview	
Year Designed	
Format	
Purpose	
Material	
Dimensions (L x W x H) [mm]	
Tightest Tolerance [mm]	
Overall tolerance [mm]	
Surface Roughness (Smoothest) [μm]	
Parallelism [mm]	
Perpendicularity [mm]	
Possible Conventional Manufacturing Methods	Primary:
	Machining:
Eligibility [Included or Excluded]	
Reasoning	

Appendix 1 shows the results of this screening process and the Table 7 illustrates the summary of the inclusion and exclusion of the spare parts for further analysis.

Table 7. Results of spare parts screening summary.

Spare Parts Screening Summary			
Entity	Included [No.]	Excluded [No.]	Total [No.]
Individual Parts	9	7	16
Assemblies	6	1	7
Total Parts	26	10	36

The reasons for exclusion for further analysis of 10 parts out of 36 parts are presented in the following Table 8.

Table 8. Reasoning of exclusion of spare parts for further analysis.

Reasons for Exclusion	
Exclusion Scenario	Reasoning
Cheap to Manufacture	The part consists of a simple geometric design which is easy to manufacture through readily available stock material at a low cost.
Short Lead Time	The part would require workshop finishing even after AM which would increase lead time.
Too Long and Narrow	The length of the part is too long for direct and indirect AM. A high level of straightness and flatness can be hard to manufacture through AM assisted casting (rapid tooling) due to high level of narrowness in the design.
Too big	The part size is too big to be manufactured through direct and indirect AM. In addition, straightness and flatness can be hard to manufacture through AM assisted casting (rapid tooling) due to high level of narrowness in the design.

4 Computer Aided Design

A prerequisite of AM is 3-dimensional (3D) data of a part to be manufactured in a format that is compatible to it. While there are several CAD data exchange formats such as IGES, Initial Graphics Exchange Specification and STEP, Standard for the Exchange of Product model data, AM compatible formats are AMF, Additive Manufacturing File format and STL, occasionally referred as Stereolithography or Standard Tessellation Language. According to ISO/TC 261 (2015), STL format describes the surface geometry of a part as a tessellation of triangles used to communicate 3D geometries to AM machines in order to manufacture the physical parts whereas AMF describes the native support for materials, colours, lattices, textures, constellations and metadata in addition to the 3D geometry represented by a triangular mesh that may even be curved. In order to fulfil this prerequisite, the available data format of the selected models is analysed and eventually converted to STL format. STL is selected over AMF since it consists of a relatively smaller file size. Hence, it can provide a denser mesh with the same amount of file size.




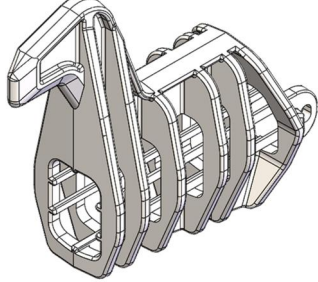
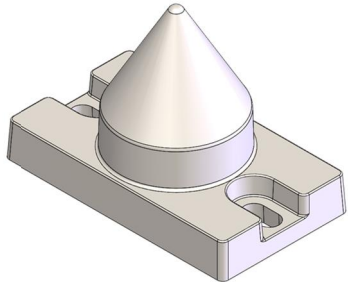
Appendix 1 presents the data format associated with each spare part and Table 9 illustrates the summary of the spare parts data format. In total, 2D data of 11 parts is modelled into 3D data using Creo Parametric, however, 3D data from 2 of these parts was eventually also received. In addition, a parametric model of DOP Turbine is also programmed with 8 parameters to provide ease of user interface. Lastly, seven moulds of the selected components are also modelled using Creo Parametric in order to evaluate the production of AM rapid tooling. This selection was based on spare parts which had a relatively bigger size leading to very high costs for direct or indirect AM of the part itself.


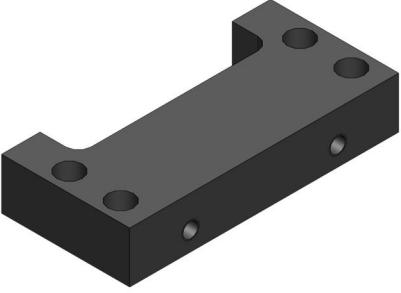
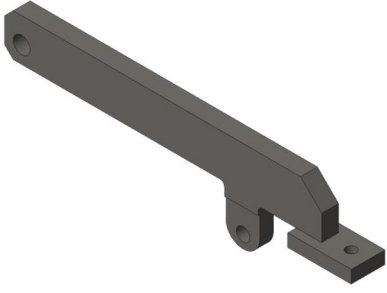
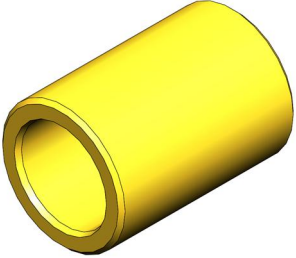
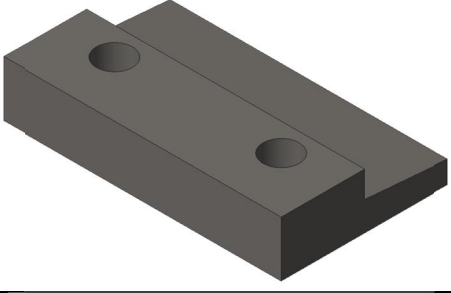
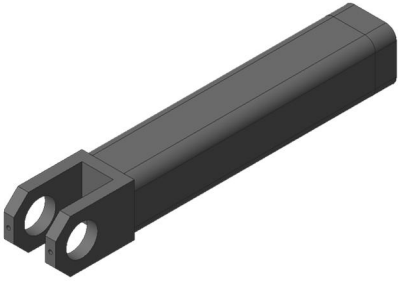
Table 9. Spare parts data format summary.

Spare Parts Data Format Summary			
Entity	2D Data [No.]	3D Data [No.]	Total [No.]
Individual Parts	5	4	9
Assemblies	4	2	6
Total Parts	16	10	26

Once the 3D data of all the spare parts was finalised, STL formats were created using the native CAD program of the models that are Creo Parametric or Solidworks. In addition, the STL files were validated for printability using the 3D Print tool of Creo Parametric. Table 10 presents an overview of the models with an isometric view.

Table 10. An Overview of CAD 3-dimensional spare parts.

Overview of 3-Dimensional Spare Parts						
Serial No.	Part Name	Material Classification	Manufacturing Method	Bounding Box [mm]	Source	Isometric View
1	DOP Turbine	Metal	Subtractive Manufacturing	200 x 200 x 963.5	Modelled*/Partially Provided	
2	Upper Shank	Metal	Subtractive Manufacturing	455 x 125 x 77	Modelled	
3	Chain Wheel	Metal	Subtractive Manufacturing	345 x 345 x 20	Modelled	
4	Hangbar	Polymer	Injection Moulding	210 x 200 x 66	Provided	
5	Positioning Cone	Polymer	Injection Moulding	200 x 115 x 141	Provided	

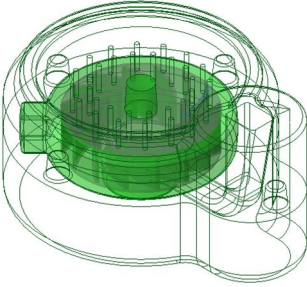
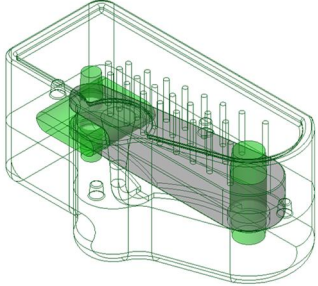
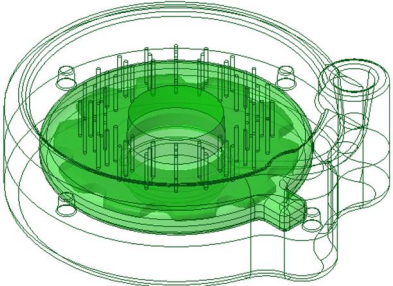
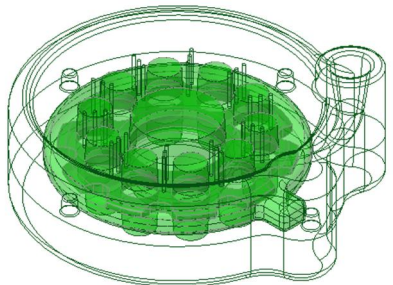
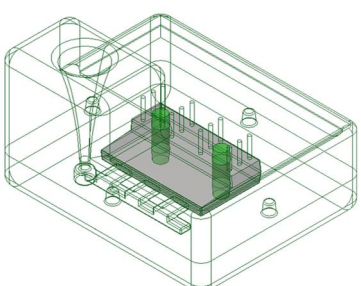
6	Cutting Blade	Metal	Subtractive Manufacturing	183 x 183 x 16	Modelled	
7	Guide Frame	Metal	Subtractive Manufacturing	210 x 100 x 40	Provided	
8	Roll Support	Metal	Subtractive Manufacturing	420 x 110 x 40	Modelled	
9	Sliding Bush	Metal	Subtractive Manufacturing	70 x 70 x 100	Provided	
10	Rail Fastener	Metal	Subtractive Manufacturing	100 x 60 x 20	Modelled	
11	Fork Bar	Metal	Subtractive Manufacturing	50 x 50 x 325	Modelled/Provided	

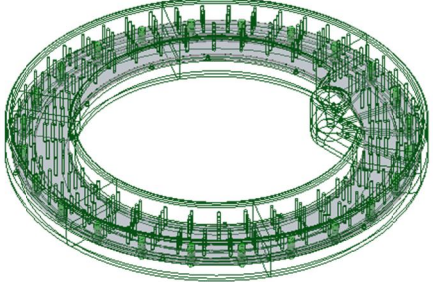
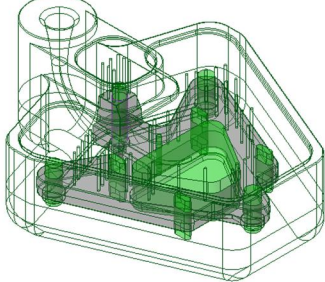
12	Stopper Flange Assembly	Metal & Polymer	Subtractive Manufacturing	236 x 236 x 95	Modelled/Provided	
13	Adjustable Mounting Plate	Metal	Subtractive Manufacturing	476 x 424 x 103	Modelled	
14	Bush	Metal	Subtractive Manufacturing	90 x 90 x 25	Modelled	
15	Brake Flange	Metal	Subtractive Manufacturing	1580 x 1580 x 35	Modelled	

**Parametric Model*

The following Table 11 illustrates the moulds that are modelled for rapid tooling, in this case, AM sand moulds. Each mould contains a top mould, bottom mould and a core that are presented in an isometric view. The top and bottom moulds are illustrated by a wire frame and these incorporate sprue, gates, runners, risers and guides which have been modelled by taking advantage of the design freedom of AM. The feeding height of the sprue is modelled to be at least 75mm from the part cavity because it cancels the effect of thermal expansion, inwards for convex and outwards for concave surfaces of the sand mould according to Campbell (2001). The core and the part cavity are represented by a transparent view in green for the aid of visualization.

Table 11. An overview of modelled moulds of spare parts for rapid tooling.

Overview of 3-Dimensional Moulds of Spare Parts for Rapid Tooling					
Serial No.	Part Name	Material Classification	Bounding Box [mm]	Source	Isometric View
1	DOP Turbine: Blade Housing	Sand Mould	430.0 x 340.0 x 211.0	Modelled*	
2	Upper Shank	Sand Mould	566.4 x 316.1 x 263.5	Modelled	
3	Chain Wheel	Sand Mould	483.5 x 541.8 x 200.0	Modelled	
4	Chain Wheel Opt.	Sand Mould	494.0 x 541.7 x 200.0	Modelled	
5	Rail Fastener	Sand Mould	160.0 x 117.0 x 200.0	Modelled	

7	Brake Flange	Sand Mould	1630.0 x 1630.0 x 210.0	Modelled	
6	Adjustable Mounting Plate	Sand Mould	576.0 x 683.0 x 278.0	Modelled	

*Courtesy of Aalto University Foundry

5 Cost and Lead Time Analysis

In this chapter, the cost effectiveness and lead time of the selected spare parts is evaluated with respect to additive manufacturing and subtractive manufacturing by means of qualitative methods. Further information was requested and acquired regarding the current state of subtractive manufacturing. Table 12 lists the additional attributes which were requested for further analysis. Appendix 2 describes these attributes with respect to each spare part.

Table 12. List of additional attributes acquired for selected spare parts.

Additional Attributes of Spare Parts
Equipment/Machinery [-]
Subtractive Method [-]
Downtime [Yes/No]
Type of Loading [Static/Variable/Shock]
Lead time [Weeks]
Cost [€]

For the purpose of this study, a total of 7 major service providers were selected and contacted in order to evaluate the cost and lead time of additively manufactured spare parts and/or rapid tooling such as investment casting patterns and sand moulds. Consequently, the quotations including the costs and lead time were received. In addition, a metal based PBF AM algorithm from Aalto University was also used to evaluate the cost and lead time of the selected components. In this case, the properties of SLM Solutions 500 HL with quad lasers of 700W each are used to print Maraging Steel 1.2709. Table 13 presents these service providers in alphabetical format with respect to direct AM, indirect AM and AM rapid tooling that were used for this study.

Table 13. List of AM Service Providers for Additive Manufacturing Cost and Lead Time Analysis.

Description	Additive Manufacturing		
	Direct	Indirect	Rapid Tooling
3D Systems: Quickparts	✓	✗	✓
ExOne: Karlebo	✗	✗	✓
iMaterialise	✓	✓	✗
Own Printer	✓	✗	✗
Protolabs	✓	✗	✗
Shapeways	✓	✓	✓
Stratasys	✓	✗	✓
Voxeljet: Hetitec	✗	✗	✓

According to the current manufacturing methods, the spare parts were categorized as injection moulding parts and subtractive manufacturing parts. Injection moulding parts are manufactured with a lot size of 1s in case of Positioning Cone and 100s in case of Hangbar during one setup. On the other hand, the subtractive manufacturing parts are produced with a lot size of 1. The aforementioned lot sizes typically refer to the execution of one customer order. According to the current demand, the injection moulding parts were analysed by means of cost per part of the selected AM method with respect to variable production volume defined as small series production from several AM service providers and their breakeven points were calculated with respect to injection moulding. Considering the fact that these IM spare parts are made up of polymers such as Polypropylene

(PP), ISO/ASTM approved AM method of PBF and its variant, SLS of Polyamide (PA) is selected to conduct these analyses. According to Granta Design Limited (2017), PA can exhibit approximately 75% higher tensile strength than that of PP. In this case, the tensile strength of additively manufactured PA is calculated to be approximately 43% higher than that of injection moulding PP. In order to compliment the cost effectiveness of AM, an additional AM method, ME of PLA is also selected and presented in the IM parts analyses. In this case, the additively manufactured PLA exhibits 48% higher tensile strength than injection moulded PP however, it may be subjected to long term creep depending on the level of plasticizers in its composition. Subsequently, according to the current demand, the subtractive manufacturing parts were evaluated by means of cost per part with respect to different AM methods and materials to compensate those of the original model. Taxation and shipping costs are omitted from the cost analyses due to industrial usage of services and the fact that most selected AM service providers operate globally from several locations. All cost analyses were followed by a lead time investigation to evaluate and compare how fast the product is manufactured. The lead times are measured in business days including 2 business days for international delivery and excluding weekends and public holidays.

5.1 Results of Injection Moulding Parts

5.1.1 Anode Hangbar

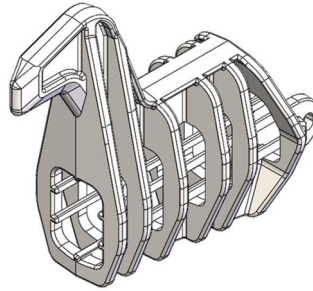


Figure 10. Injection Moulded Anode Hangbar containing a bounding box of 210mm x 200mm x 66mm.

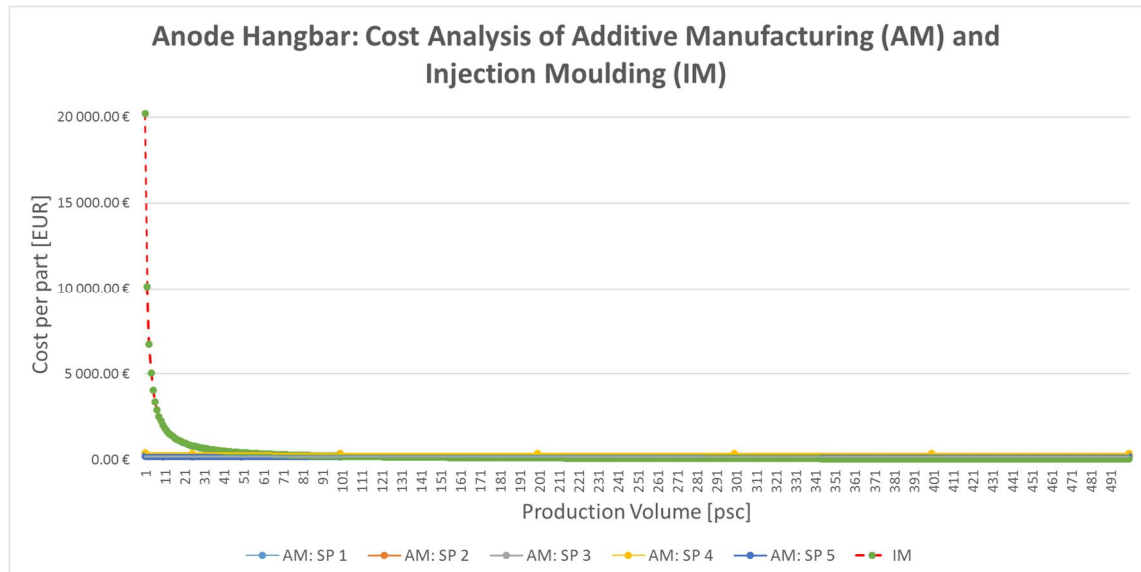
As described in Appendix 2, Anode Hangbar is a component of anode top insulator. It is manufactured via injection moulding and consists of a polymer. The component experiences variable loading and it doesn't necessarily effect downtime of the equipment in case it is damaged. A CAD model is shown in the following Figure 10.

5.1.1.1 Cost per Part by means of Production Volume

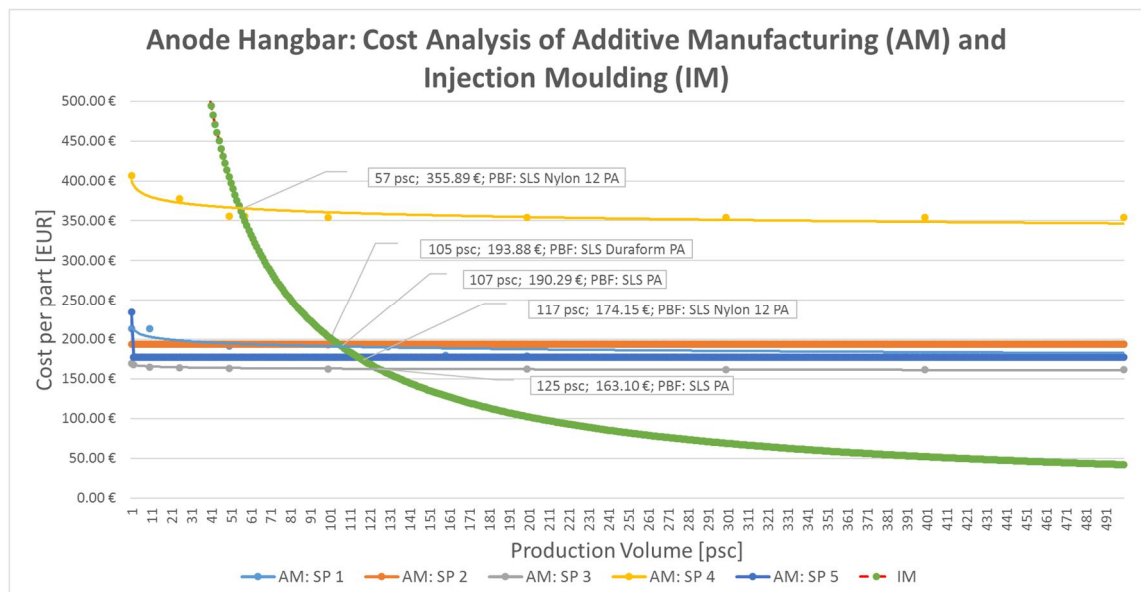
The behaviour of cost per part with respect to the production volume of this spare part can be seen in the following graphs. Graph 1 illustrates an overview of the cost analysis. As it can be seen, the cost per part of IM represented by the dashed red line starts just above the 20000€ threshold, which is the cost of the mould and it decreases with an exponential decay towards a steady state value. The cost per part including the parameters of IM presented in Table 1 is described in following Equation 3.

$$IM \text{ Cost per Part}(N) = \left(\frac{200\text{€} + 1.5\text{€}(N) + 20000\text{€}}{N} \right) \quad (3)$$

Where N is number of spare parts [No.]



Graph 1. An overview of Anode Hangbar cost analysis comparing injection moulding and additive manufacturing.



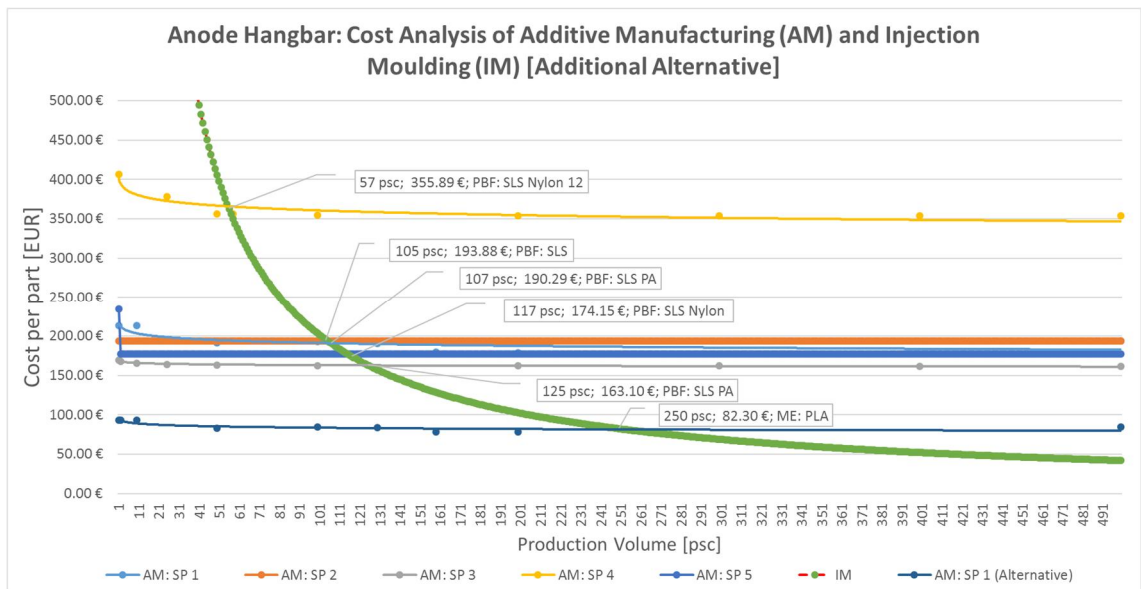
Graph 2. Breakeven cost analysis of Anode Hangbar.

The cost per part of AM seems to be constant according to the overview presented in Graph 1. However, Graph 2 illustrates a clearer, zoomed-in version of Graph 1 in which the cost per part of AM varies to some extent. The breakeven points or the crossover points between the two manufacturing methods are also presented with labels including the number of breakeven parts, cost per part, ISO/ASTM standardised AM method and the material of the part. It can be observed that each service provider follows a unique methodological algorithm for its quotations.

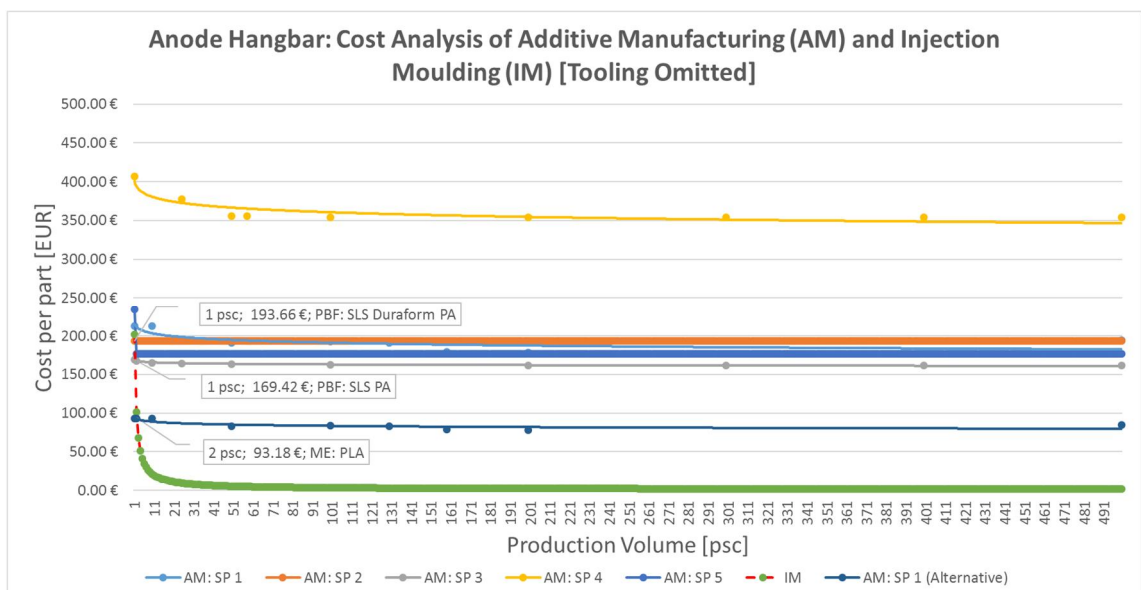
The cost per part, in a decreasing order of SP4, SP1 and SP3 decreases with a slight logarithmic decay. This is due to the fact that small series production through AM decreases costs per part as confirmed by (Piili, et al., 2015; Salmi, et al., 2016). It is also observed that the intensity of the decay decreases as the cost per part decreases. On the other hand, the cost per part of SP2 is constant since this price was negotiated to be valid for all lot sizes which was approximately 40% cheaper than the price that was originally

received from their parts on demand service with a lot size/production volume of 1. Furthermore, cost per part of SP5 decreases dramatically after the first build by approximately 24% and stays constant for the rest of the production volume. A basic analysis draws the fact that the prices quoted by these service providers are quite negotiable to an extent and as the cost per part is decreased, the number of breakeven parts increase. SP3 supplies the highest number of breakeven parts with a value of 125 psc for this analysis, confirming the most economical manufacturing method and service provider whereas, SP4 markets the lowest breakeven point of 57 pieces, yet still economical than IM.

The following Graph 3 illustrates another alternative AM method, ME and material, PLA with one of the most effective mechanical properties that pushes the number of breakeven parts even further to 250 pieces from SP1 however, at the cost of lower accuracy, higher levels of anisotropy and higher surface roughness. This method with specific material is marketed with relatively higher cost per part with respect to PBF of PA according to other service providers used in this analysis other than SP1.



Graph 3. Breakeven cost analysis of Anode Hangbar illustrating an additional alternative.

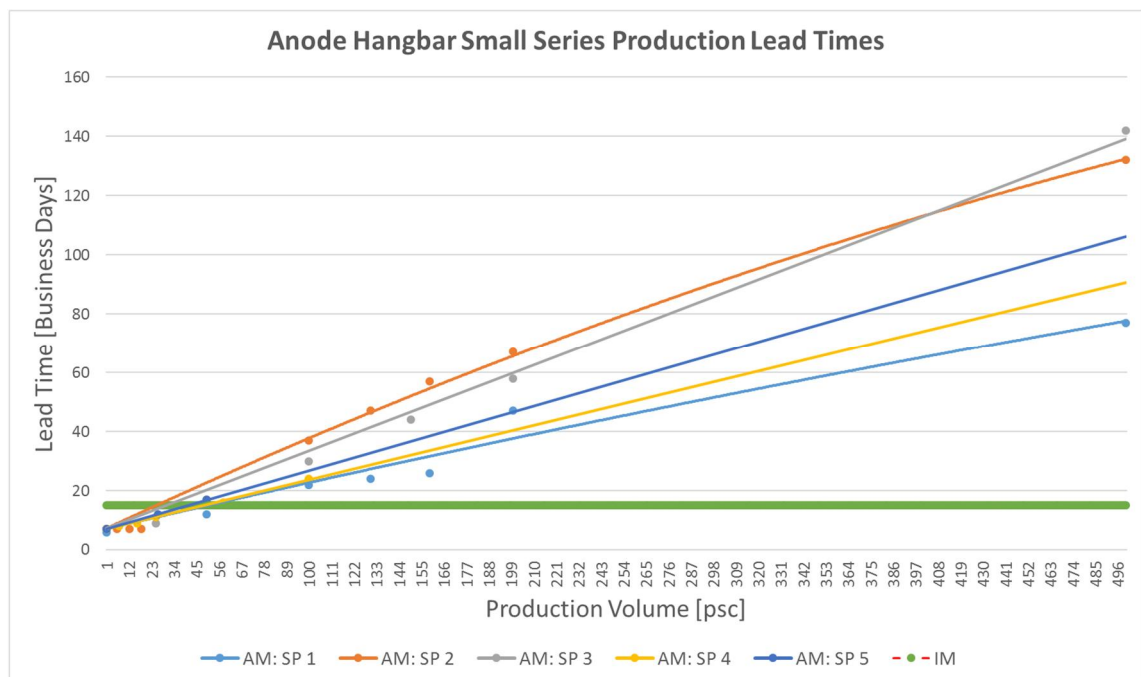


Graph 4. Breakeven cost analysis of Anode Hangbar without tooling costs.

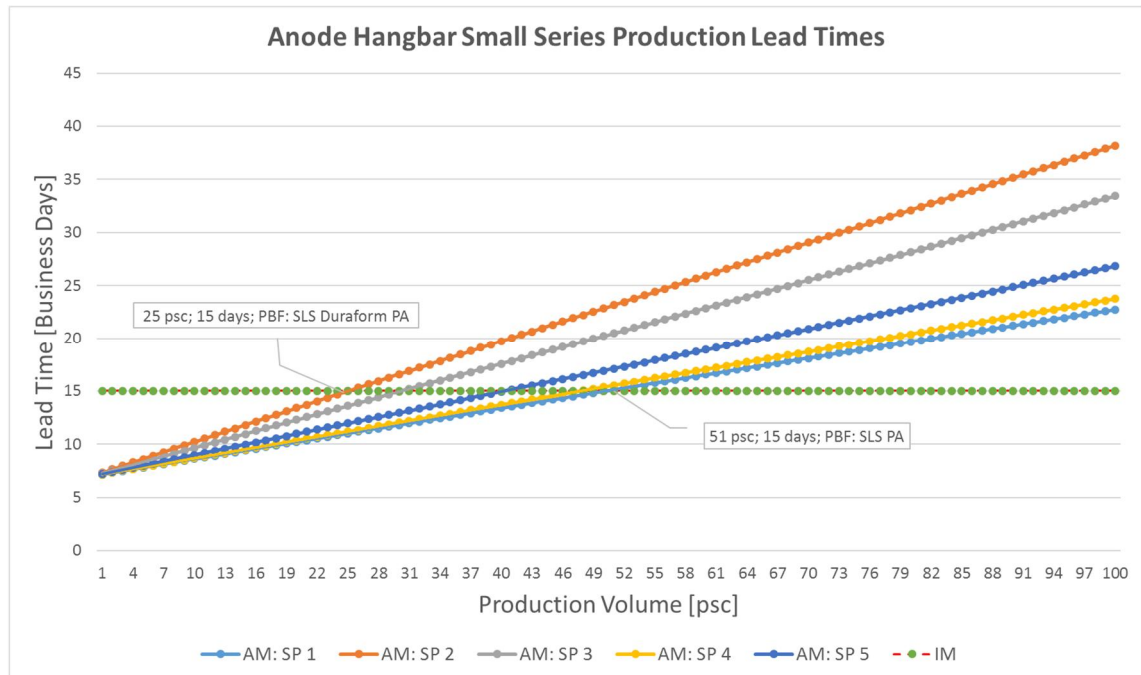
Another case scenario, in which tooling cost is omitted is presented in Graph 4. As tooling incorporates a major amount of total cost per part which is amortized over the number of produced parts, cost per part of IM starts from a reasonable value of 202 € and rapidly drops well below the cost per part of AM. In this case, manufacturing up to 2 parts via AM is still economical than IM according to the number of breakeven parts of 2 pieces which is recorded for ME from SP1. In addition, 1 part can be manufactured economically via SLS of PA from SP2 and SP3 as seen from the breakeven points illustrated in Graph 4.

5.1.1.2 Lead Times by means of Production Volume

A third dimension of the previously presented cost per part with respect to production volume can be seen in the following graphs that is the lead time which is measured in business days excluding weekends and public holidays. The lead times also include 2 business days for expedited international delivery since the selected AM service providers operate globally from several locations. The behaviour of estimated lead times with respect to production volume of 500 psc and 100 psc can be seen in Graph 5 and Graph 6 respectively. The green data points representing lead time of IM are used as a reference for comparing the lead times of AM from listed service providers in Table 13. According to the source, a lot size of 100 psc to 200 psc can be produced in 3 weeks' time at the latest with the ready-made mould and in 8 weeks' time without the mould. Hence, a benchmark of 15 business days is used since the mould already exists. A line of best fit, trendline is drawn to estimate the lead time behaviour for each service provider according to the acquired data. As it can be seen from the graphs, the lead times increase linearly and polynomially.



Graph 5. An overview of lead times of Anode Hangbar with respect to production volume.



Graph 6. A closer view of Anode Hangbar lead times by means of production volume.

The trendlines for each service provider are plotted in Graph 6 in order to evaluate the breakeven points with respect to IM benchmark. As a result, a maximum production volume of approximately 51 psc can be manufactured through AM supplied by SP1 in 15 business days. Correspondingly, a minimum production volume of approximately 25 psc can be manufactured via AM according to SP2 in 15 business days. Furthermore, the highest breakeven point of 250 psc from Graph 3 would be manufactured in approximately 45 working days. The estimated lead times provided for the alternative method of ME of PLA were equal to those that are presented for SLS of PA from SP1. It should be noted that these lead times are estimations provided by the listed AM suppliers which depend on several factors such as number of pending orders, number of operational machines and the part geometry and volume leading to the ability of the part to nest in the build chamber. In addition, the presented lead times provided by SP2 are according to the 3D Systems UK capacity only and hence, these can be decreased when considering their other global locations especially in Holland, Italy and France. Finally, according to the discussions held with the listed service providers, it is fair to state that the level of expedition of lead times is quite negotiable to an extent.

5.1.2 Positioning Cone

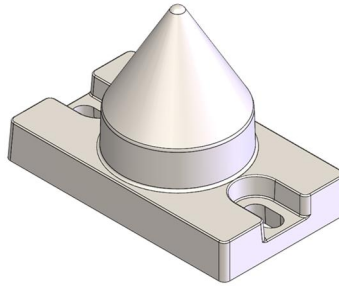


Figure 11. Injection Moulded Positioning Cone containing a bounding box of 200mm x 115mm x 141mm.

Positioning Cone is a component of Anode Cathode Crane and Grab that is used for alignment purposes. It is manufactured through injection moulding and it is composed of Polypropylene. The component undergoes shock and variable loading and it doesn't necessarily cause downtime of the equipment in case it malfunctions. A CAD model of the component can be seen in following Figure 11.

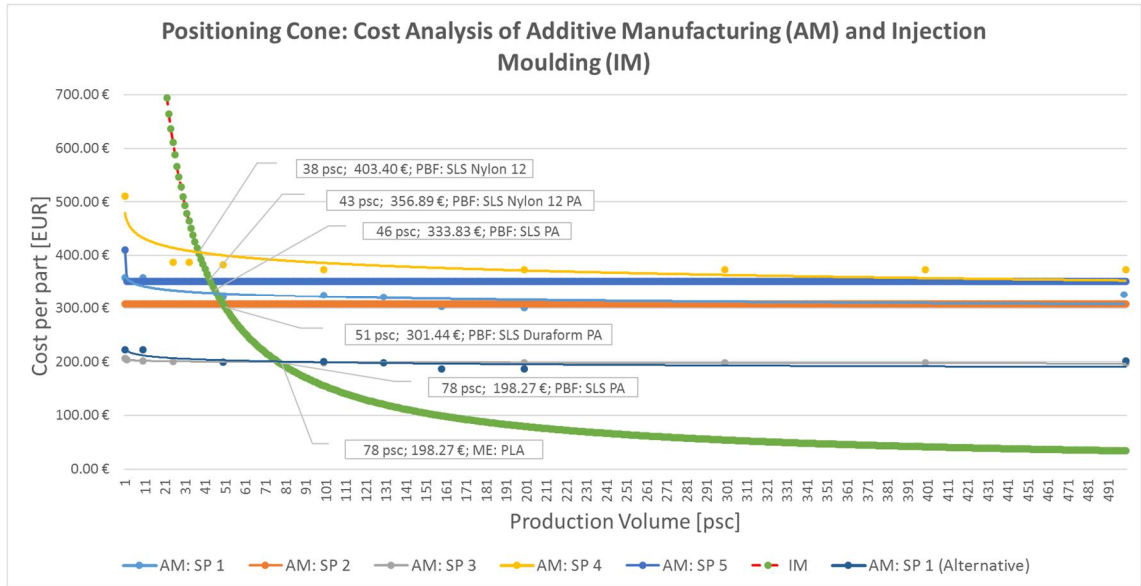
5.1.2.1 Cost per Part by means of Production Volume

In order to compliment the results of IM spare part of Anode Hangbar presented in Section 5.1.1, another cost effectiveness and lead time analysis is conducted for Positioning Cone. The behaviour of cost per part with respect to the production volume of this spare part can be seen in the following graphs. In this case, the cost per part of IM starts just above the 15000€ threshold contrary to the 20000€ presented in Graph 1, which is the cost of the mould and it decreases with an exponential decay towards a steady state value similarly to Graph 1. The cost per part including the parameters of IM presented in Table 1 is described in following Equation 4.

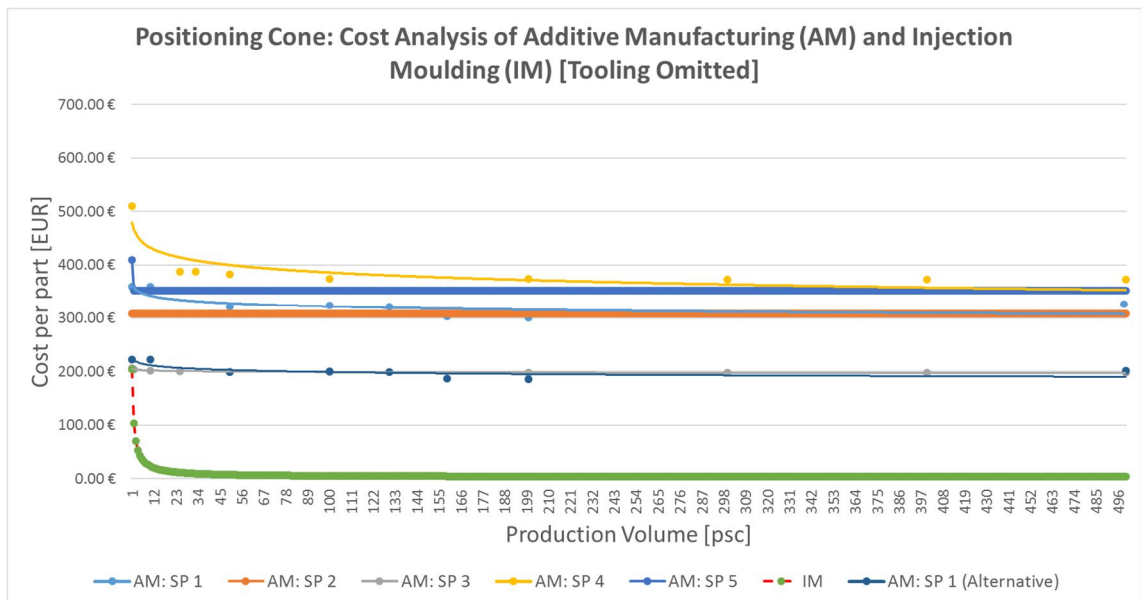
$$IM \text{ Cost per Part}(N) = \left(\frac{200€ + 3.4€(N) + 15000€}{N} \right) \quad (4)$$

Where N is number of spare parts [No.]

As seen in Graph 7, the behaviour of trends of the cost per part with respect to production volume from each service provider is quite similar to that of Anode Hangbar shown in Graph 2 however, the cost per part of this part is higher than the Anode Hangbar in all cases. This increase is caused by a larger bounding box as well as 40% higher volume of Positioning Cone. Similarly, in this case, SP3 supplies the highest number of breakeven parts however, with a value of 78 psc for this analysis, confirming the most economical manufacturing method and service provider whereas, SP4 markets the lowest breakeven point of 38 pieces, yet still economical than IM. When considering the additional alternative AM method of ME of PLA from SP1, it is observed that it consists of the same number of breakeven parts as that of PBF through SLS of PA with a value of 78 psc as seen from the same Graph 7. Similarly, this alternative method is observed to be more expensive than SLS of PA according to quotations of both methods from each service provider except SP1.



Graph 7. Breakeven cost analysis of Positioning Cone.

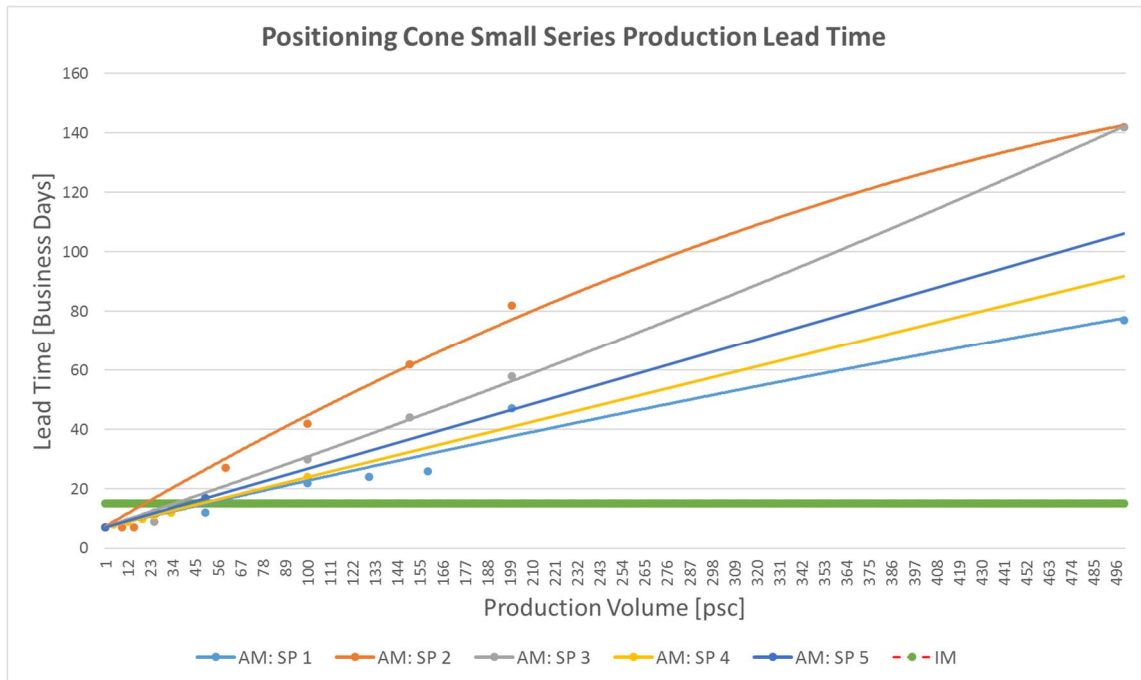


Graph 8. Breakeven cost analysis of Positioning Cone excluding cost of tooling.

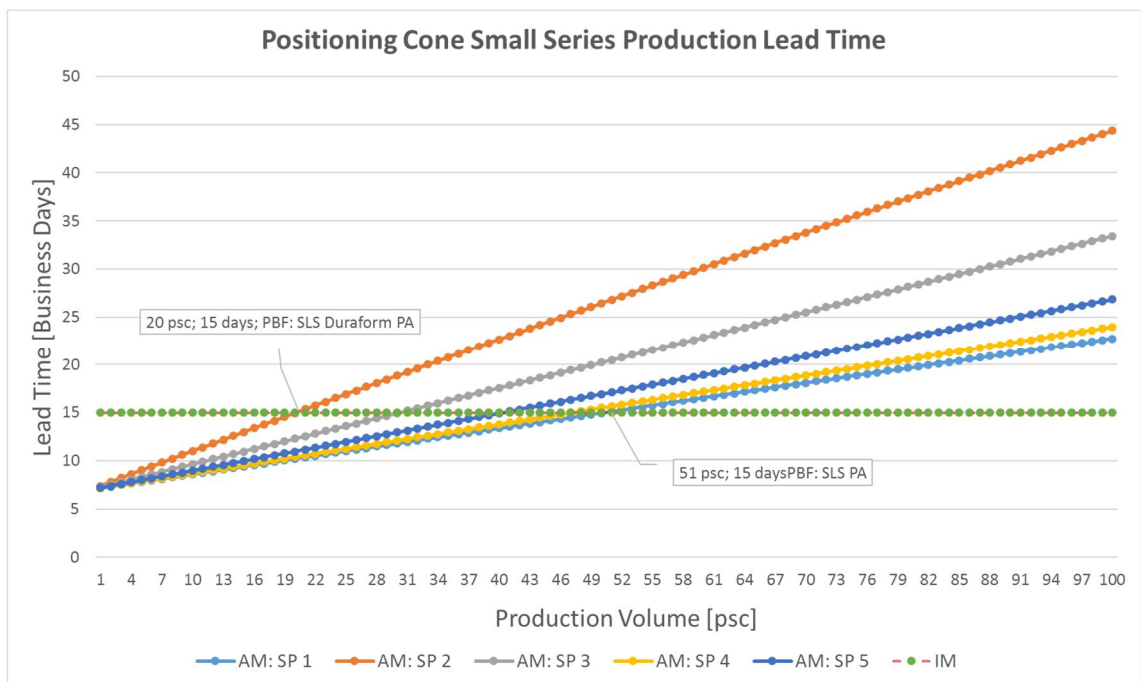
When omitting the cost of tooling, no breakeven points are observed according to Graph 8 nevertheless, the cost of 1 psc of SP3 is very close to that of the cost of 1 psc of IM with a difference of approximately 1%.

5.1.2.2 Lead Times by means of Production Volume

A lead time analysis with similar parameters of those used in Section 5.1.1.2 is conducted for this spare part as well. The behaviour of estimated lead times with respect to production volume of 500 psc and 100 psc can be seen in Graph 9 and Graph 10 respectively. According to the source, a lot size of 2 psc to 4 psc can be produced in 3 weeks times at the latest with the mould and in 20 weeks without the mould. Hence, a similar benchmark of 15 business days is used to that of Anode Hangbar due to existence of the mould. A similar trend of that presented in Anode Hangbar can be seen from these graphs. The lead times increase linearly and polynomially depending on the estimated data received from each service provider.



Graph 9. An overview of lead times of Positioning Cone with respect to production volume.



Graph 10. A closer view of Positioning Cone lead times by means of production volume.

After plotting the trendlines calculated in Graph 9 to that of Graph 10, the range of break-even points is observed. As a result, a maximum production volume of approximately 51 psc can be manufactured through AM supplied by SP1 in 15 business days. On the other hand, a minimum production volume of approximately 20 psc can be manufactured via AM according to SP2 in 15 business days. Furthermore, the highest breakeven point of 78 psc from Graph 7 would be manufactured in approximately 19 working days. The estimated lead times provided for the alternative method of ME of PLA were equal to those that are presented for SLS of PA from SP1. The same level of estimations presented in Section 5.1.1.2 are used for this analysis as well and according to the discussions held with the listed service providers, it is fair to state that the level of expedition of lead times is quite negotiable to a fair extent.

5.1.3 Summary of Injection Moulding Parts

According to the above analyses, it can be deduced that AM can be beneficial in contrast to IM for injection moulding components in terms of cost and lead time up to an extent. The following Table 14 provides a summary of this extent.

Table 14. AM summary of benefits in contrast to IM.

AM Cost Effectiveness and Lead Time Summary		
Anode Hangbar		
Benefit Scenario	Parts [psc]	
	Including IM Tooling Cost	Excluding IM Tooling Cost
Economical	Up to 250	Up to 2
Shorter Lead Time	Up to 51	Up to 51
Economical and Shorter Lead Time	Up to 51	Up to 2
Positioning Cone		
Benefit Scenario	Parts [psc]	
	Including IM Tooling Cost	Excluding IM Tooling Cost
Economical	Up to 78	0
Shorter Lead Time	Up to 51	Up to 51
Economical and Shorter Lead Time	Up to 51	0

5.2 Results of Subtractive Machining Parts

5.2.1 Turbine Blade Housing

As seen from Appendix 2, the DOP turbine consists of 5 main components that are blade, top plate, bottom plate, shaft and flange with a composition of steel. The machining process involves cutting, drilling and milling. The main joining method of these components is welding. The turbine has a direct impact on downtime of the equipment, hence lead times are of critical importance. Due to the fact that shaft is a simple round bar, it resembles a typical base material that is readily available in the market at an economical cost. The flange also consists of a basic geometry and requires the need of basic cutting, milling and drilling. In case, the flange is manufactured via AM, it would still need to be sent to a workshop for drilling purposes leading to increased lead times. The bottom and top plates can be easily cut through sheets readily available in the market. On the other hand, the blades of the turbine consist of relatively the most geometrically complex component and are milled leading to excessive tooling and material removal. This enabled the opportunity to utilize the shape complexity features of design for AM. In addition, the top and bottom plates can be manufactured in the same process as the blade leading to part consolidation and less assembly components. Since direct metal AM requires the need of support structures which are eventually removed through machining, the feasibility of this method is hindered. Subsequently, the functional environment of the component consists of liquid immersion hence, the indirect metal AM is also omitted due to the level of porosity accumulated in its parts. As a result of the aforementioned constraints and freedoms, AM rapid tooling of sand mould is selected to assist casting in order to manufacture the turbine blade housing consisting of top plate, bottom plate and the blade as seen in Figure 12. The CAD model of the AM sand mould can be seen in Table 11.

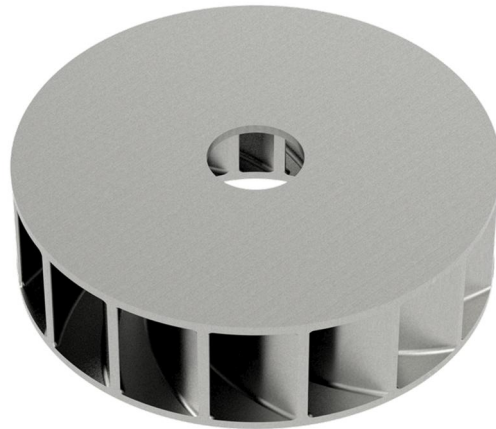
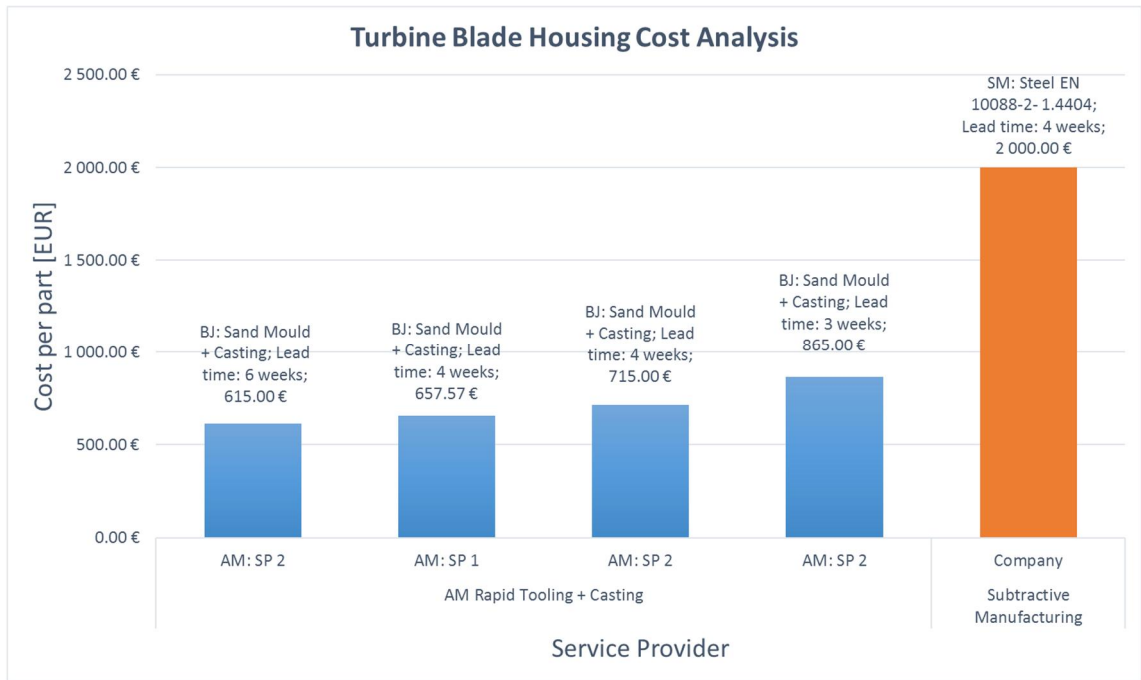


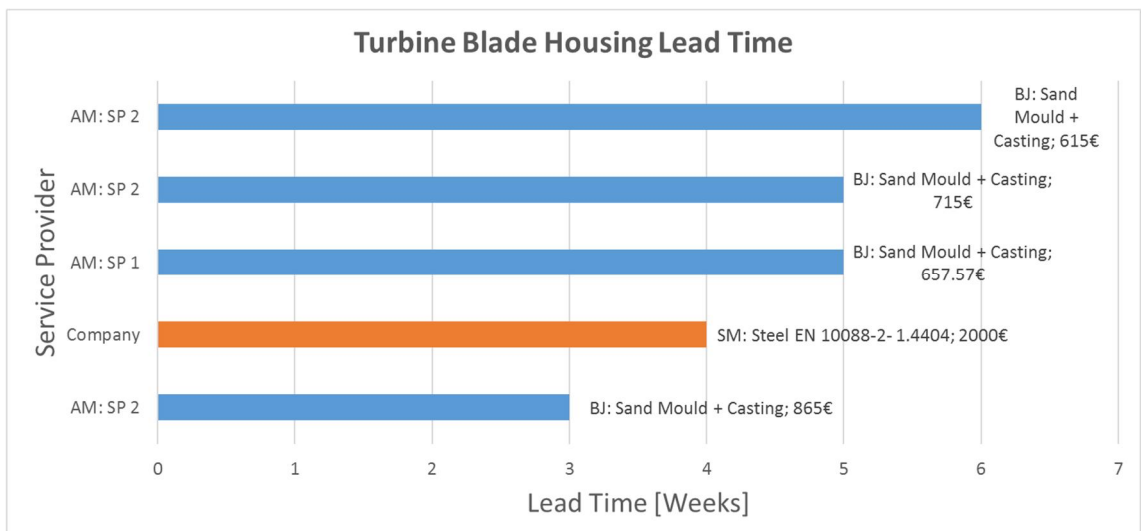
Figure 12. A render of Turbine Blade Housing with a size of 200 [mm] x 200 [mm] x 56 [mm].

5.2.1.1 Cost and Lead Time Analysis

The following graphs present the cost effectiveness and lead time analysis of this component from Karlebo which represents ExOne and Hetitec which represents Voxeljet in the Nordic region. ExOne and Voxeljet are the two main global key players when it comes to AM of sand moulds. The current cost of subtractively manufacturing the Turbine Blade Housing presented in Figure 12 and Appendix 2 including its associated lead time, are also presented in the following analyses. The cost per part of the flange, the shaft and their assembly onto Turbine Blade Housing is approximately thousand euros. Graph 11 presents the cost analysis and Graph 12 illustrates the lead time analysis. Both graphs consist of labels which include the ISO/ASTM approved method, material and lead time or cost per part depending on the graph for ease of evaluation. SP2 has provided three quotations in which the cost per part of the sand mould increases which shorter lead times as seen in Graph 11 or Graph 12. Comparatively, only one quotation was received from SP1 which economically supersedes the one from SP2 with the same lead time. In order to approximate the total cost of AM assisted casting and its associated lead time, a quotation was received from a casting foundry leading to a value of 365€ with a lead time of 2 weeks. This value included a setup cost of 200€ which can be combined for producing other components as well leading to multiple castings within the same setup cost.



Graph 11. Turbine blade housing cost analysis.



Graph 12. Turbine blade housing lead time analysis.

5.2.1.2 Summary

According to the above analyses, it can be deduced that AM can be beneficial in contrast to SM for this component in terms of cost and lead time up to an extent. The following Table 15 provides a summary of this extent.

Table 15. Turbine Blade Housing AM summary of benefits in contrast to Subtractive Manufacturing.

Turbine Blade Housing: AM Cost Effectiveness and Lead Time Summary		
Benefit Scenario	Validity [Yes/No]	Description
Economical	Yes	Considering cost per part of AM rapid tooling of 250€ from SP 2 and cost per part of 365€ for casting totals to approximately 615€ with a lead time of approximately 6 weeks.
Shorter Lead Time	Yes	Considering the lead time per part of 1 week for AM rapid tooling from SP 2 and the lead time of 2 weeks for casting totals to approximately 3 weeks with a cost of approximately 865€.
Economical and Shorter Lead Time	Yes	Considering cost per part of AM rapid tooling of 500€ from SP 2 and cost per part of 365€ for casting totals to approximately 865€ with a lead time of approximately 3 weeks.

5.2.2 Upper Shank



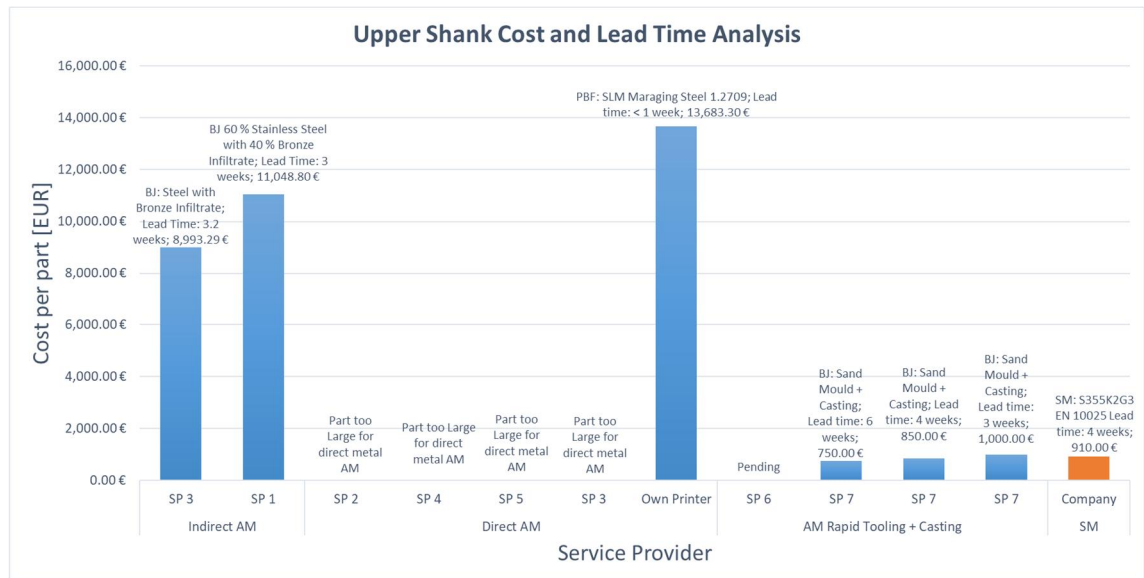
Figure 13. A CAD model of Upper Shank (Left) and its sand mould (Right) containing a bounding box of 455mm x 125mm x 77mm and 566.4mm x 316.1mm x 263.5mm, respectively.

As described in Appendix 2, Upper Shank is part of a lifter assembly and it involves several machining processes such as flame cutting, milling, drilling, broaching and grinding in order to be manufactured through stainless steel. A CAD of the model can be seen in Figure 13. The component has a direct impact on the downtime of the lifter equipment hence, its lead time is of dire importance. Due to the relatively long length of the part and geometric features, its cost effectiveness and lead times are analysed for AM rapid tooling to assist casting as well on top of the analysis for direct and indirect AM. Consequently, the sand mould of the component is modelled and it's presented in Table 11.

5.2.2.1 Cost and Lead Time Analysis

The following Graph 13 illustrates the cost per part of the component with respect to indirect AM, direct AM and AM rapid tooling. The lead times of the part are also labelled according to the material, method and service provider under consideration. The cost per part of the current SM is also presented for comparison. As expected, the cost per part of the direct and indirect AM are steeply high however, the lead times of these methods are incredibly fast. In general, as the lead time decreases, the cost per part increases. In case of direct AM through own printer, the cost per part is approximately 13700€ with a lead time of less than one week. The geometrical dimensions of the component are too large

for direct metal AM according to 4 service providers as shown in Graph 13. On the other hand, the cost per part of AM rapid tooling of sand mould are quite reasonable. Three quotations from SP 2 exhibit the similar phenomena where the cost per part of the sand mould is increased with faster lead times. The cost of casting the component is approximated to couple of hundred euros with a lead time of approximately 2 weeks which has been added to the presented values. In addition, the cost of finishing process such as drilling or surface treatment of the part is approximated to hundred euros which has been also added on top of the existing values.



Graph 13. Cost and lead time analysis of Upper Shank.

5.2.2.2 Conclusion

According to the above analyses, it can be deduced that AM can be beneficial in contrast to SM for this component in terms of cost and lead time up to an extent. The following Table 16 provides a summary of this extent.

Table 16. Upper Shank AM summary of benefits in contrast to Subtractive Manufacturing.

Upper Shank: AM Cost Effectiveness and Lead Time Summary		
Benefit Scenario	Validity [Yes/No]	Description
Economical	Yes	Considering cost per part of AM rapid tooling of 300€ from SP 7 and cost per part of couple of hundred euros for casting and finishing processes totals to approximately 700-800€ with a lead time of approximately 6-8 weeks.
	No	The cost per part of direct metal AM and indirect metal AM exceeds those of the SM method currently under operation.
Shorter Lead Time	Yes	Considering the lead time per part of less than 1 week for direct AM and finishing processes with a cost of approximately 14000€. Considering lead time per part of 1 week for AM rapid tooling of sand mould and 2 weeks of casting and finishing totalling to approximately 3 weeks.
Economical and Shorter Lead Time	No	The lead time of economical AM assisted casting exceeds that of the current subtractive manufacturing method. The cost per part of shorter lead times exceeds that of the current subtractive manufacturing method.

5.2.3 Chain Wheel

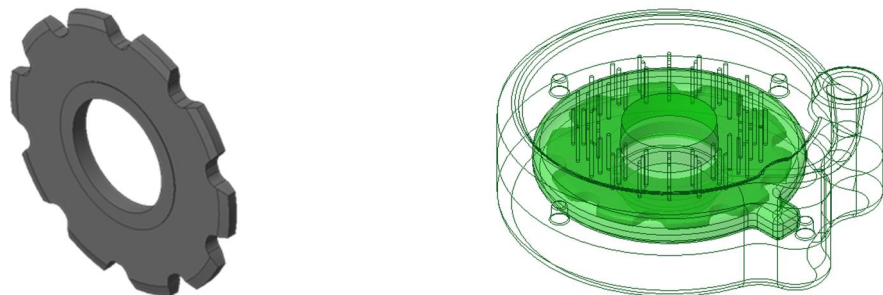
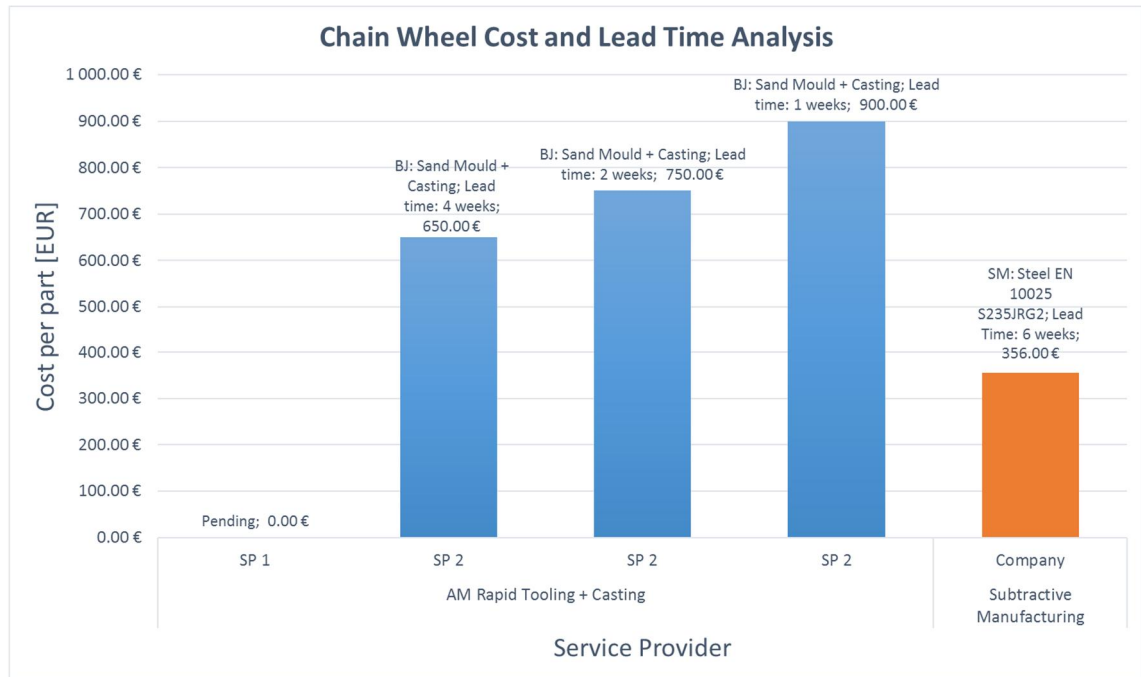


Figure 14. A CAD model of Chainwheel (Left) and its sand mould (Right) containing a bounding box of 345mm x 345mm x 20mm and 483.5mm x 541.8mm x 200.0mm, respectively.

As described in Appendix 2, Chainwheel represents a chain sprocket mechanism such as lift transfer device or a conveyor system. The material of the component is stainless steel. A CAD of the part can be seen in Figure 14. The component experiences static as well as shock loads and it has a direct impact on the downtime of the equipment in case it malfunctions. Hence, lead time is of crucial importance. Due to the large size of the component, AM rapid tooling is taken into consideration for manufacturing. The sand mould of the part is shown in Figure 14. The cost of manufacturing this component via direct and/or indirect AM would be in thousands of euros indeed, very expensive compared to the current SM method.

5.2.3.1 Cost and Lead Time Analysis

The following Graph 14 illustrates the costs, lead times and the ISO/ASTM approved AM method in comparison to the current subtractive manufacturing method. Three quotations of AM sand mould from SP 2 exhibit the similar phenomena where the cost per part of the sand mould is increased with faster lead times. The cost of casting and finishing is approximated to couple of hundred euros with a lead time of approximately 2 weeks.



Graph 14. Cost and Lead Time Analysis of Chainwheel.

5.2.3.2 Conclusion

According to the above analyses, it can be deduced that AM may be beneficial in contrast to SM for this component in terms of cost and lead time to an extent. The following Table 17 provides a summary of this analysis.

Table 17. Chainwheel AM summary of benefits in contrast to Subtractive Manufacturing.

Chainwheel: AM Cost Effectiveness and Lead Time Summary		
Benefit Scenario	Validity [Yes/No]	Description
Economical	No	Considering cost per part of AM rapid tooling of 250€ from SP 2 and cost per part of couple of hundred euros for casting and finishing processes totals to approximately 550-750€ with a lead time of approximately 6-8 weeks.
Shorter Lead Time	Yes	Considering the lead time per part of 1 week for AM rapid tooling from SP 2 and the lead time of 2 weeks for casting and finishing processes totals to approximately 3 weeks with a cost of approximately 800-900€.
Economical and Shorter Lead Time	No	The cost per part of shorter lead times exceeds that of the current SM method.

5.2.4 Cutting Blade



Figure 15. A CAD model of Cutting Blade containing a bounding box of 183mm x 183mm x 16mm.

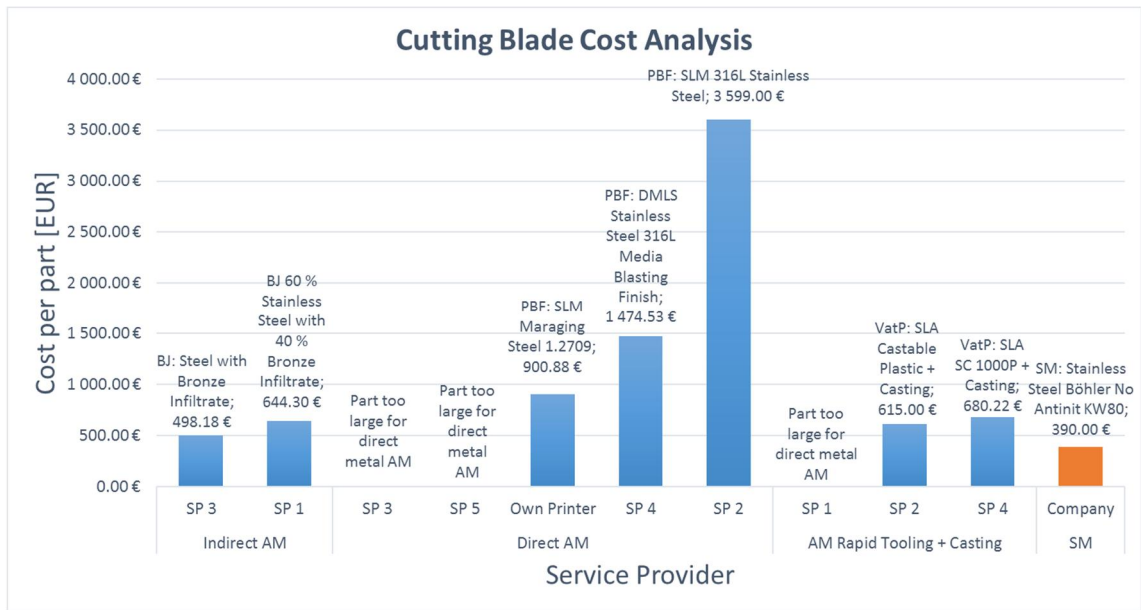
Cutting blade is a component of lug strip cutting machine as described in Appendix 2. Its purpose is to cut sheets of metal. A CAD model of the component can be seen in Figure 15. The manufacturing method of the component involves cutting, facing, grinding and surface hardening. The component undergoes variable and shock loads and it has a direct impact on the downtime of the equipment in case it is damaged. Hence, shorter lead time is of critical importance. The component is analysed for indirect AM, direct AM and AM rapid tooling.

5.2.4.1 Cost and Lead Time Analysis

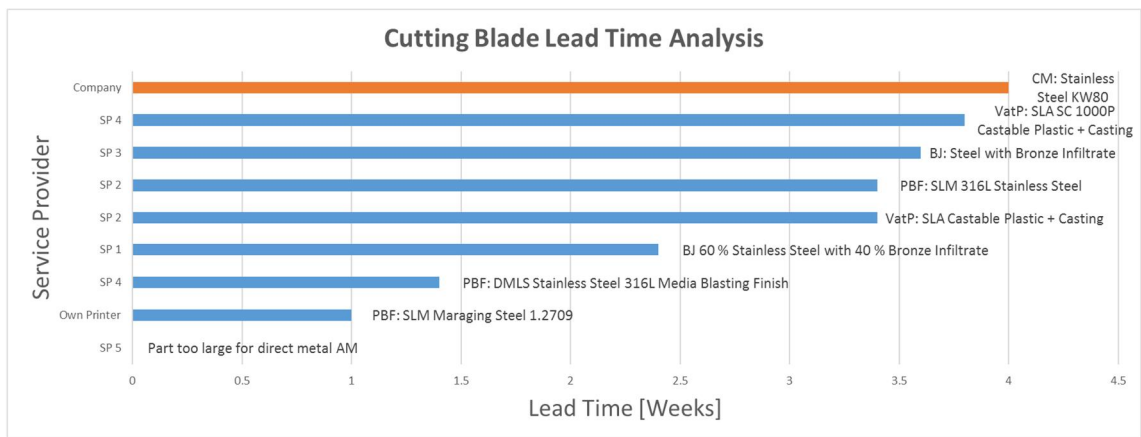
The following Graph 15 presents the costs per part of the Cutting Blade with respect to each service provider and with respect to the category of AM in terms of direct, indirect and rapid tooling. The bars of the graph are also labelled with the type of AM method, material as well as the exact value of the cost per part. The current cost per part of SM is also presented in contrast. Likewise, Graph 16 illustrates the lead times associated with each of the cost per part presented in the Graph 15 according to the service provider and the AM method.

According to the results of the analyses, the lead time can be decreased up to 1 week which is approximately 75% faster in case of additively manufacturing the part with own printer at the cost per part of approximately twice as much compared to the current SM

process. When considering the service provider for direct metal AM, the lead time can be approximately 65% faster according to SP4 at the cost per part of approximately 4 times as much as the current SM process. In case of indirect metal AM, the lead time can be approximately 40% faster according to SP1 at the cost per part of approximately 22% higher than that of the current SM process. The cost per part of AM rapid tooling of investment casting patterns is quite lower than that of the current SM process, however, when the cost of casting is added on top of these values, it exceeds the cost per part of the current subtractive manufacturing.



Graph 15. Cost analysis of Cutting Blade.



Graph 16. Lead analysis of Cutting Blade.

5.2.4.2 Conclusion

According to the above analyses, it can be deduced that AM may be beneficial in contrast to SM for this component in terms of cost and lead time to an extent. The following Table 18 provides a summary of this extent.

Table 18. Cutting Blade AM summary of benefits in contrast to Subtractive Manufacturing.

Cutting Blade: AM Cost Effectiveness and Lead Time Summary		
Benefit Scenario	Validity [Yes/No]	Description
Economical	No	Considering cost per part of AM rapid tooling of 165€ from SP2 and cost per part of couple of hundred euros for casting and finishing processes totals to approximately 565-665€ with a lead time of approximately 3-4 weeks.
Shorter Lead Time	Yes	Considering the lead time per part of 1 week for direct metal AM in case of own printer, the lead time per part of 1.4 week for direct metal AM from SP4 and the lead time per part of 2.4 weeks for indirect metal AM from SP1.
Economical and Shorter Lead Time	No	The cost per part of shorter lead times exceeds that of the current SM method.

5.2.5 Guide Frame

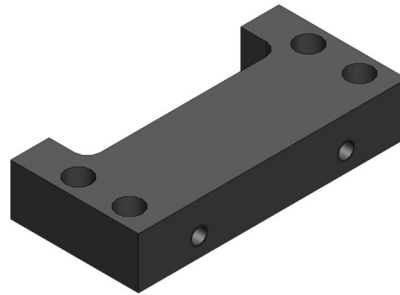


Figure 16. A CAD model of Guide Frame containing a bounding box of 210mm x 100mm x 40mm.

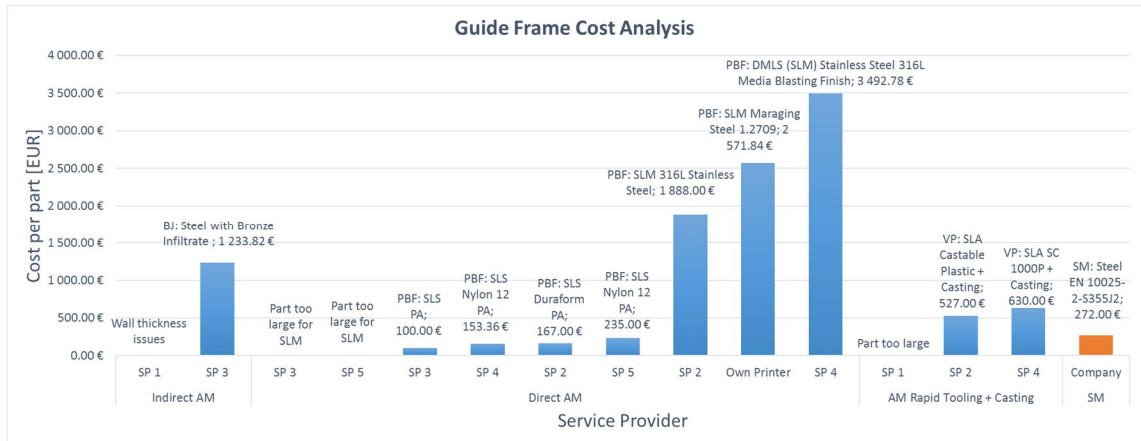
As described in Appendix 2, Guide Frame is component of Bale assembly. Its purpose is to support a moving polymer shaft. The component is manufactured out of stainless steel and the process involves flame cutting, milling and drilling. Since it doesn't affect the downtime of the equipment, the lead time is not as crucial. The part experiences mild static loading hence, it may be produced with a polymer. In addition, due to its reasonable size of geometric dimensions, the component is analysed for direct AM, indirect AM and AM rapid tooling. A CAD model of the component is shown in Figure 16.

5.2.5.1 Cost and Lead Time Analysis

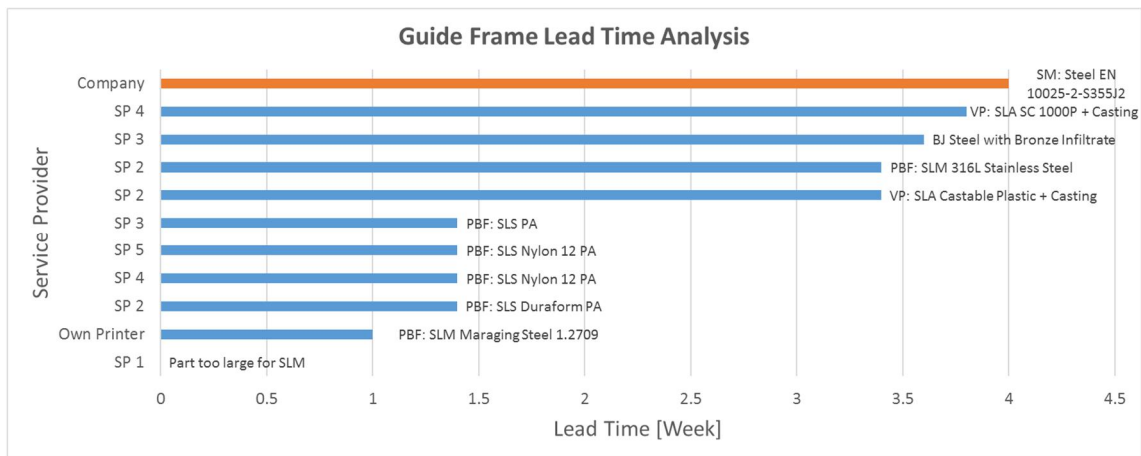
The following Graph 17 presents the costs per part of the Guide Frame with respect to each service provider and with respect to the category of AM in terms of direct, indirect and rapid tooling. The bars of the graph are also labelled with the type of AM method, material as well as the exact value of the cost per part. The current cost per part of SM is also presented in contrast. Likewise, Graph 18 illustrates the lead times associated with each of the cost per part presented in the Graph 17 according to the service provider and the AM method.

According to the results presented in the graphs, it can be deduced that if the part is made from PA polymer directly via AM, it can be up to 63% cheaper than the current price of

SM at a 65% faster lead time. In addition, the cost per part of direct metal AM is very high at the benefit of shortest lead time of approximately one week if manufactured by own printer. It is also observed that the geometric elements of the part do not fulfil the AM manufacturing criteria according to some service providers for certain AM methods. AM assisted casting represents the costs per part of the investment casting pattern and casting. The cost of casting and finishing is approximated to couple of hundred euros with a lead time of approximately 2 weeks.



Graph 17. Cost analysis of Guide Frame.



Graph 18. Lead time analysis of Guide Frame.

5.2.5.2 Conclusion

According to the above analyses, it can be deduced that AM can be beneficial in contrast to SM for this component in terms of cost and lead time to an extent. The following Table 19 provides a summary of this analysis.

Table 19. Guide Frame AM summary of benefits in contrast to Subtractive Manufacturing.

Guide Frame: AM Cost Effectiveness and Lead Time Summary		
Benefit Scenario	Validity [Yes/No]	Description
Economical	Yes	Considering the cost per part of 100.00€ for direct polymer AM from SP3 with a lead time of approximately 1.4 weeks.
	No	Considering the cost per part of AM rapid tooling of investment casting pattern of 177.00€ and cost per part of casting and finishing of couple of hundred euros totals to approximately 477-577€ with approximately 3.4 weeks. In addition, the cost per part of metal AM is very high.
Shorter Lead Time	Yes	Considering the lead time per part of 1 week for direct metal AM in case of own printer, the lead time per part of 1.4 week for direct polymer AM from SP3 and the lead time per part of 3.6 weeks for indirect metal AM from SP3.
Economical and Shorter Lead Time	Yes	Considering the cost per part of 100.00€ for direct polymer AM from SP3 with a lead time of approximately 1.4 weeks.

5.2.6 Roll Support

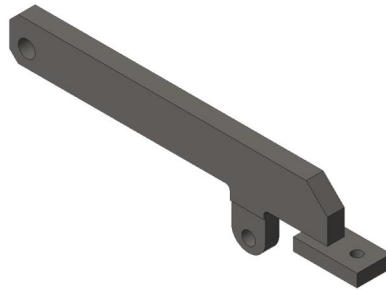


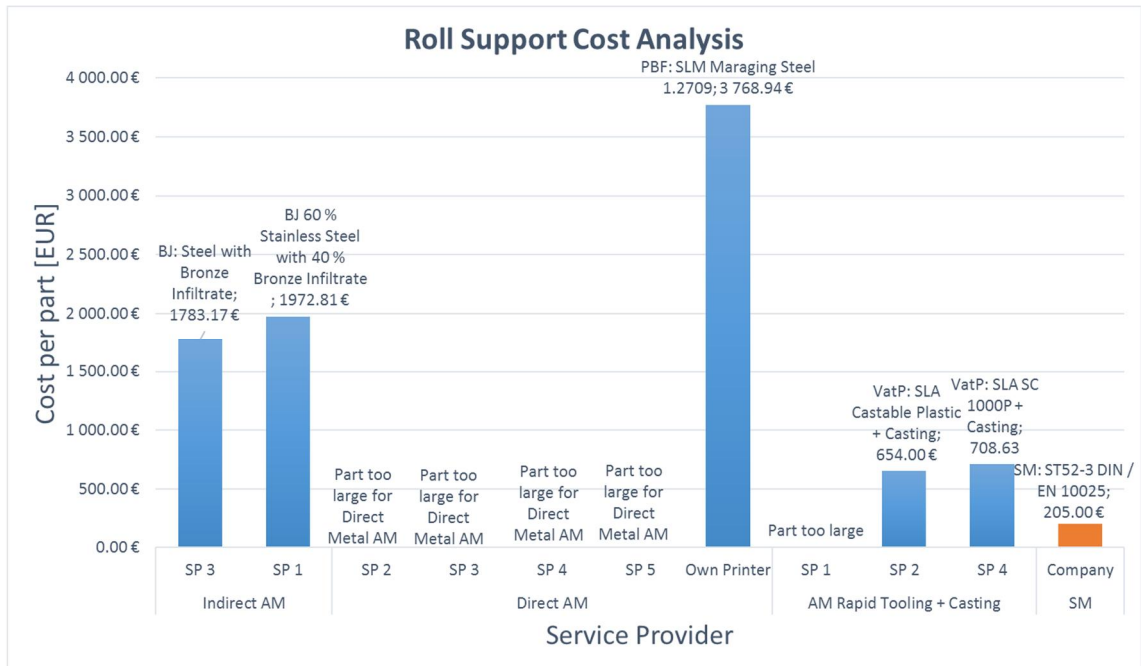
Figure 17. A CAD model of Roll Support containing a bounding box of 420mm x 110mm x 40mm.

As explained in Appendix 2, Roll Support is a component of Anode Holder and it's made of stainless steel. Its current manufacturing methods involve flame cutting, welding, drilling and milling. A CAD model of the component can be seen in Figure 17. The component does impact downtime however, it can be repaired on site through welding in few days depending on the severity of damage. In addition, being a roll support, it does experience shock loading. Even though the component has a relatively long geometric length, the component is analysed for manufacturing through direct AM and indirect AM in addition to AM rapid tooling to produce a metallic part.

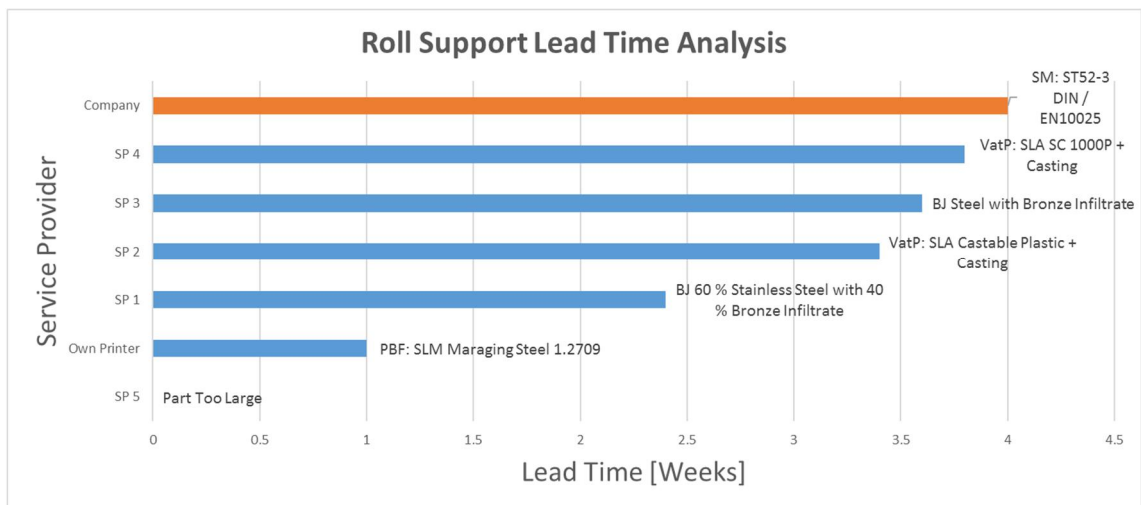
5.2.6.1 Cost and Lead Time Analysis

Graph 19 and Graph 20 present the cost analysis and lead time analysis of Roll Support, respectively. As expected, the geometric length of the part is too large for direct metal AM as per four service providers however, the cost per part is calculated for this method via own printer leading to shortest possible lead time of one week with the highest cost

per part compared to other methods. The indirect metal AM from SP1 and SP3 also provides faster lead times at the cost of expensive parts. In addition, it is observed that the investment casting patterns for AM assisted casting cost more than the cost per part of the current SM method.



Graph 19. Cost analysis of Roll Support.



Graph 20. Lead time analysis of Roll Support.

5.2.6.2 Conclusion

According to the above analyses, it can be deduced that AM may be beneficial in contrast to SM for this component in terms of cost and lead time to an extent. The following Table 20 provides a summary of this analysis.

Table 20. Roll Support AM summary of benefits in contrast to Subtractive Manufacturing.

Roll Support: AM Cost Effectiveness and Lead Time Summary		
Benefit Scenario	Validity [Yes/No]	Description
Economical	No	The cost per part of direct AM, indirect AM and AM rapid tooling exceeds those of the SM method currently under operation.
Shorter Lead Time	Yes	Considering the lead time per part of 1 week of direct metal AM in case of own printer and the lead time per part of 2.4 week for indirect metal AM from SP1. Considering the lead time per part of AM rapid tooling of 1.4 weeks from SP2 and lead time of 2 weeks for casting and finishing processes totals to approximately 3.4 weeks.
Economical and Shorter Lead Time	No	The cost per part of direct AM, indirect AM and AM rapid tooling exceeds those of the SM method currently under operation.

5.2.7 Sliding Bush

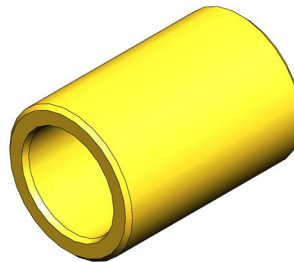
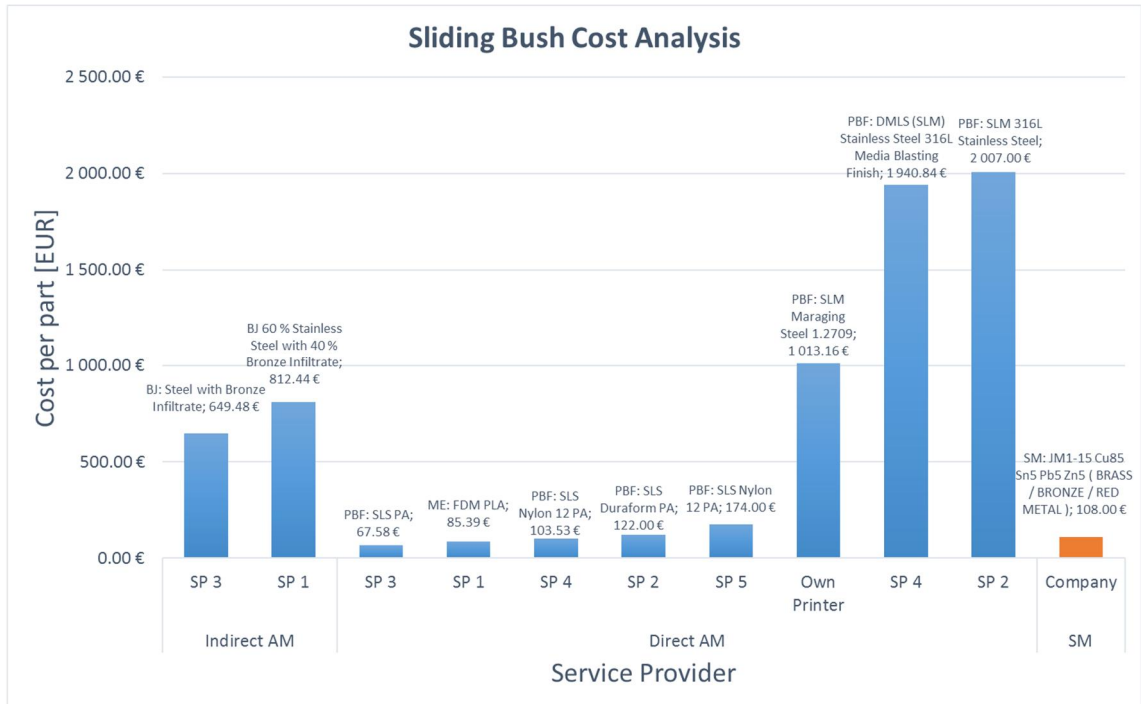


Figure 18. A CAD model of Sliding Bush containing a bounding box of 70mm x 70mm x 100mm.

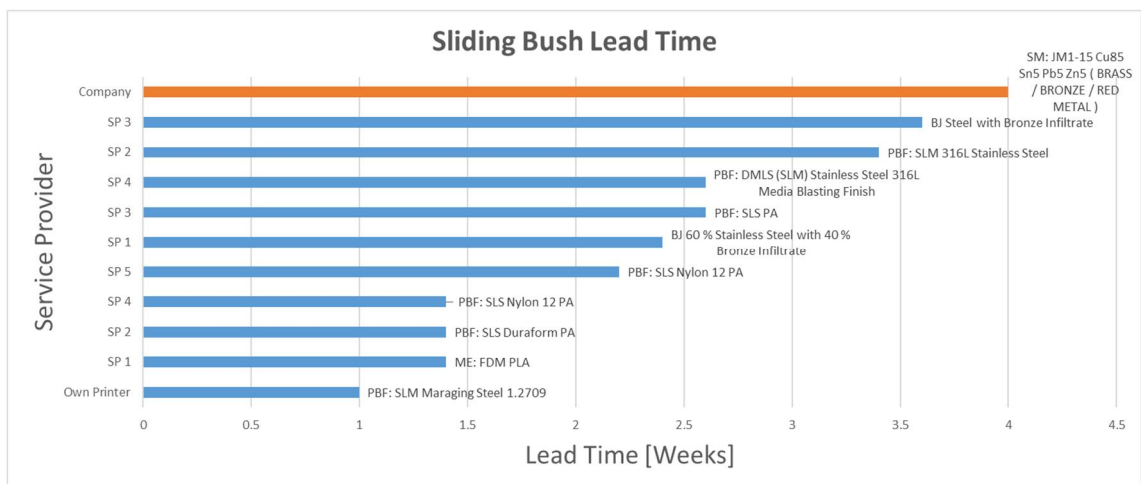
As described in Appendix 2, the Sliding Bush is a component of the Bale assembly. It is composed of either brass or bronze. Its manufacturing methods involve casting and milling. A CAD model of the component can be seen in Figure 18. It experiences variable loading with relatively low stresses and it doesn't impact downtime of the equipment. Hence, an engineering approach is considered by analysing the direct polymer AM in addition to the direct and indirect metal AM.

5.2.7.1 Cost and Lead Time Analysis

Graph 21 and Graph 22 represent the cost analysis and lead time analysis of Sliding Bush, respectively. The cost analysis describes the cost per part from the listed service providers with respect to direct AM, indirect AM and SM. The data is also labelled by means of ISO/ASTM standardised AM method, its variant, material and the value of the cost per part. Lead time analysis is presented from highest to lowest. As seen from Graph 22, all AM lead times are faster than the SM lead time. According to the results of Graph 21, the cost per part of direct AM via PBF of SLS using PA from SP3 can be up to approximately 37% cheaper than that of the current SM with a 35% faster lead time. The cost of metal AM remains high at the benefit of shorter lead times. The shortest lead time of 1 week can be achieved when considering manufacturing by own printer at the expense of approximately 10 times higher cost per part compared to the current SM method.



Graph 21. Cost analysis of Sliding Bush.



Graph 22. Lead time analysis of Sliding Bush.

5.2.7.2 Conclusion

According to the above analyses, it can be deduced that AM may be beneficial in contrast to SM for this component in terms of cost and lead time to an extent. The following Table 21 provides a summary of this analysis.

Table 21. Guide Frame AM summary of benefits in contrast to Subtractive Manufacturing.

Guide Frame: AM Cost Effectiveness and Lead Time Summary		
Benefit Scenario	Validity [Yes/No]	Description
Economical	Yes	Considering the cost per part of 67.58 € for direct polymer AM from SP3 with a lead time of approximately 2.6 weeks.
	No	Considering the cost per part of direct and indirect metal AM of 1013.16 € via own printer and 649.48 € via SP3 with a lead time of 1 week and 3.6 weeks, respectively.
Shorter Lead Time	Yes	Considering the lead time per part of 1 week of direct metal AM in case of own printer, the lead time per part of 2.4 weeks of indirect metal AM from SP1 and the lead time per part of 1.4 weeks of direct polymer AM from SP1/SP2/SP4.
Economical and Shorter Lead Time	Yes	Considering the cost per part of 67.58 € for direct polymer AM from SP3 with a lead time of approximately 2.6 weeks.

5.2.8 Rail Fastener

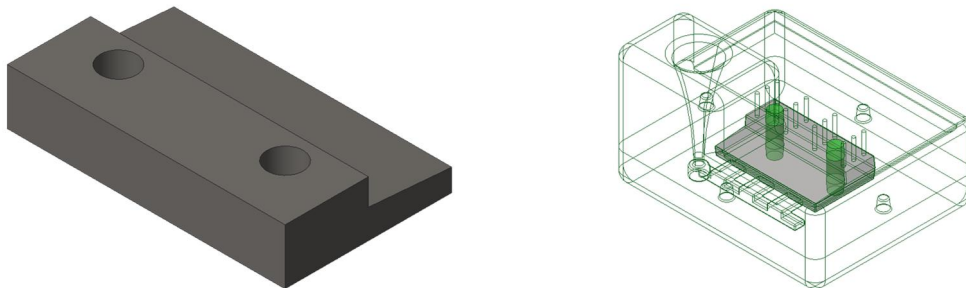


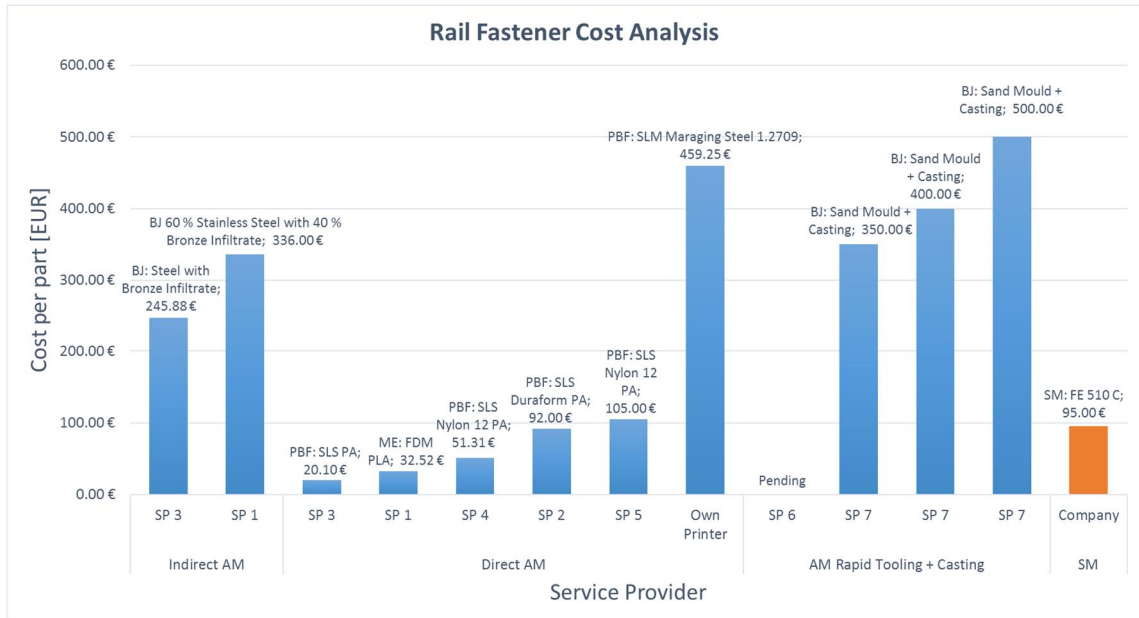
Figure 19. A CAD model of Rail Fastener (Left) and its sand mould (Right) containing a bounding box of 100mm x 60mm x 20mm and 160.0mm x 117.0mm x 200.0mm, respectively.

As explained in Appendix 2, Rail Fastener is part of an Anode Storage Beam. The part consists of iron and its manufacturing processes involve flame cutting, milling and drilling. A CAD model of the component can be seen in Figure 19. It undergoes static loading and it doesn't affect downtime of the equipment. In order to compete with the current SM method, this component is analysed with respect to direct AM, indirect AM and AM rapid tooling. In case of direct AM, metal and polymer are considered. However, due to the high levels of stresses involved in loading and boundary conditions of this part, only metal is recommended. An isometric view of the CAD model of the sand mould of this component can be seen in Figure 19.

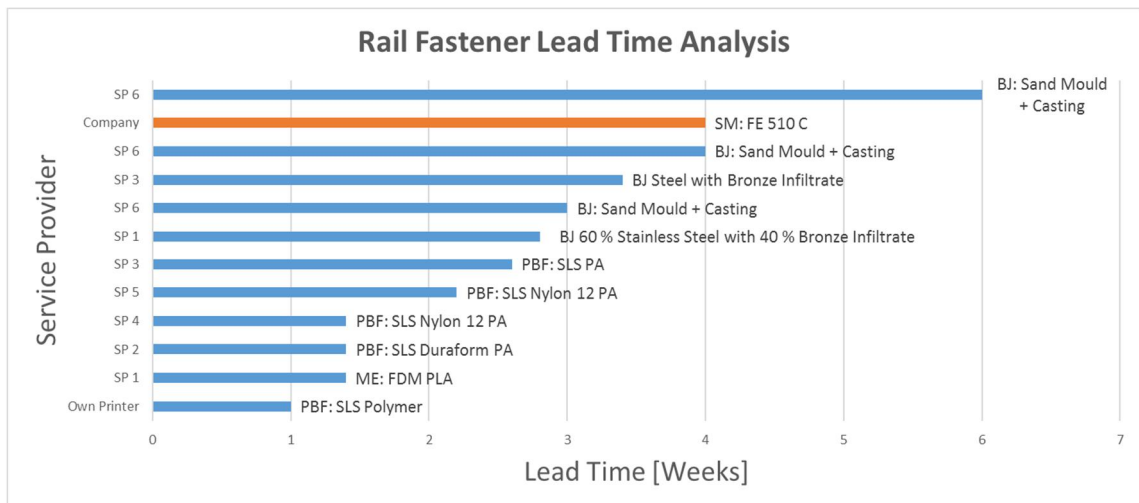
5.2.8.1 Cost and Lead Time Analysis

The following Graph 23 and Graph 24 represent the cost analysis and lead time analysis of Rail Fastener, respectively. The data is labelled by means of ISO/ASTM standardised AM method, its variant, material and the value of the cost per part. The cost per part for each category of AM is presented from lowest to highest and the lead time analysis is presented from lowest to highest. As seen from the cost and lead time analysis, the cost

per part of direct and indirect metal AM is quite high in contrast to the current SM method at the benefit of faster lead times. In addition, when considering the cost of casting and finishing processes over the cost of AM rapid tooling, the cost per part grows beyond that of SM however, at the benefit of shorter lead time. In case, the component is to be made of polymer, the cost per part can be decreased up to approximately 79% that of the SM of metal with approximately 50% faster lead time.



Graph 23. Cost analysis of Rail Fastener.



Graph 24. Lead time analysis of Rail Fastener.

5.2.8.2 Conclusion

According to the above analyses, it can be deduced that AM may be beneficial in contrast to SM for this component in terms of cost and lead time to an extent. The following Table 22 provides a summary of this extent.

Table 22. Rail Fastener AM summary of benefits in contrast to Subtractive Manufacturing.

Rail Fastener: AM Cost Effectiveness and Lead Time Summary		
Benefit Scenario	Validity [Yes/No]	Description
Economical	Yes	Considering the cost per part of 20.10 € for direct polymer AM from SP3 with a lead time of approximately 2.6 weeks.
	No	Considering the cost per part of direct and indirect metal AM of 459.25 € via own printer and 245.88 € via SP3 with a lead time of 1 week and 3.4 weeks, respectively. In addition, the cost per part of AM rapid tooling exceeds that of SM process.
Shorter Lead Time	Yes	Considering the lead time per part of 1 week of direct metal AM in case of own printer, the lead time per part of 2.8 weeks of indirect metal AM from SP1 and the lead time per part of 1.4 weeks of direct polymer AM from SP1/SP2/SP4. In addition, considering the lead time of 1 week for AM rapid tooling of sand mould and the lead time of 2 weeks for casting and finishing processes totals to approximately 3 weeks.
Economical and Shorter Lead Time	Yes	Considering the cost per part of 20.10 € for direct polymer AM from SP3 with a lead time of approximately 2.6 weeks.

5.2.9 Fork Bar

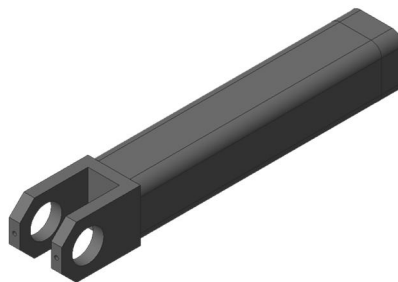


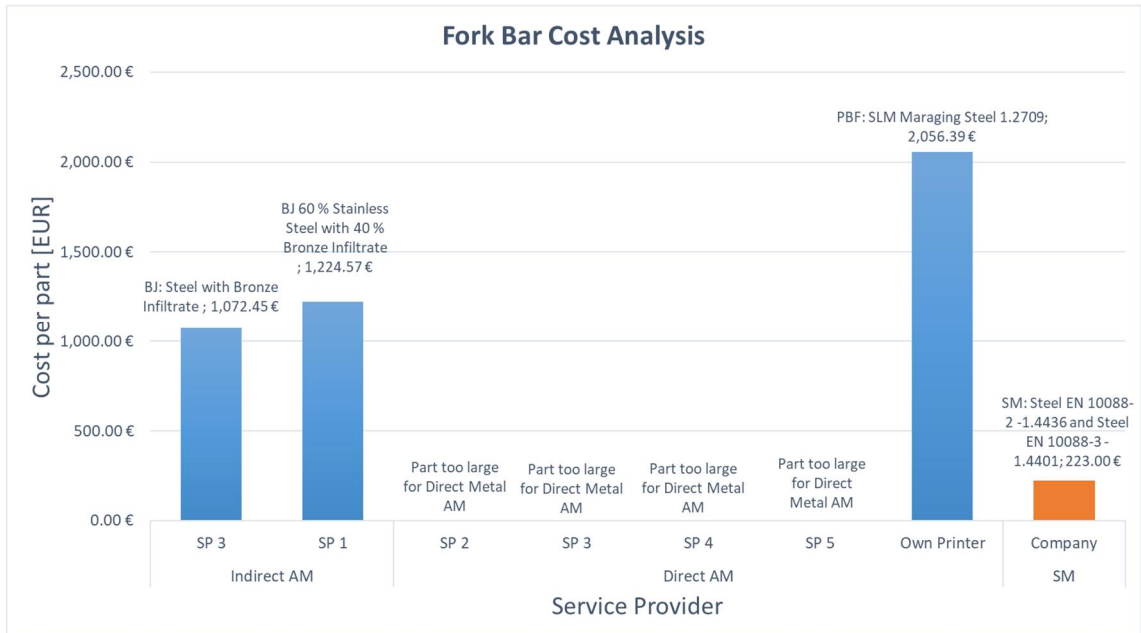
Figure 20. A CAD model of Fork Bar containing a bounding box of 50mm x 50mm x 325mm.

As described in Appendix 2, Fork Bar is a component of aligning comb assembly. Fork Bar consists of three parts that are hollow section, steel plate and a square bar which are composed of stainless steel. Its manufacturing processes involve flame cutting, cutting, milling, facing, drilling, and welding. A CAD model of the component can be seen in Figure 20. It doesn't affect the downtime of the equipment and it's loaded under variable loading. The current SM of the component is analysed against direct and indirect metal AM.

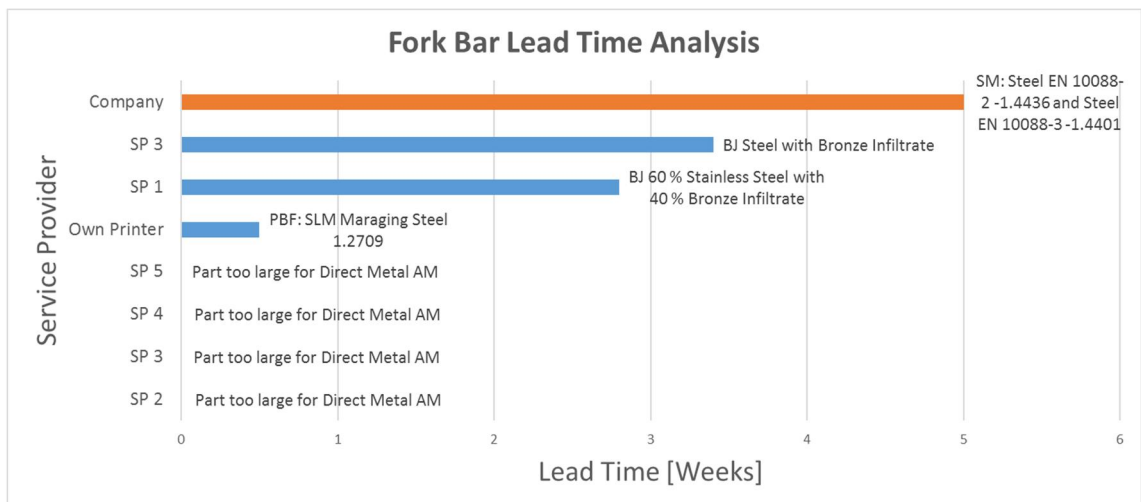
5.2.9.1 Cost and Lead Time Analysis

The following Graph 25 and Graph 26 represent the cost analysis and lead time analysis of Fork Bar, respectively. The data is labelled by means of ISO/ASTM standardised AM

method, its variant and material. The value of the cost per part is also identified in case of the cost analysis. The cost per part for each category of AM is presented from lowest to highest and the lead time is also presented from lowest to highest in the lead time analysis. As seen from the cost and lead time analysis, the cost per part of direct and indirect metal AM is quite high in contrast to the current SM method at the benefit of faster lead times. In addition, the geometrical length of the part is too long to be manufactured via direct metal AM according to 4 service providers.



Graph 25. Cost analysis of Fork Bar.



Graph 26. Lead time analysis of Fork Bar.

5.2.9.2 Conclusion

According to the above analyses, it can be deduced that AM may be beneficial in contrast to SM for this component in terms of cost and lead time to an extent. The following Table 23 provides a summary of this extent.

Table 23. Fork Bar AM summary of benefits in contrast to Subtractive Manufacturing.

Fork Bar: AM Cost Effectiveness and Lead Time Summary		
Benefit Scenario	Validity [Yes/No]	Description
Economical	No	The cost per part of direct AM and indirect metal AM exceeds those of the SM method currently under operation.
Shorter Lead Time	Yes	Considering the lead time per part of 1 week of direct metal AM in case of own printer and the lead time per part of 2.8 week for indirect metal AM from SP1.
Economical and Shorter Lead Time	No	The cost per part of direct AM and indirect AM exceeds those of the SM method currently under operation.

5.2.10 Stopper Flange Assembly

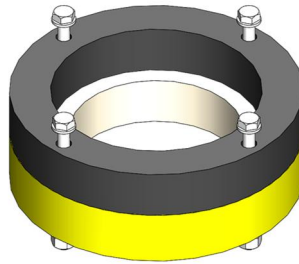
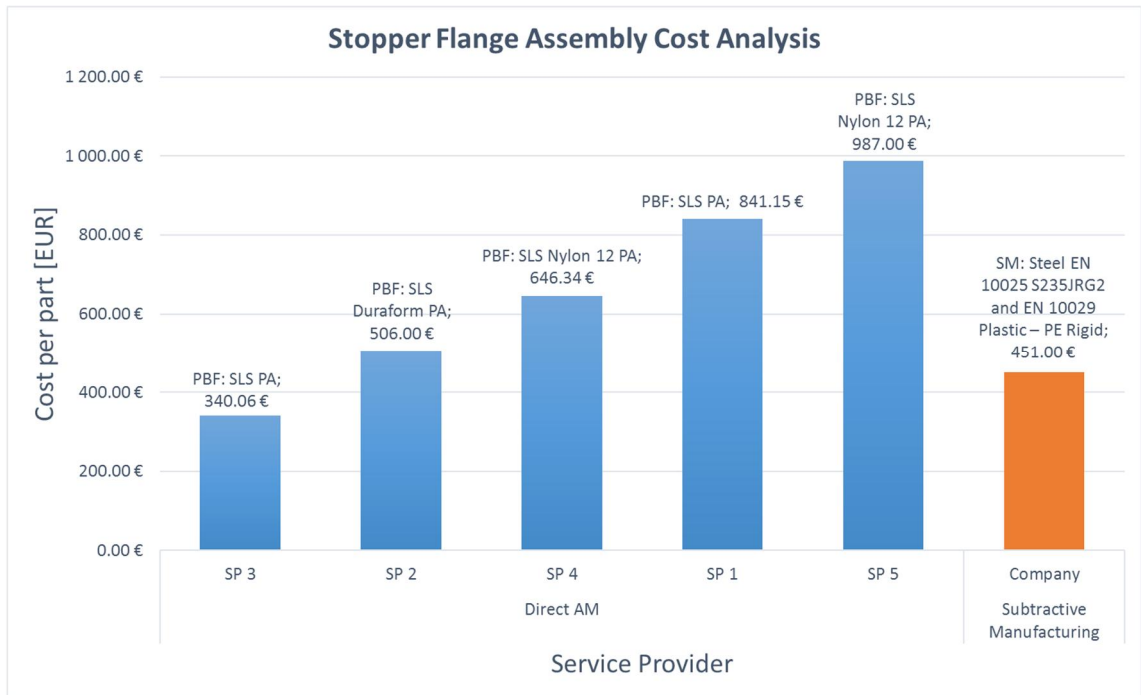


Figure 21. A CAD model of Stopper Flange Assembly containing a bounding box of 236mm x 236mm x 95mm.

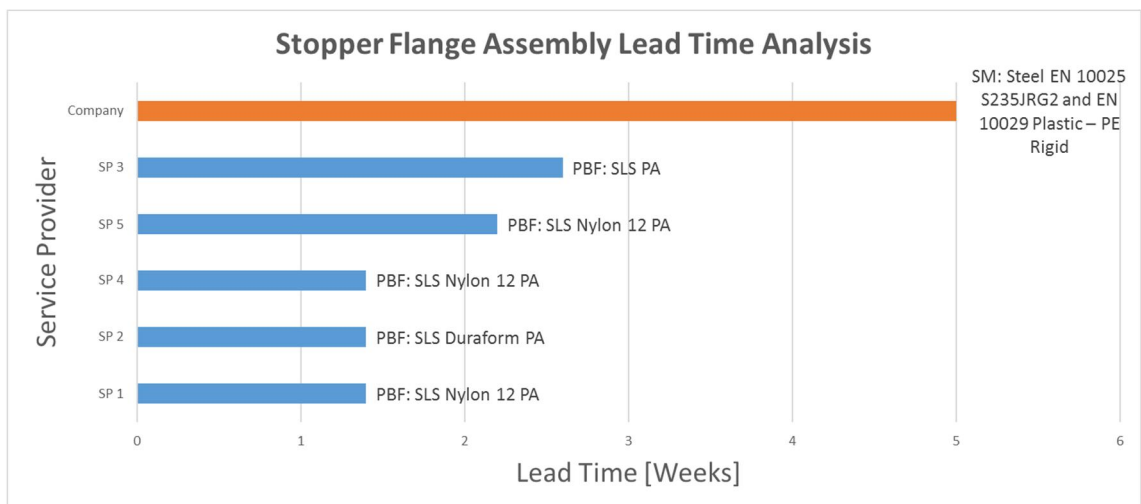
Stopper Flange Assembly is part of an Anti-Sway Frame Assembly as described in Appendix 2. The Stopper Flange Assembly consists of three main components including stopper flange, flange and the sliding ring. The stopper flange and the flange are composed of stainless steel whereas, the sliding ring is made up of Polyethylene polymer. The manufacturing methods of this component include cutting, milling and drilling. A CAD model of the component can be seen in Figure 21. The downtime of the equipment is not affected by this component. Since the part experiences variable and shock loading of low stress intensity, the part is analysed considering direct polymer AM.

5.2.10.1 Cost and Lead Time Analysis

The following Graph 27 and Graph 28 represent the cost analysis and lead time analysis of Stopper Flange Assembly, respectively. The data is labelled by means of ISO/ASTM standardised AM method, its variant and material. The value of the cost per part is also identified in case of the cost analysis. The cost per part for AM is presented from lowest to highest and compared to that of the SM. The lead time is also presented from lowest to highest. As a result of this analyses, it can be deduced that direct AM of PBF via SLS of PA can be up to approximately 25% economical from SP3 than the current SM methods.



Graph 27. Cost analysis of Stopper Flange Assembly.



Graph 28. Lead time analysis of Stopper Flange Assembly.

5.2.10.2 Conclusion

According to the above analyses, it can be deduced that AM may be beneficial in contrast to SM for this component in terms of cost and lead time to an extent. The following Table 24 provides a summary of this extent.

Table 24. Stopper Flange Assembly AM summary of benefits in contrast to Subtractive Manufacturing.

Stopper Flange Assembly: AM Cost Effectiveness and Lead Time Summary		
Benefit Scenario	Validity [Yes/No]	Description
Economical	Yes	Considering the cost per part of 340.06 € of direct polymer AM of PBF via SLS of PA with a lead time of approximately 2.6 weeks.
Shorter Lead Time	Yes	Considering the lead time per part of 1.4 weeks of direct polymer AM from SP1/SP2/SP4.
Economical and Shorter Lead Time	Yes	Considering the cost per part of 340.06 € of direct polymer AM of PBF via SLS of PA with a lead time of approximately 2.6 weeks.

5.2.11 Adjustable Mounting Plate

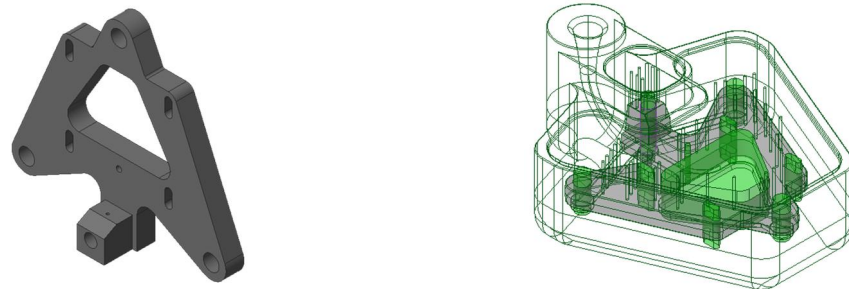
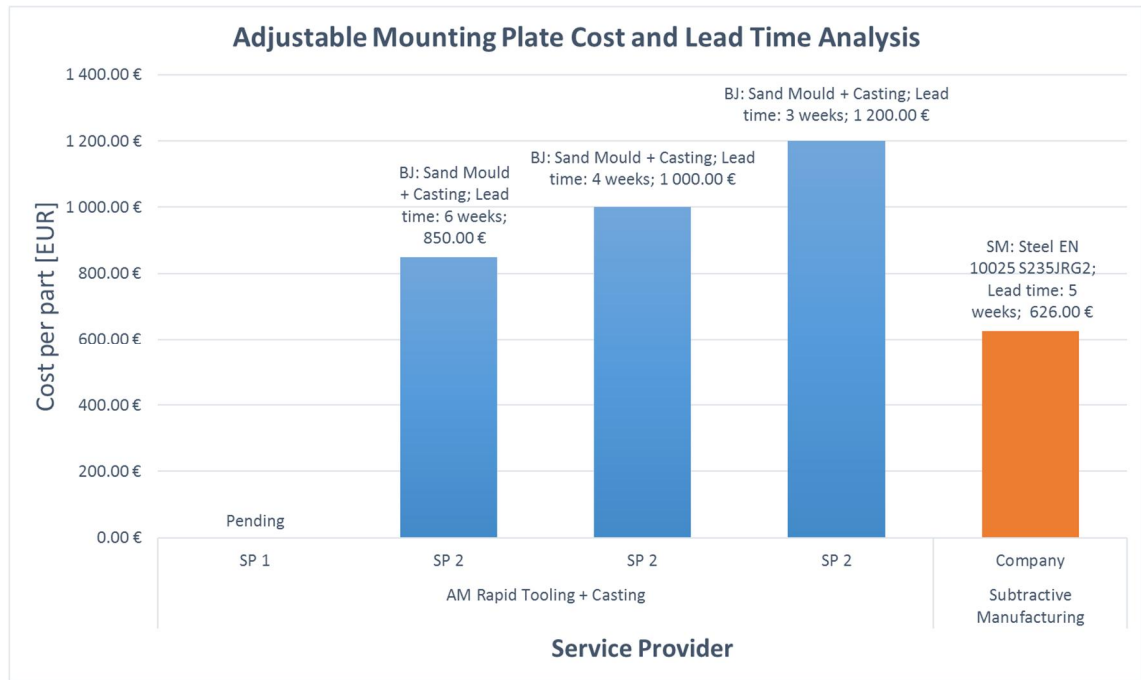


Figure 22. A CAD model of Adjustable Mounting Plate (Left) and its sand mould (Right) containing a bounding box of 476mm x 424mm x 103mm and 576.0mm x 683.0mm x 278.0mm, respectively.

Adjustable Mounting Plate is a component of a lifting device as explained in Appendix 2. It consists of two parts that are adjustable mounting plate and a relatively smaller part called plate. Both parts of Adjustable Mounting Plate are composed of stainless steel. Its manufacturing methods include flame cutting, milling, facing and welding. A CAD model of the component can be seen in Figure 22. The component is subjected to variable loading and it has a direct impact on the downtime of the equipment in case it is damaged. Due to a large geometrical size of the component, it is analysed for AM rapid tooling. An isometric view of the modelled sand mould for this component can be seen in Figure 22.

5.2.11.1 Cost and Lead Time Analysis

The following Graph 29 presents the cost and lead time analysis of Adjustable Mounting Plate. The data is labelled by means of ISO/ASTM standardised AM method, material, lead time and the value of cost per part. Three quotations were received from SP 2 in which the cost per part of AM sand mould increases as the lead time decreases. The cost of casting per part is approximated to couple of hundred euros with a lead time of approximately 2 weeks.



Graph 29. Cost and lead time analysis of Adjustable Mounting Plate.

5.2.11.2 Conclusion

According to the above analyses, it can be deduced that AM can be beneficial in contrast to SM for this component in terms of cost and lead time up to an extent. The following Table 25 provides a summary of this extent.

Table 25. Adjustable Mounting Plate AM summary of benefits in contrast to Subtractive Manufacturing.

Adjustable Mounting Plate: AM Cost Effectiveness and Lead Time Summary		
Benefit Scenario	Validity [Yes/No]	Description
Economical	No	Considering cost per part of AM rapid tooling of 400€ from SP 2 and cost per part of couple of hundred euros for casting and finishing totals to approximately 800-900€ with a lead time of approximately 6 weeks.
Shorter Lead Time	Yes	Considering the lead time per part of 1 week for AM rapid tooling from SP 2 and the lead time of 2 weeks for casting totals to approximately 3 weeks with a cost of approximately 1150-1250€.
Economical and Shorter Lead Time	No	The cost per part with shorter lead time exceeds that of the cost per part of the SM process.

5.2.12 Bush

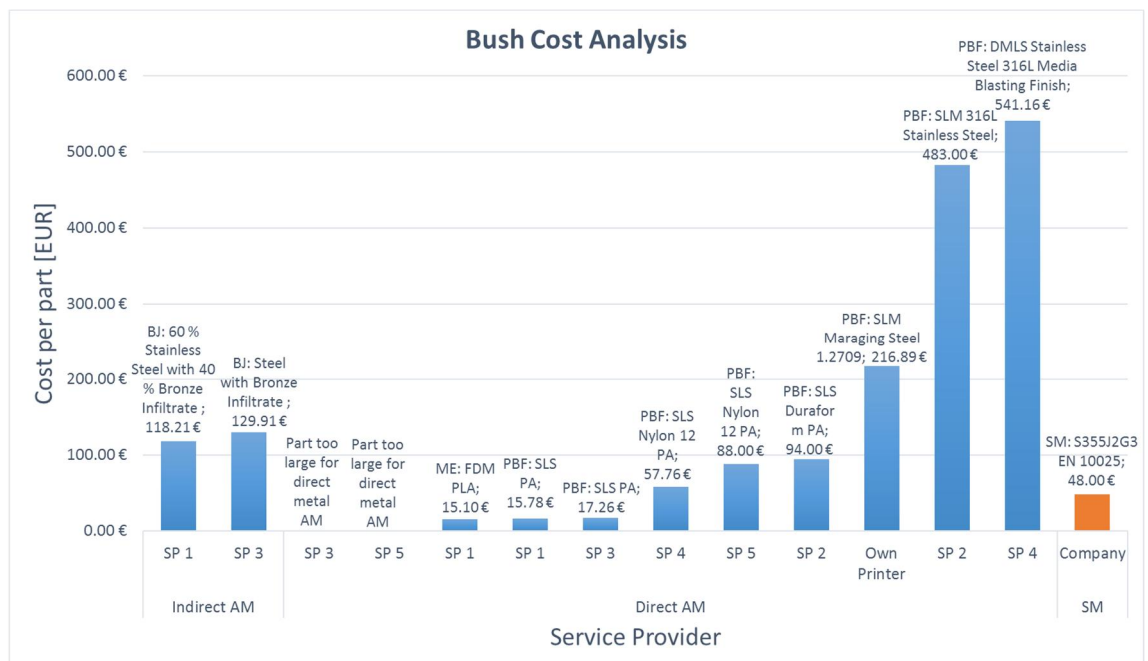


Figure 23. A CAD model of Stopper Flange Assembly containing a bounding box of 90mm x 90mm x 25mm.

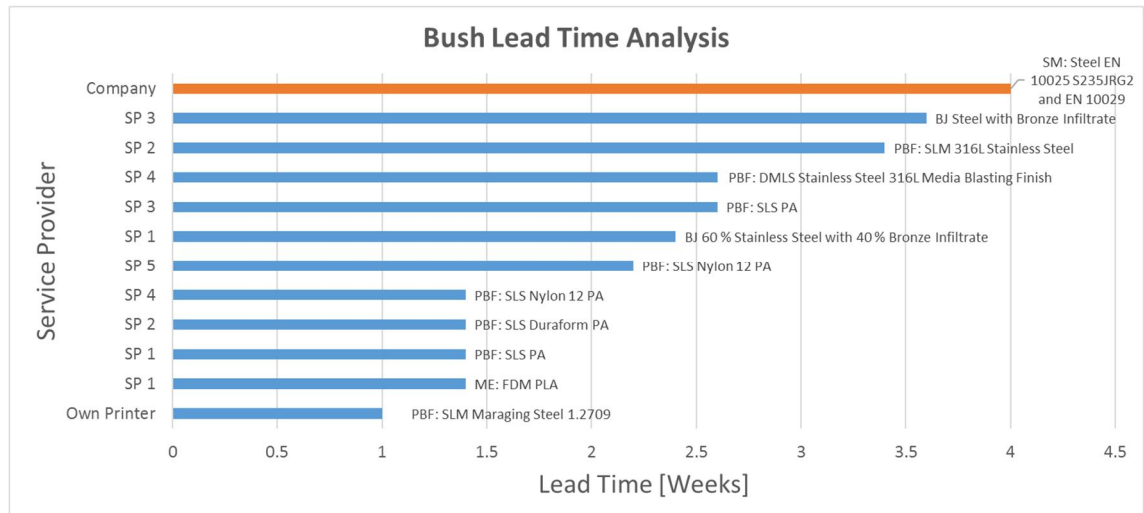
Bush is a component of a Transfer Device as explained in Appendix 2. The material of the component is stainless steel and its manufacturing methods include cutting, milling and drilling. A CAD model of the component can be seen in Figure 23. The component experiences static loading and it directly effects the downtime of the equipment in case it is malfunctioning. The component is analysed for direct AM and indirect AM of metals and polymers due to the compatibility of its geometrical size.

5.2.12.1 Cost and Lead Time Analysis

The following Graphs 30 and 31 illustrate the cost analysis and lead time analysis of the Bush, respectively. The data is labelled by means of ISO/ASTM standardised AM method, its variant and material. The value of the cost per part is also identified in case of the cost analysis. The cost per part for each category of AM is presented from lowest to highest and the lead time is also presented from lowest to highest. As observed from these analyses and the previous analyses, the cost per part of direct and indirect metal AM remains relatively quite high at the benefit of achieving shorter lead times. The direct polymer AM of ME via FDM of PLA offers approximately 69% economical cost per part at a 65% faster lead time from SP1 in contrast to SM method. In addition, direct polymer AM of PBF via SLS of PA can be up to approximately 67% cheaper with a 65% faster lead time from SP1 in comparison to the current SM method.



Graph 30. Cost analysis of Bush.



Graph 31. Lead time analysis of Bush.

5.2.12.2 Conclusion

According to the above analyses, it can be deduced that AM can be beneficial in contrast to SM for this component in terms of cost and lead time up to an extent. The following Table 26 provides a summary of this extent.

Table 26. Bush AM summary of benefits in contrast to Subtractive Manufacturing.

Bush: AM Cost Effectiveness and Lead Time Summary		
Benefit Scenario	Validity [Yes/No]	Description
Economical	Yes	Considering the cost per part of 15.10 € for direct AM via ME of PLA and 15.78 € for direct AM of PBF via SLS of PA from SP1 with a lead time of approximately 1.4 weeks.
	No	Considering the cost per part of direct metal AM of 216.89 € via own printer and indirect metal AM of 118.21 € via SP1 with a lead time of 1 week and 2.4 weeks, respectively.
Shorter Lead Time	Yes	Considering the lead time per part of 1 week of direct metal AM in case of own printer, the lead time per part of 2.4 weeks of indirect metal AM from SP1 and the lead time per part of 1.4 weeks of direct polymer AM from SP4 and/or SP2 and/or SP1.
Economical and Shorter Lead Time	Yes	Considering the cost per part of 15.10 € and 17.26 € for direct polymer AM from SP1 and SP3 with a lead time of approximately 1.4 weeks and 2.6 weeks, respectively.

5.2.13 Brake Flange

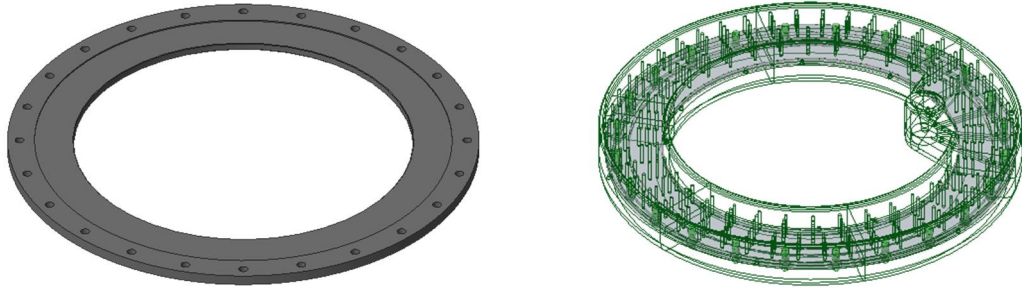
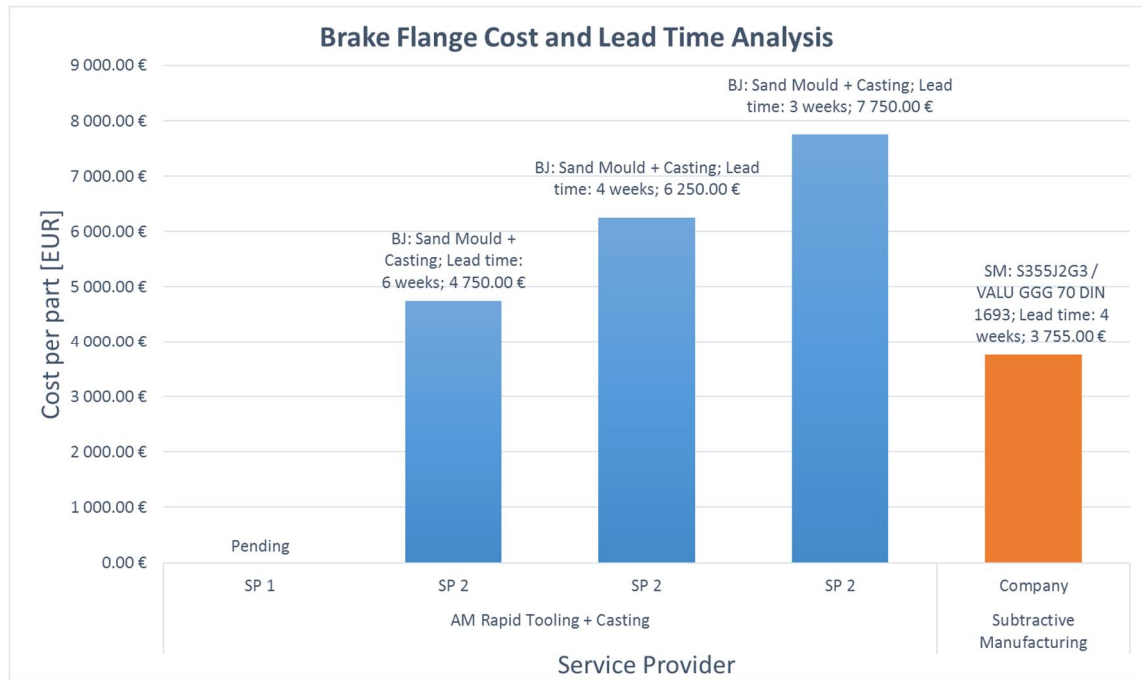


Figure 24. A CAD model of Brake Flange (Left) and its sand mould (Right) containing a bounding box of 1580mm x 1580mm x 35mm and 1630.0mm x 1630.0mm x 210.0mm, respectively.

Brake flange is a component of Casting Table as explained in Appendix 2. The material of the component is either stainless steel or cast iron. Its manufacturing methods involve flame cutting, milling and drilling. The component contains variable loading and it has a direct impact on downtime of the equipment in case it is damaged. It possesses the largest geometrical dimension of the selected parts for further analysis with a diameter of 1.58 meters. A CAD model of the component can be seen in Figure 24. Due to the aforementioned reason, it is analysed against AM rapid tooling to assist casting of the component. Since the geometrical size of the component is still large for additively manufacturing the sand mould, the part and its corresponding mould are split into 5 partitions. The partitioned moulds can be manufactured via existing technology and these can be eventually joined together via adhesion to form a complete mould of the part. A CAD model of the partitioned sand mould of the component can also be seen in Figure 24.

5.2.13.1 Cost and Lead Time Analysis

The following Graph 32 presents an approximation of the cost per part of AM rapid tooling of sand mould with respect to the current SM method. The data is labelled by means of ISO/ASTM standardised AM method, material, cost per part and the corresponding lead time. As observed from the graph, the cost per part of the AM sand mould increases as the lead time is shortened. Overall, the cost per part of the sand mould exceeds that of the cost per part of the current SM method even before the cost of casting and finishing processes is applied to it.



Graph 32. Cost and lead time analysis of Brake Flange.

5.2.13.2 Conclusion

According to the above analyses, it can be deduced that AM can be beneficial in contrast to SM for this component in terms of cost and lead time up to an extent. The following Table 27 provides a summary of this extent.

Table 27. Brake Flange AM summary of benefits in contrast to Subtractive Manufacturing.

Brake Flange: AM Cost Effectiveness and Lead Time Summary		
Benefit Scenario	Validity [Yes/No]	Description
Economical	No	The cost of AM rapid tooling of sand mould exceeds that of the current SM process.
Shorter Lead Time	Yes	Considering the lead time per part of 1 week for AM rapid tooling from SP 2 and the lead time of 2 weeks for casting and finishing processes totals to approximately 3 weeks with a cost of approximately 7500-8000 €.
Economical and Shorter Lead Time	No	The cost per part with shorter lead time exceeds that of the cost per part of the SM process.

5.2.14 Summary of Subtractive Manufacturing Parts

According to the above 13 analyses, it can be deduced that AM can be beneficial in contrast to subtractive manufacturing of components in terms of cost and lead time on a case by case scenario. The following Table 28 provides a summary of the conducted analyses.

Table 28. AM summary of benefits in contrast to subtractive manufacturing parts.

AM Cost Effectiveness and Lead Time Summary		
Benefit Scenario	Validity [Yes/No]	Description
Economical	Yes	All 5 components, that were considered for direct polymer AM proved to be economical in all cases. Approximately 22% (2/9) of all components that were considered for AM rapid tooling for casting proved to be economical.
	No	All 8 components that were considered for indirect and direct metal AM proved to be expensive to manufacture in all cases. Indirect metal AM was cheaper to manufacture than direct metal AM in all cases.
Shorter Lead Time	Yes	Indirect AM, direct AM and AM rapid tooling proved to be faster to manufacture for all of their respective components.
Economical and Shorter Lead Time	Yes	Approximately 46% (6/13) of components proved to be economical to manufacture at faster lead time through AM.

6 Performance

This chapter of the study investigates the effect of shape optimization and topology optimization on cost, lead time and performance of the selected components. Shape optimization is performed on Chainwheel and topology optimization is performed on Upper Shank. Both optimization involve static analysis for maximizing Von Mises stress up to a selected factor of safety according to the loading and boundary conditions. Displacement or deformation of the components is also taken into consideration to fulfil a minimum safety criterion.

6.1 *Shape Optimization: Chain Wheel*

6.1.1 Objective

The objective of this computer aided engineering through finite element method simulations and possible optimizations is to reduce the weight of a Chainwheel also referred to as a driving sprocket in order to enhance its manufacturability for additive manufacturing. The sprocket was modelled using Creo Parametric M050 according to the provided CAD drawing and CAE analysis was performed on Creo Simulate. The loads projected on the sprocket were calculated according to the literature review and the given information. The stress concentrations of the sprocket were analysed and an optimization approach was taken into consideration with respect to the factor of safety.

6.1.2 Load Calculations

The loads projected on the sprocket were calculated according to the hydraulic motor and planetary gears which were used to power the sprocket.



Figure 25. Hydraulic Motor: M+S Hydraulics B/MR250C.

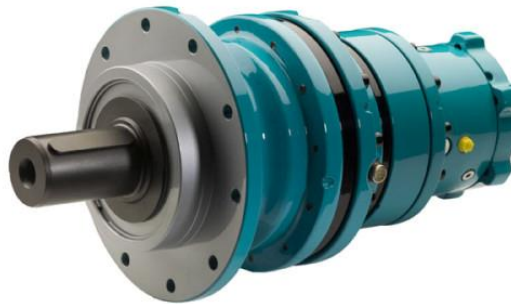


Figure 26. Planetary Gear: Brevini ED – 2090-FE-25-00.

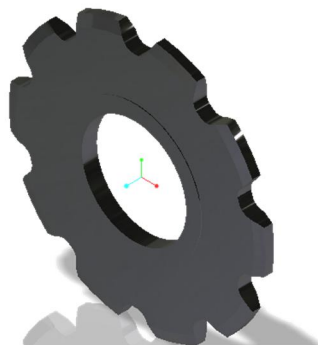


Figure 27. A CAD model of the Chainwheel/Sprocket.

6.1.2.1 Specifications

Motor Specifications (M+S Hydraulics Plc., 2015):

Motor Displacement per rotation, V_r : $250.1 \times 10^{-6} [m^3/rev]$

Max. Change in Pressure, Δp_{max} : 175 bar

Max. Torque, T_{max} : 540 Nm

$$T = \Delta p \left(\frac{V_r}{2\pi} \right) \eta_{hm} \quad (5)$$

Where T is torque [Nm]
 Δp is pressure [Pa]
 V_r is motor displacement per rotation $[\frac{m^3}{rev}]$
 η_{hm} is motor mechanical efficiency [%]

$$\eta_{hm} = \frac{T_{max} \times 2\pi}{\Delta p_{max} \times V_r} = 0.775 = 77.5\% \quad (6)$$

Given Pressure drop: $\Delta p = 130 \text{ bar} = 13 \text{ MPa} = 13 \times 10^6 \text{ Pa}$

$$T_{motor} = 13 \times 10^6 \left(\frac{250.1 \times 10^{-6}}{2\pi} \right) 0.775 = 401.03 \text{ Nm} \quad (7)$$

Gear Specifications (Brevini UK Ltd., 2017; Martikka, et al., 1985):

Gear ratio, $i_{eff} = 24.48$

$$i_{eff} = \frac{T_{sprockets}}{T_{motor}} \quad (8)$$

$$T_{sprockets} = i_{eff} \times T_{motor} = 9817.21 \text{ Nm} \quad (9)$$

$$T_{sprocket} = \frac{T_{sprockets}}{\text{No. of Sprockets}} = \frac{9817.21}{2} = 4908.61 \text{ Nm} \quad (10)$$

$$F_{Total} = \frac{T_{sprocket}}{R_{Pitch}} = \frac{4908.61}{161.81 \times 10^{-3}} = 30335.64 \text{ N} \quad (11)$$

Where $T_{sprockets}$ is the torque applied on sprockets [Nm]
 $T_{sprocket}$ is the torque applied on one sprocket [Nm]
 F_{Total} is the total amount of force [N]
 R_{Pitch} is the sprocket pitch radius [m]

$$F_{Teeth} = \frac{F_{Total}}{z \times q} = \frac{30335.64}{5 \times 0.9} = 6741.25 \text{ N} \quad (12)$$

Where F_{Groove} is the force on sprocket teeth [N]
 Z is the number of teeth [Number]
 q is the loading factor [-]

Chain Drive Contact Angle

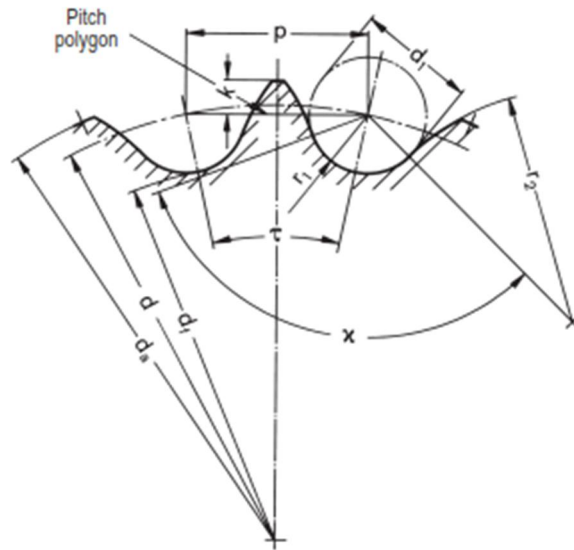


Figure 28. Chain roller and sprocket schematic. (Joh. Winklhofer Beteiligungs GmbH & Co. KG, 2016)

Where

- p is pitch of the chain [mm]
- d_1 is roller maximum diameter [mm]
- d is the sprocket pitch radius [mm]
- d_f is root sprocket diameter [mm]
- d_a is top sprocket diameter [mm]
- r_1 is tooth radius [mm]
- τ is angle of tooth [deg.]
- χ is roller contact angle [deg.]
- r_2 is profile radius of the tooth [mm]
- k is the tooth height above pitch polygon [mm]
- z is the number of teeth [Number]

$$\chi_{total} = 124^\circ \quad (13)$$

$$\chi_{directional} = \frac{124^\circ}{2} = 62^\circ \quad (14)$$

$$\chi_{effective} = \chi_{directional} - \tan^{-1}\left(\frac{5.055}{15.01}\right) = 62^\circ - 18.61^\circ = 43.39^\circ \quad (15)$$

Where

- χ_{total} is the total roller contact angle [°]
- $\chi_{directional}$ is the directional roller contact angle [°]
- $\chi_{effective}$ is the effective roller contact angle [°]

6.1.3 Mode of Failure

6.1.3.1 Factor of Safety

According to Jelaska (2012), from manufacturers and user experiences the factor of safety of a gear, sprocket in this case ranges from 1.2 to 1.5.

$$\text{Factor of safety: } FOS = \frac{\sigma_{yield}}{\sigma_{applied}} = 1.2 \text{ to } 1.5 \quad (16)$$

Where: σ_{yield} is the yield stress of the material
 $\sigma_{applied}$ is the applied stress of the material

6.1.3.2 Deformation

For this study, the maximum allowable deformation is taken as 1 mm according to the chain sprocket mechanism.

$$\text{Deformation}_{allowable} = 1 \text{ [mm]} \quad (17)$$

6.1.4 Materials

6.1.4.1 Sprocket

The sprocket was assigned Structural steel properties as following:

Table 29. Material Properties of Sprocket.

Hot- rolled Structural Steel S235J2 EN 10025	
Density	7850 [Kg/m ³]
Young's Modulus	206000 [MPa]
Poisson's Ratio	0.3
Coefficient of Thermal Expansion	1.5×10^{-5} [/K]
Tensile Yield Stress	235 [MPa]
Tensile Ultimate Stress	360 [MPa]
Specific Heat Capacity	440 [J/kgK]
Thermal Conductivity	38 [W/mk]

6.1.4.2 Weld Filler

The weld filler was assigned properties with an addition of 150 MPa to the yield stress and 80 MPa to the Tensile Ultimate Stress in order to convey its dominance with respect to the base material.

6.1.4.3 Shaft

The shaft was assigned structural steel properties as following:

Table 30. Material Properties of Shaft.

Hot- rolled Structural Steel S355J2 EN 10025	
Density	7850 [Kg/m ³]
Young's Modulus	200000 [MPa]
Poisson's Ratio	0.32
Coefficient of Thermal Expansion	1.2×10^{-5} [/K]
Tensile Yield Stress	345 [MPa]
Tensile Ultimate Stress	482.549 [MPa]
Specific Heat Capacity	500 [J/kgK]
Thermal Conductivity	30 [W/mk]

6.1.5 Static Analysis

A static analysis was performed on Creo Simulate using the loads and their projection calculated above. The sprocket was constrained with a fillet weld onto a fixed shaft and the corresponding loads were applied to the sprocket teeth. The details of loading and boundary conditions, contact interfaces, mesh size and results are presented in this analysis.

6.1.5.1 Loading and Boundary Conditions

Loading Constraints

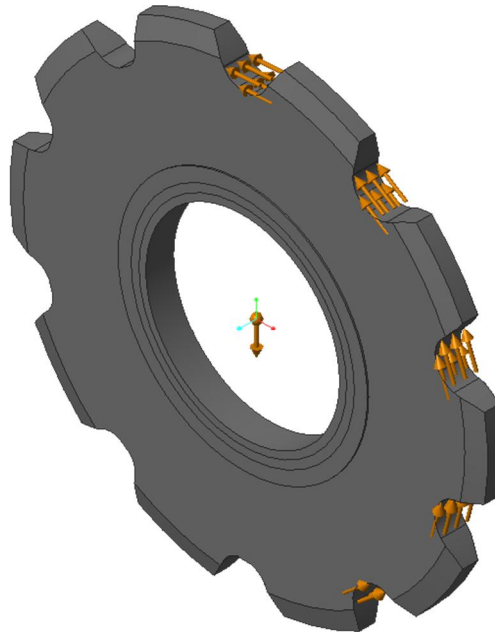


Figure 29. A force of 6741.25 N tangential to the pitch diameter is applied on effective contact angle of 43.39° on 5 gear teeth.

Boundary Constraints

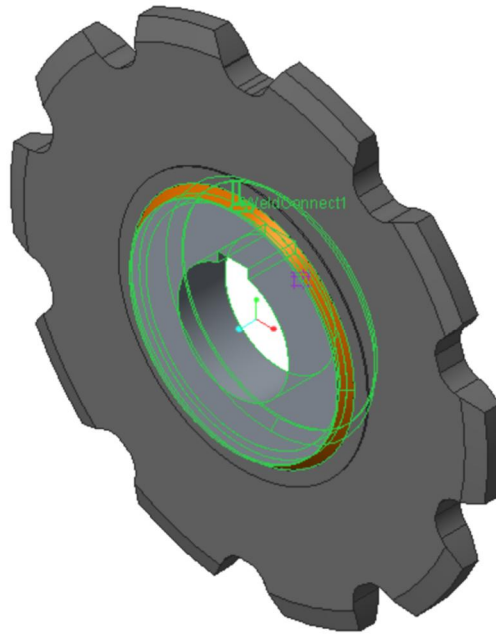


Figure 30. The sprocket was constrained with two fillet welds onto the shaft which was fixed.

Contact Interfaces

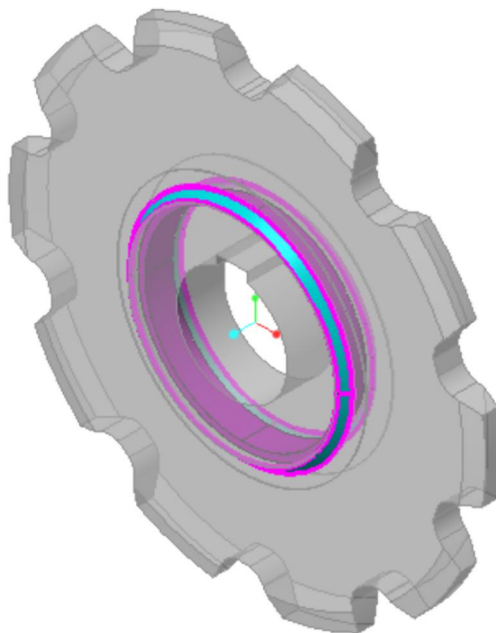


Figure 31. Weld surface shown in Cyan and bonded surface shown in purple.

Mesh Size

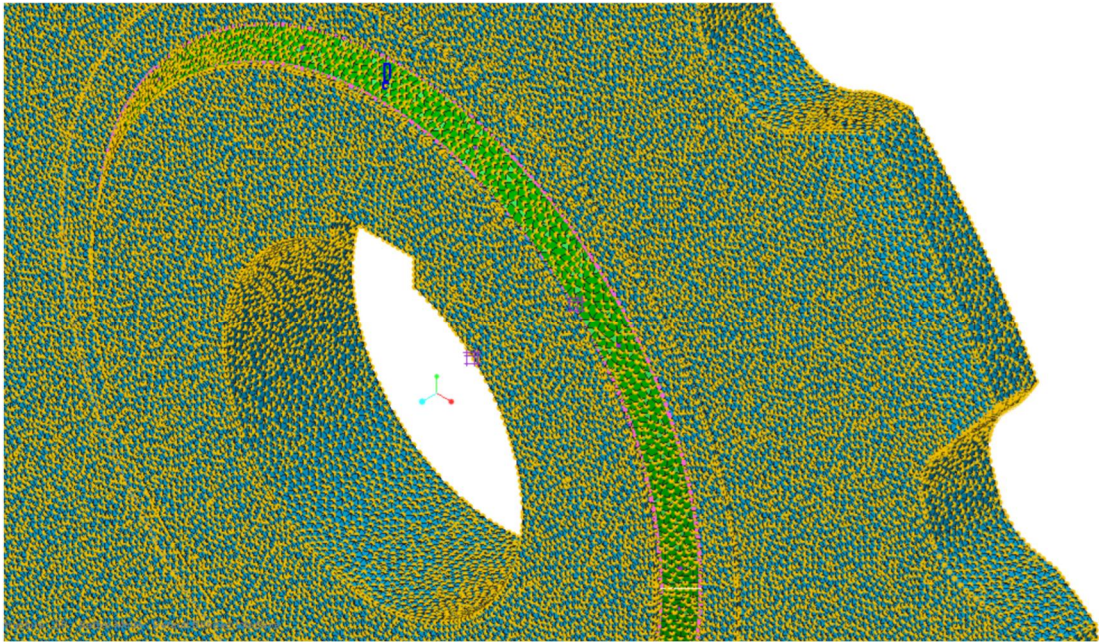


Figure 32. A mesh size of 2mm is created for the sprocket, weld constraint and the shaft.

6.1.5.2 Results

6.1.5.2.1 Von Mises Stress [MPa]

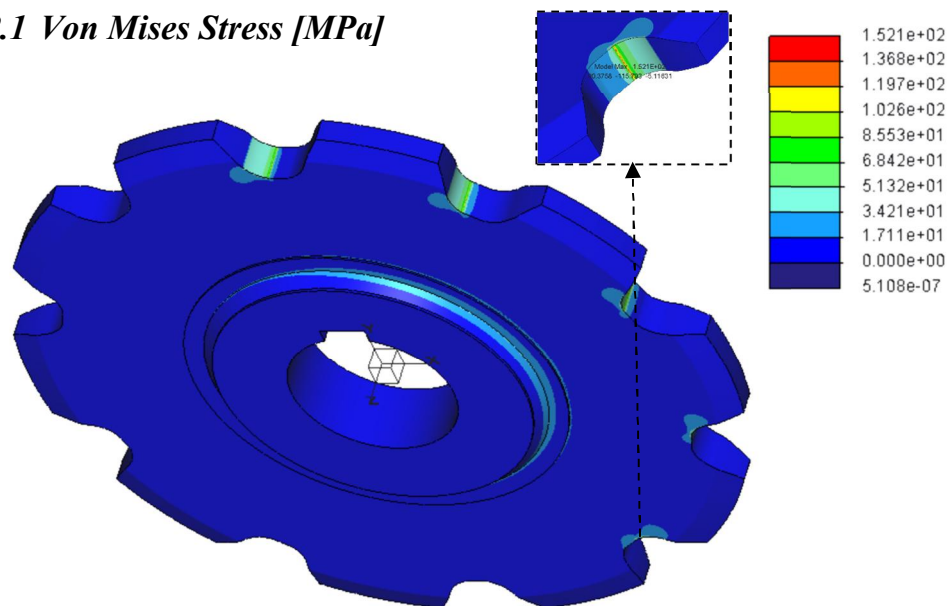


Figure 33. A maximum Von Mises stress of 152.1 MPa is observed close to the flank root.

$$\text{Factor of safety: } FOS = \frac{235}{152.1} = 1.55 \approx 1.6 \quad (18)$$

As observed from above Figure 33 and the factor of safety, the blue region occupies a non-existence level of stress which can be used as an opportunity for weight optimization.

6.1.5.2.2 Deformation [mm]

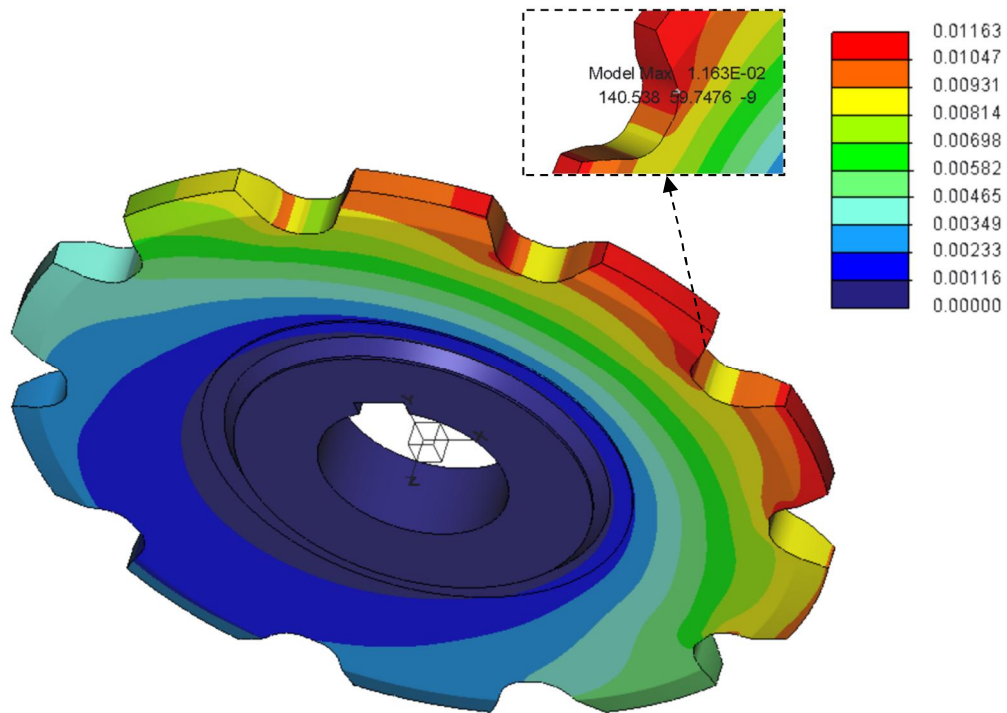


Figure 34. A maximum deformation of 0.01163 mm is observed on the sprocket flank root.

$$0.01163 \text{ [mm]} < Deformation_{allowable} ; \textit{Within Range} \quad (19)$$

6.1.5.3 Model Properties

Table 31. Original Model Results.

<i>Sprocket Properties</i>							
<i>Iteration</i> [No.]	<i>Volume</i> [mm ³]	<i>Surface Area</i> [mm ²]	<i>Mass</i> [Kg]	<i>Weight</i> [N]	<i>Max. Von Mises Stress</i> [MPa]	<i>Max. Displacement</i> [μm]	<i>Factor of Safety</i>
Original	1.24e + 6	1.68e + 05	9.73	95.45	152.1	11.63	1.6

6.1.6 Optimization Study

In order to reduce the weight and minimize mass of the sprocket, 10 circular cuts were made with a consistent diameter. This diameter was used to perform a dimensional optimization design study leading to evaluation of the behaviour of stresses and deformations in the sprocket. The diameters of the circular cut pattern were 40mm, 45mm, 50 mm and 55 mm according to the 1st, 2nd, 3rd and 4th iteration. The results of the optimization can be seen in the subsequent text.

6.1.6.1 1st Iteration Results

The results of a circular cut diameter of 40mm are as following.

6.1.6.1.1 Von Mises Stress [MPa]

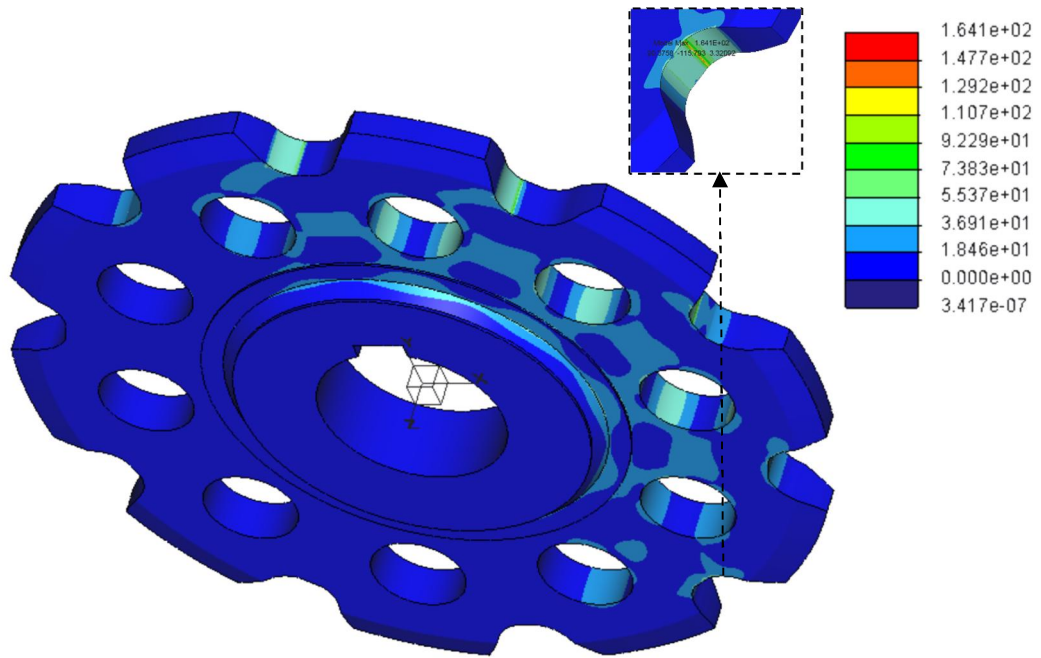


Figure 35. A maximum Von Mises stress of 164.1MPa is observed close to the flank root of the 40mm circular cut pattern sprocket.

$$\text{Factor of safety: } FOS = \frac{235}{164.1} = 1.43 \approx 1.4 ; \text{Within Range} \quad (20)$$

6.1.6.1.2 Deformation [mm]

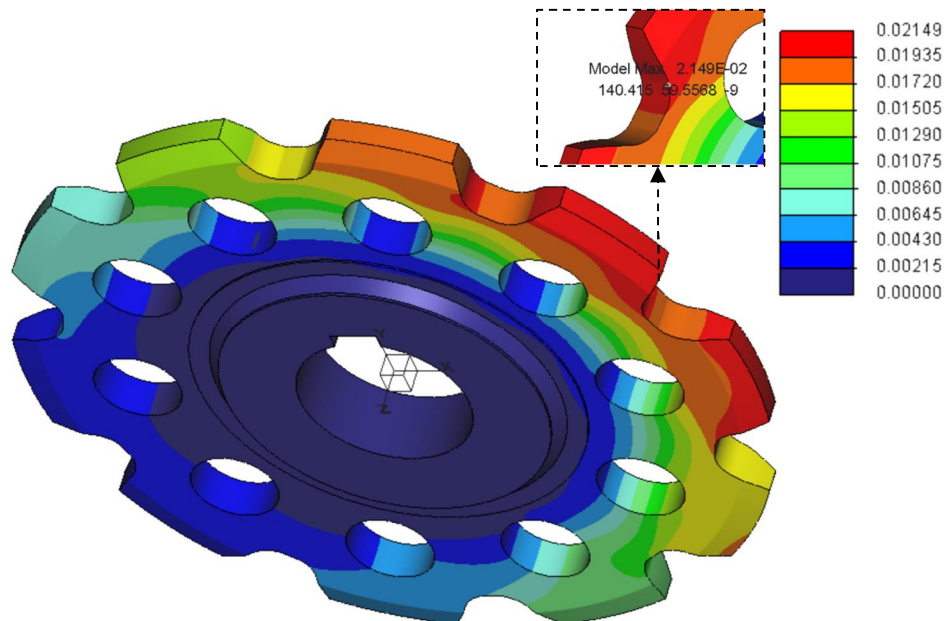


Figure 36. A maximum deformation of 0.02149 mm is observed on the sprocket flank root of the 40mm circular cut pattern sprocket.

$$0.02149 \text{ [mm]} < Deformation_{allowable} ; \text{Within Range} \quad (21)$$

6.1.6.2 Model Properties

Table 32. 1st Iteration Results with 40mm diameter cut pattern.

Sprocket Properties							
Iteration [No.]	Volume [mm ³]	Surface Area [mm ²]	Mass [Kg]	Weight [N]	Max. Von Mises Stress [MPa]	Max. Displacement [μm]	Factor of Safety
Original	1.24e+06	1.68e+05	9.73	95.45	152.1	11.63	1.6
1	1.01e+06	1.65e+05	7.95	77.99	164.1	21.49	1.4

6.1.6.3 2nd Iteration Results

The results of a circular cut diameter of 45mm are as following.

6.1.6.3.1 Von Mises Stress [MPa]

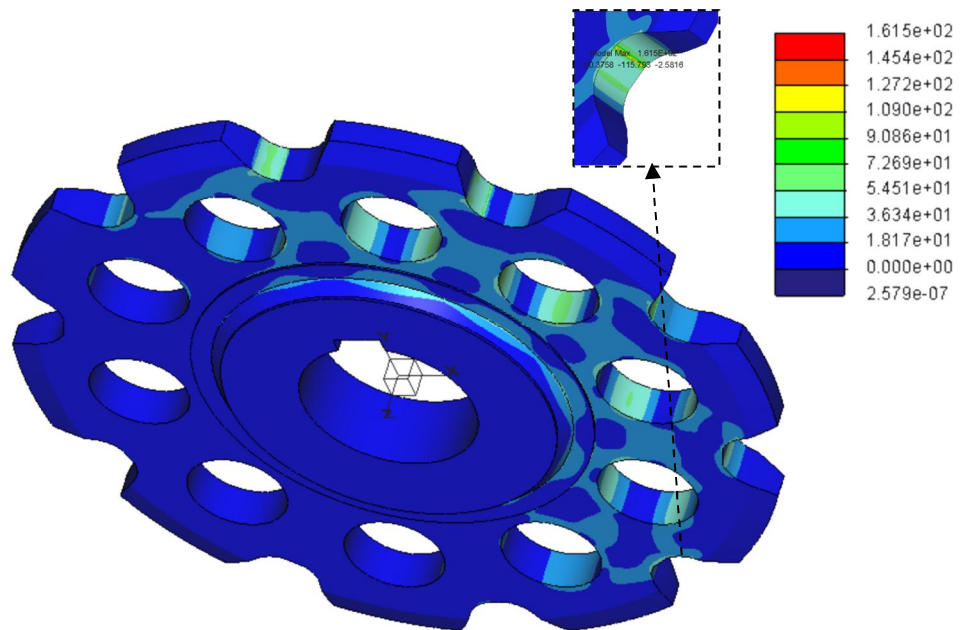


Figure 37. A maximum Von Mises stress of 161.5MPa is observed close to the flank root of the 45mm circular cut pattern sprocket.

$$\text{Factor of safety: } FOS = \frac{235}{161.5} = 1.45 \approx 1.5 ; \text{Within Range} \quad (22)$$

6.1.6.3.2 Deformation [mm]

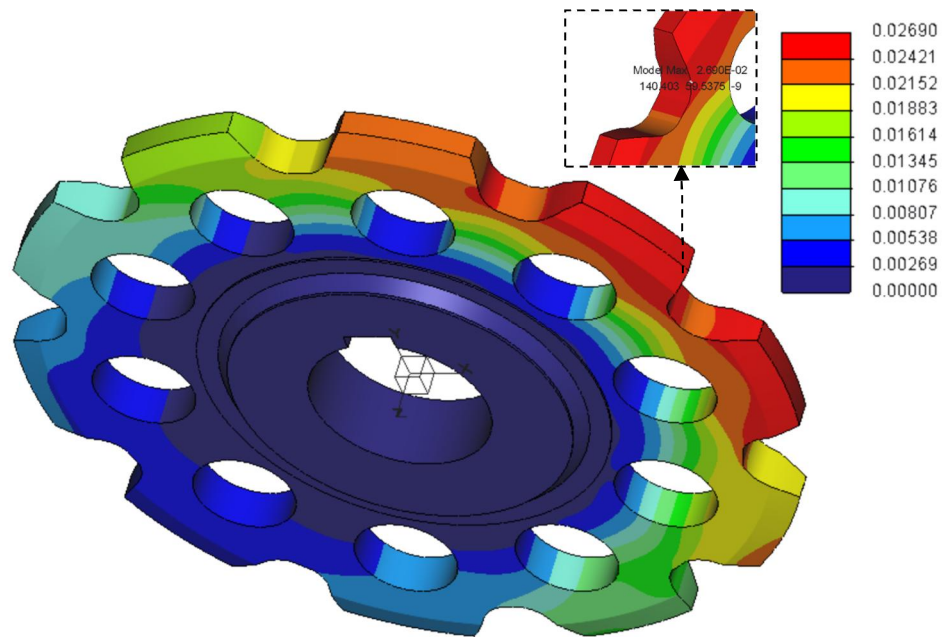


Figure 38. A maximum deformation of 0.02690mm is observed on the sprocket flank root of the 45mm circular cut pattern sprocket.

$$0.02690 \text{ [mm]} < Deformation_{allowable} ; \textit{Within Range} \quad (23)$$

6.1.6.4 Model Properties

Table 33. 2nd Iteration Results with 45mm diameter cut pattern.

<i>Sprocket Properties</i>							
<i>Iteration [No.]</i>	<i>Volume [mm³]</i>	<i>Surface Area [mm²]</i>	<i>Mass [Kg]</i>	<i>Weight [N]</i>	<i>Max. Von Mises Stress [MPa]</i>	<i>Max. Displacement [μm]</i>	<i>Factor of Safety</i>
Original	1.24e+06	1.68e+05	9.73	95.45	152.1	11.63	1.6
1	1.01e+06	1.65e+05	7.95	77.99	164.1	21.49	1.4
2	0.95e+06	1.61e+05	7.48	73.38	161.5	26.90	1.5

6.1.6.5 3rd Iteration Results

The results of a circular cut diameter of 50mm are as following.

6.1.6.5.1 Von Mises Stress [MPa]

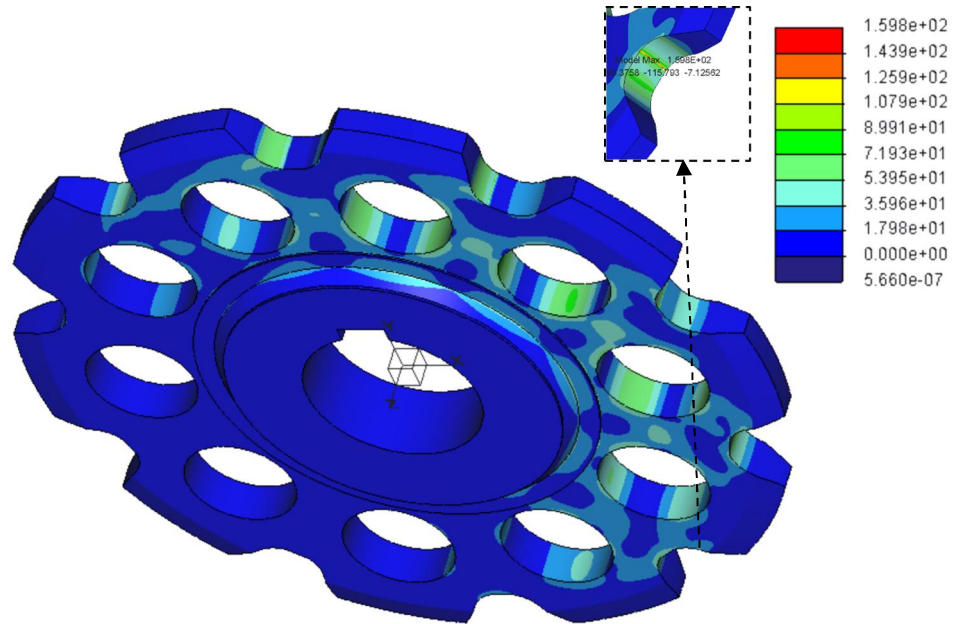


Figure 39. A maximum Von Mises stress of 159.8MPa is observed close to the flank root of the 50mm circular cut pattern sprocket.

$$\text{Factor of safety: } FOS = \frac{235}{159.8} = 1.47 \approx 1.5 ; \text{Within Range} \quad (24)$$

6.1.6.5.2 Deformation [mm]

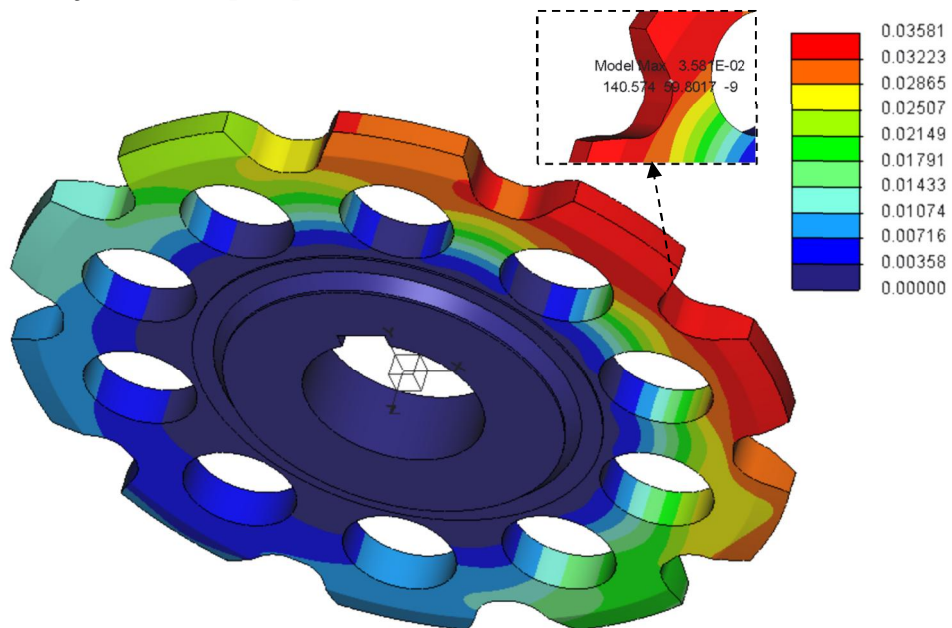


Figure 40. A maximum deformation of 0.03581mm is observed on the sprocket flank root of the 50mm circular cut pattern sprocket.

$$0.03581 \text{ [mm]} < \text{Deformation}_{\text{allowable}} ; \text{Within Range} \quad (25)$$

6.1.6.6 Model Properties

Table 34. 3rd Iteration Results with 50mm diameter cut pattern.

<i>Sprocket Properties</i>							
<i>Iteration [No.]</i>	<i>Volume [mm³]</i>	<i>Surface Area [mm²]</i>	<i>Mass [Kg]</i>	<i>Weight [N]</i>	<i>Max. Von Mises Stress [MPa]</i>	<i>Max. Displacement [μm]</i>	<i>Factor of Safety</i>
Original	1.24e+06	1.68e+05	9.73	95.45	152.1	11.63	1.6
1	1.01e+06	1.65e+05	7.95	77.99	164.1	21.49	1.4
2	0.95e+06	1.61e+05	7.48	73.38	161.5	26.90	1.5
3	0.89e+06	1.57e+05	6.95	68.18	159.8	35.81	1.5

6.1.6.7 4th Iteration Results

The results of a circular cut diameter of 55mm are as following.

6.1.6.7.1 Von Mises Stress [MPa]

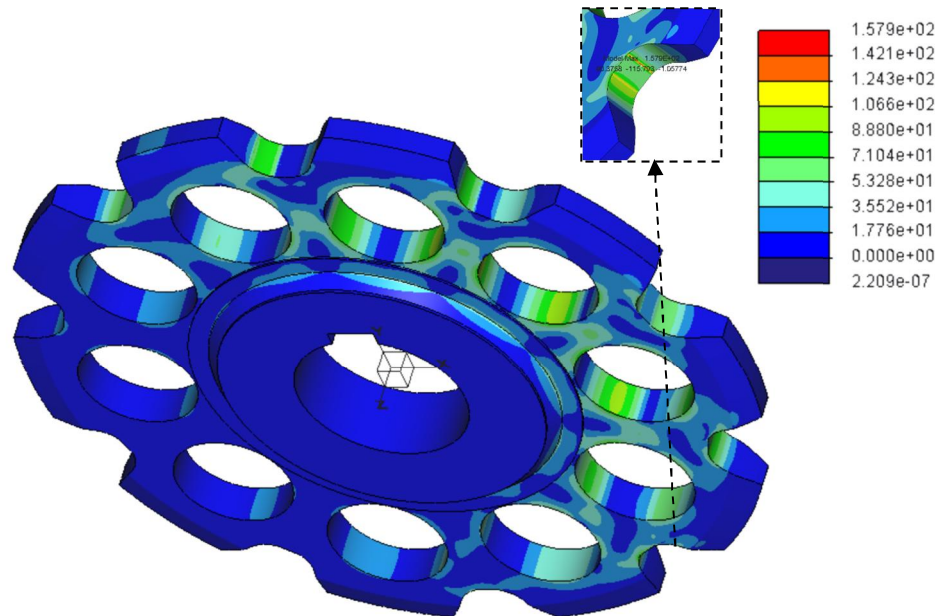


Figure 41. A maximum Von Mises stress of 157.9MPa is observed close to the flank root of the 55mm circular cut pattern sprocket.

$$\text{Factor of safety: } FOS = \frac{235}{157.9} = 1.49 \approx 1.5 ; \text{Within Range} \quad (26)$$

6.1.6.7.2 Deformation [mm]

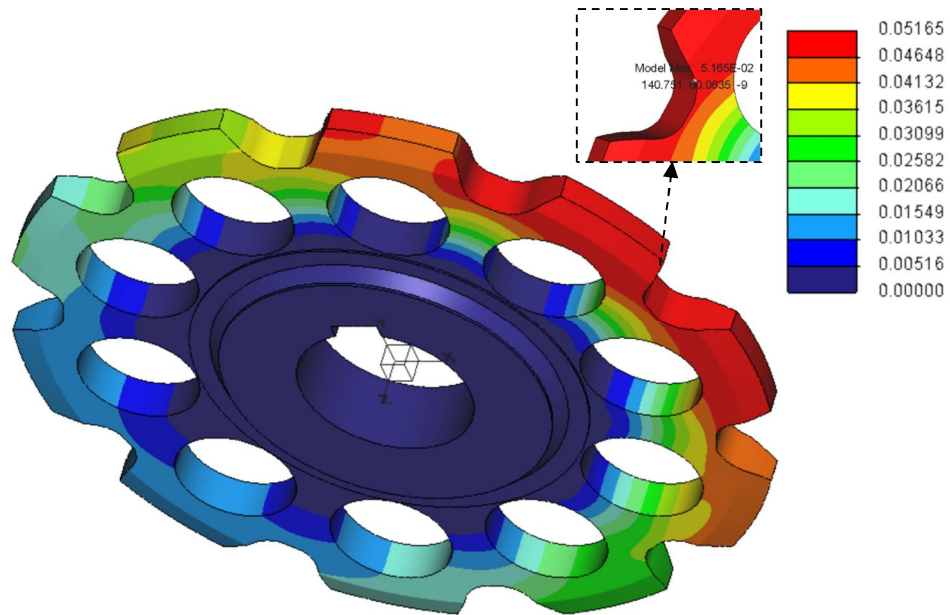


Figure 42. A maximum deformation of 0.05165mm is observed on the sprocket flank root of the 55mm circular cut pattern sprocket.

$$0.05165 \text{ [mm]} < Deformation_{allowable} ; \text{Within Range} \quad (27)$$

6.1.6.8 Model Properties

Table 35. 4th Iteration Results with 55mm diameter cut pattern.

Sprocket Properties							
Iteration [No.]	Volume [mm ³]	Surface Area [mm ²]	Mass [Kg]	Weight [N]	Max. Von Mises Stress [MPa]	Max. Displacement [μm]	Factor of Safety
Original	1.24e+06	1.68e+05	9.73	95.45	152.1	11.63	1.6
1	1.01e+06	1.65e+05	7.95	77.99	164.1	21.49	1.4
2	0.95e+06	1.61e+05	7.48	73.38	161.5	26.90	1.5
3	0.89e+06	1.57e+05	6.95	68.18	159.8	35.81	1.5
4	0.81e+06	1.51e+05	6.37	62.49	157.9	51.65	1.5

6.1.7 Conclusion

According to the results of 4th iteration of optimization shown in Table 35, the total mass and weight of the sprocket has been decreased by 34.53 % compared to the original design with a compromise of approximately 3.67% increase in Maximum Von Mises Stress with a factor of safety still within the upper limit of the prescribed range. As the diameter of the circular cut pattern of the sprocket was increased from 40mm to 55mm, the maximum Von Mises stress decreased from 164.1MPa to 157.9MPa. This incremental reduction in stress was due to the fact that energy was stored during deformation which increased by a factor of 2.4 as shown in Table 35 and stress distribution was increased as seen by the contours at the flank root and circular cuts in Figure 41 during the same transition. In case, this component is considered for direct metal AM of PBF via own printer, the cost

per part can be reduced up to approximately 34% for the optimized model and the performance of the model can be increased due to higher yield of built material associated with rapid melting and re-solidification in direct metal AM. In addition, the cost per part can be reduced up to 34% in case indirect metal AM is considered from SP1. The performance of the part can also be increased due to higher yield of built material associated with heat treatments involving debinding, sintering and infiltration in indirect metal AM. The lead times however, are not affected significantly and remain the same according to the service providers. Furthermore, the cost per part and the lead time of AM rapid tooling of redesigned sand mould for the optimized model are not affected significantly since the volume of the mould is not fluctuated significantly either. The original and the redesigned moulds of the model can be seen in Table 11. The cost per part and its associated lead time can be seen in Graph 14. In addition, the cost of casting and finishing can be reduced to an extent due to approximately 35% decrease in volume of the component even though setup cost remains the same.

6.2 Topology Optimization: Upper Shank

6.2.1 Objective

The objective of this computer aided engineering is to optimize the volume of an Upper Shank, component of a lifter assembly through topology optimization in order to enhance its performance, cost effectiveness and lead time using design for additive manufacturing. The Upper Shank was modelled using Creo Parametric M050 according to the provided CAD drawing. CAE static analysis and topology optimization were performed using Inspire 2017.1 from Solidthinking. Evolve 2017.1 from Solidthinking was also used to enhance the geometry of the final models and to perform tessellation for additive manufacturing. The loads projected on the shank were calculated according to the literature review and the given information. The stress concentrations and deformations of the shank were analysed and an optimization approach was taken into consideration with respect to the factor of safety through yield of the material as a mode of failure.

6.2.2 Load Calculations

According to the limited component and assembly drawings, forces and moments were translated onto the shank and a schematic was created as seen in Figure 43.

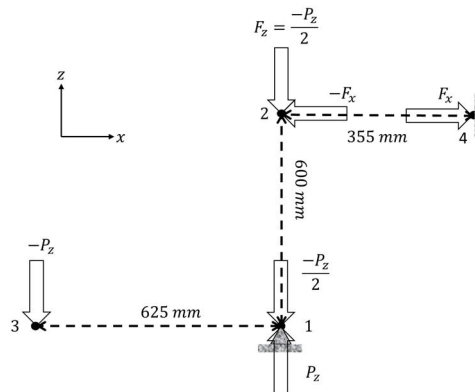


Figure 43. Schematic of force translations where point 2 acts as a hinge and point 4 acts as a fixed constraint of Upper Shank.

Assumption: Worst-case scenario by maximizing the distance between Point 3 and Point 1 from the assembly drawing

Given: Total Mass: $M_{Total} = 400 \text{ [Kg]}$

Gravity: $g = 9.81 \left[\frac{m}{s^2} \right]$

$$P_z = M_{Total} \times g = 400 \times 9.81 = 3924 \text{ [N]} \quad (28)$$

$$M_1 = P_z \times 625 = 3924 \times 625 = 2452500 \text{ [Nmm]} \quad (29)$$

$$M_1 = F_x \times 600 = 2452500 \text{ [Nmm]} \quad (30)$$

$$F_x = \frac{2452500}{600} = 4087.5 \text{ [N]} \quad (31)$$

$$F_{xus} = \frac{F_x}{2} = \frac{4087.5}{2} = 2043.75 \text{ [N]} \quad (32)$$

$$F_{xusp} = \frac{F_{xus}}{2} = \frac{2043.75}{2} = 1021.875 \text{ [N]} \quad (33)$$

$$F_z = \frac{P_z}{2} = \frac{3924}{2} = 1962 \text{ [N]} \quad (34)$$

$$F_{zus} = \frac{F_z}{2} = \frac{1962}{2} = 981 \text{ [N]} \quad (35)$$

$$F_{zusp} = \frac{F_{zus}}{2} = 490.5 \text{ [N]} \quad (36)$$

Assumption: Worst-case scenario assuming only point 2 takes the total vertical load

$$F_{zuspa} = F_{zusp} \times 2 = 981 \text{ [N]} \quad (37)$$

Where:

- P_z is the applied load to the assembly [N]
- M_1 is the moment at point 1 due to P_z [Nmm]
- F_x is the translated force in x axis acting on point 2 due to M_1 [N]
- F_{xus} is the force in x axis acting on one Upper Shank [N]
- F_{xusp} is the force in x axis acting on one pin hole of Upper Shank [N]
- F_z is the translated force in z axis acting on point 2 due to P_z [N]
- F_{zus} is the force in z axis acting on one Upper Shank [N]
- F_{zusp} is the force in z axis acting on one pin hole of Upper Shank [N]
- F_{zuspa} is the force in z axis applied on one pin hole of Upper Shank [N]

6.2.3 Mode of Failure

6.2.3.1 Factor of Safety

For the purpose of this study, an allowable range of safety of factor is taken from 1.2 to 2.5 in accordance with the yield of the material.

$$\text{Factor of safety: } FOS = \frac{\sigma_{yield}}{\sigma_{applied}} = 1.2 \text{ to } 2.5 \quad (38)$$

Where:

- σ_{yield} is the yield stress of the material
- $\sigma_{applied}$ is the applied stress of the material

6.2.3.2 Deformation

For this study, the maximum allowable deformation is taken as 1 mm according to the shank mechanism.

$$Deformation_{allowable} = 1 \text{ [mm]} \quad (39)$$

6.2.4 Static Analysis: Preliminary Baseline

In order to take into account, the performance, cost effectiveness of different AM methods and their associated lead times, a baseline static analysis was performed to evaluate the stress concentrations and deformations of original design of upper shank.

6.2.4.1 Material Properties

According to the original design, upper shank was assigned structural steel properties of Inspire as listed in the following table.

Table 36. Material Properties of Upper Shank.

Inspire: Structural Steel S355JR	
Density	7850 [Kg/m ³]
Young's Modulus	210000 [MPa]
Poisson's Ratio	0.29
Coefficient of Thermal Expansion	1.6×10^{-5} [/K]
Tensile Yield Stress	355 [MPa]

6.2.4.2 Loading and Boundary Conditions

An axial and vertical force of 1025.875 N and 981 N respectively, are applied to each pinhole of the shank represented by red arrows. The standard keyways of 8x62x68 DIN 5462 are removed and a cylindrical hole is created at a radius of 65mm, equivalent to the mid-value of the outer and inner diameter of the keyways for simplicity and mass conservation. A rigid cylindrical support is applied represented by a red cylindrical constraint in Figure 44. A mesh size of 2mm is used for the analysis.

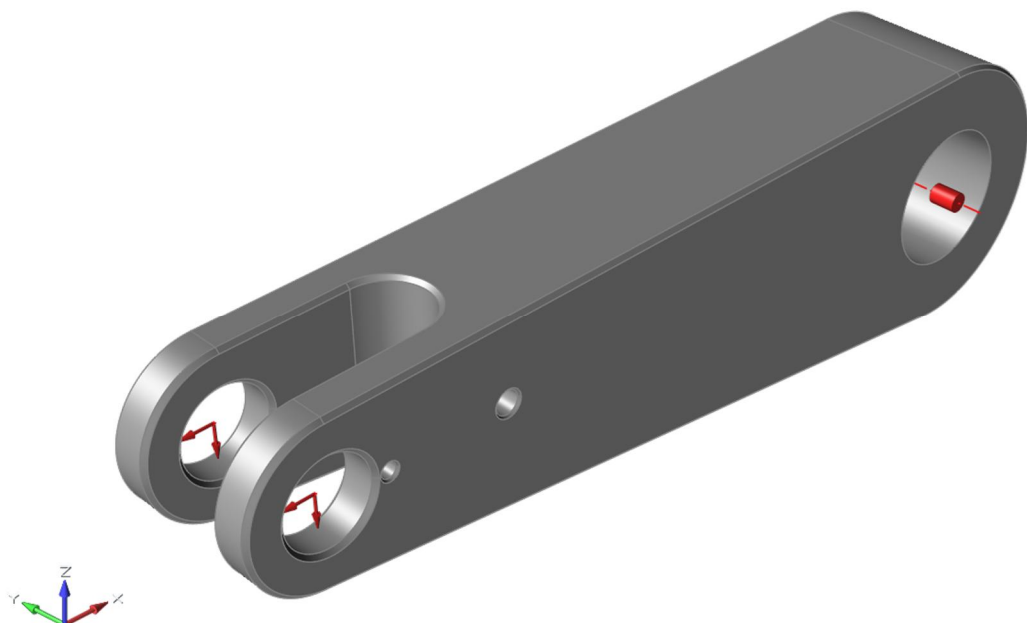


Figure 44. Loading and Boundary Conditions of the original design.

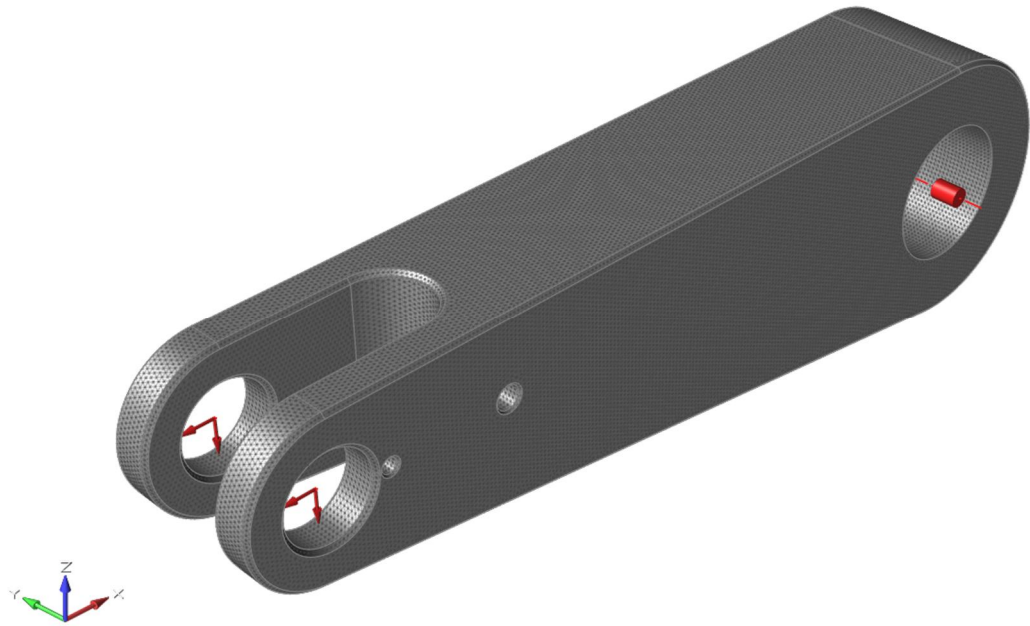


Figure 45. Upper Shank with a mesh size of 2 mm.

6.2.4.3 Results

Von Mises Stress:

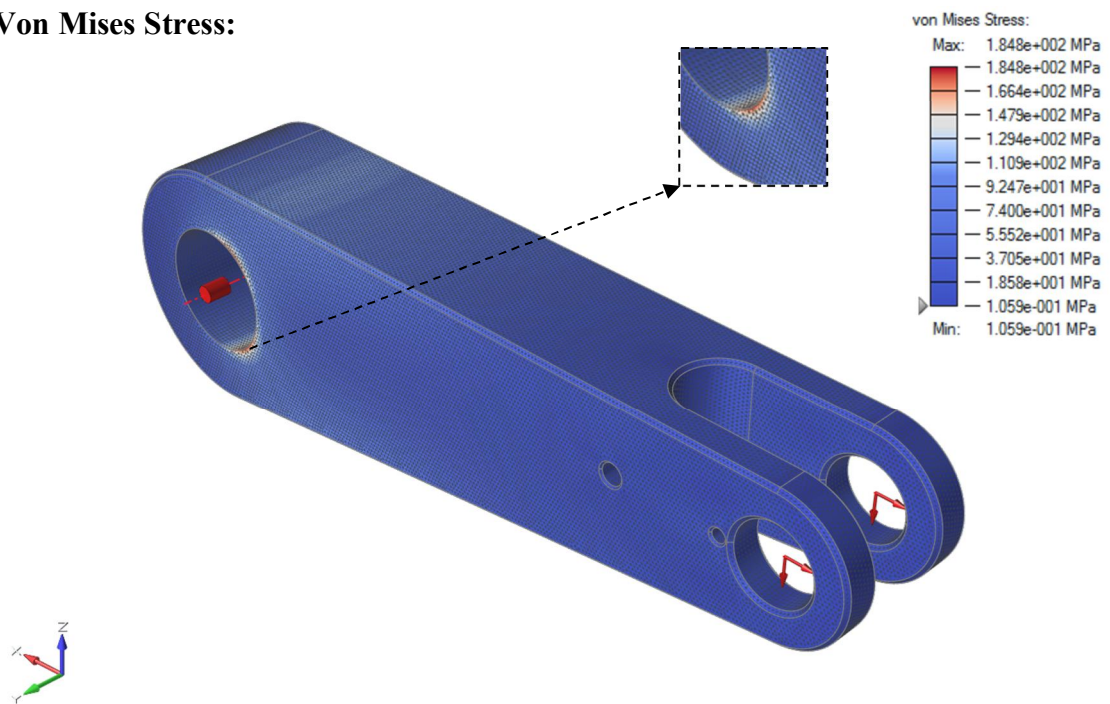


Figure 46. A maximum Von Mises stress of 184.832 MPa is observed in the vicinity of the cylindrical support with a mesh size of 2mm.

$$\text{Factor of safety: } FOS = \frac{355}{184.83} = 1.92 \approx 1.9 \quad (40)$$

As observed from above Figure 46 and the factor of safety, the blue region occupies a non-existence level of stress which can be used as an opportunity for topology optimization.

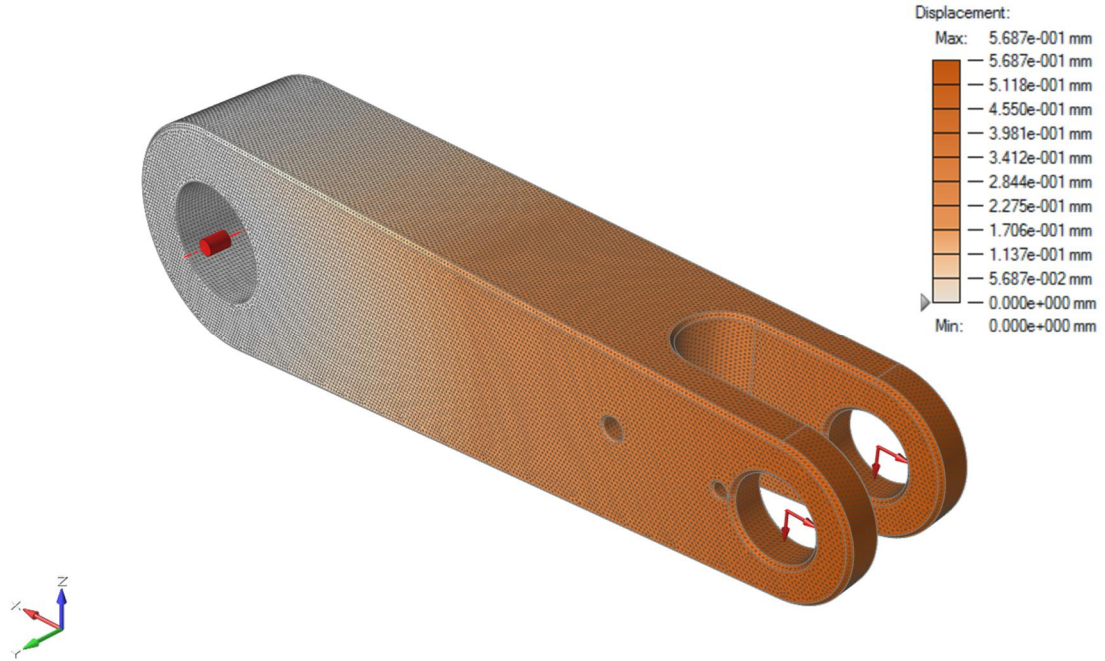
Deformation:

Figure 47. A maximum deformation of 0.5687 mm is observed at the edge of the part near the loads.

$$0.5687 \text{ [mm]} < Deformation_{allowable} ; \text{Within Range} \quad (41)$$

Table 37. Results of Original Model of Upper Shank.

Upper Shank Properties						
Iteration [No.]	Volume [mm ³]	Mass [Kg]	Weight [N]	Max. Von Mises Stress [MPa]	Max. Displacement [mm]	Factor of Safety
Original	2.74e + 06	21.52	211.11	184.83	0.569	1.9

6.2.5 Topology Optimization Preliminary Iteration

In order to take into account, the performance, cost effectiveness of different AM methods and their associated lead times, a preliminary iteration was performed which topologically optimized the basic design space of the part.

6.2.5.1 Loading and Boundary Conditions

An axial and vertical force of 1025.87 N and 981 N respectively, are applied to each pinhole of the shank represented by red arrows. The standard keyways of 8x62x68 DIN 5462 are removed and a cylindrical hole is created at a radius of 65mm, equivalent to the mid-value of the outer and inner diameter of the keyways for simplicity and mass conservation. A rigid cylindrical support is applied represented by a red cylindrical constraint in Figure 48. The brown region illustrates the design space of the optimization. A mesh size of 2mm is used for the analysis.

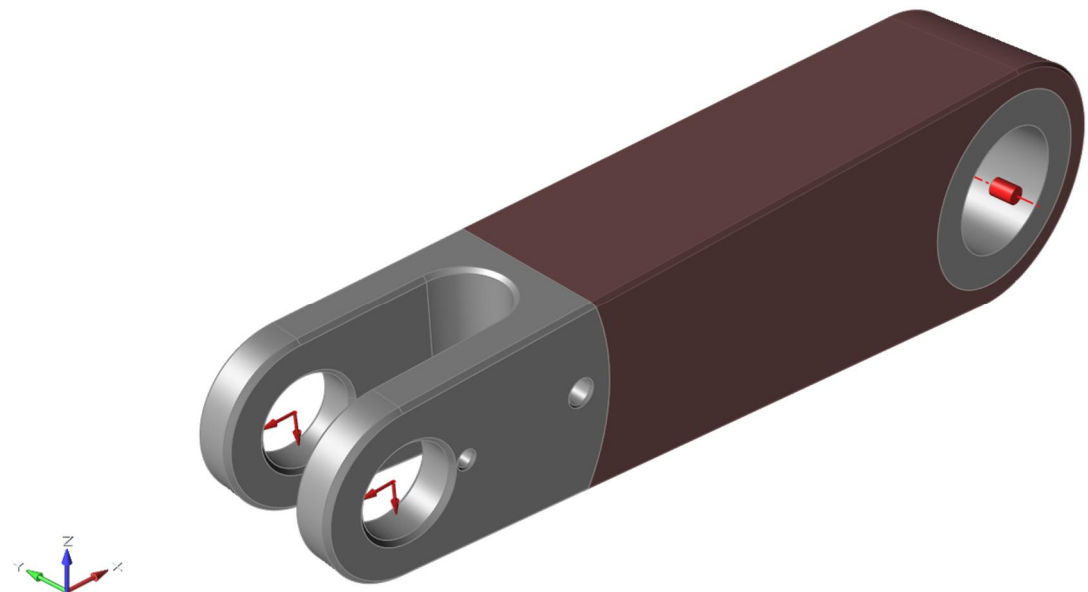


Figure 48. Loading and Boundary Conditions with design space illustrated by brown region.

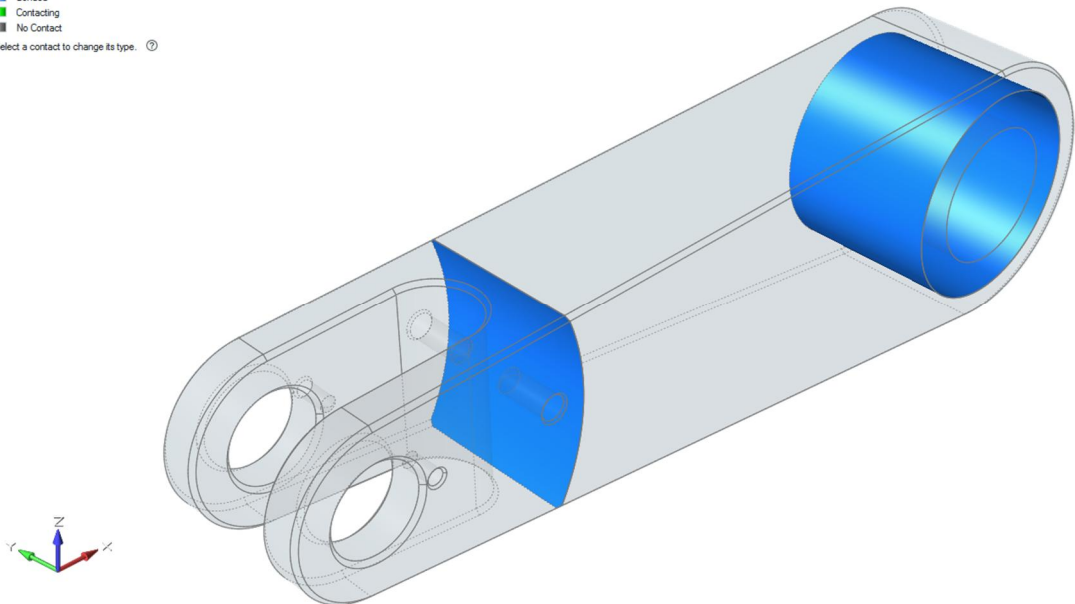
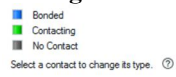


Figure 49. Upper Shank contact surfaces with respect to the design space.

6.2.5.2 Results

6.2.5.2.1 Topology Optimization

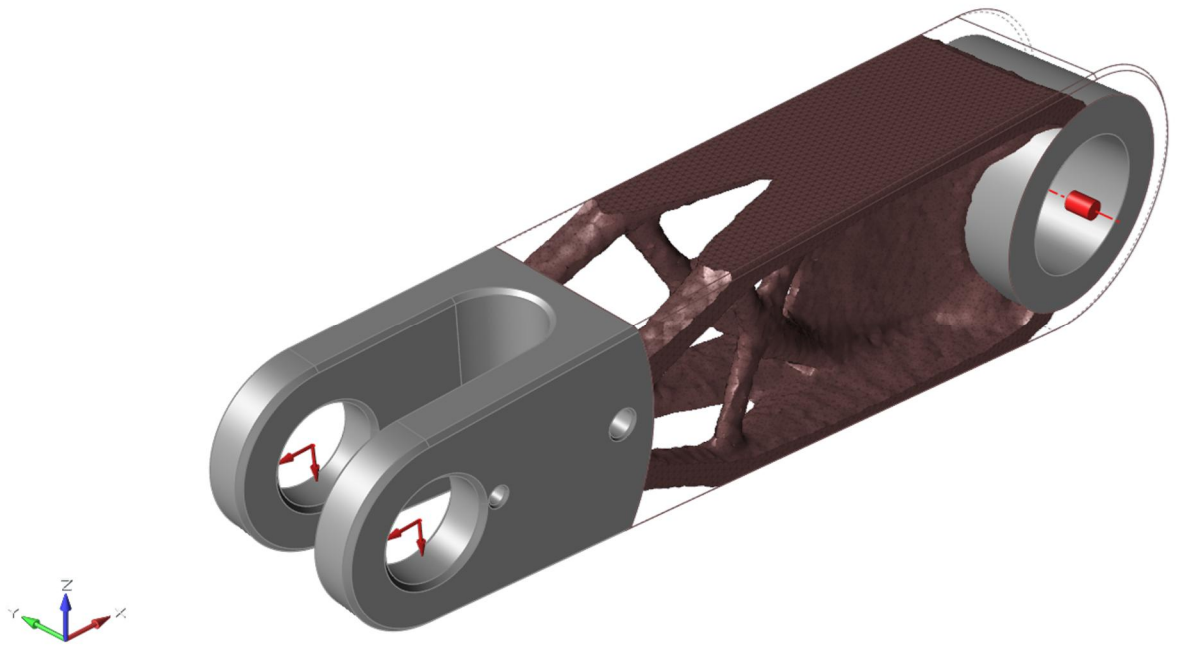


Figure 50. The result of raw topology optimization.

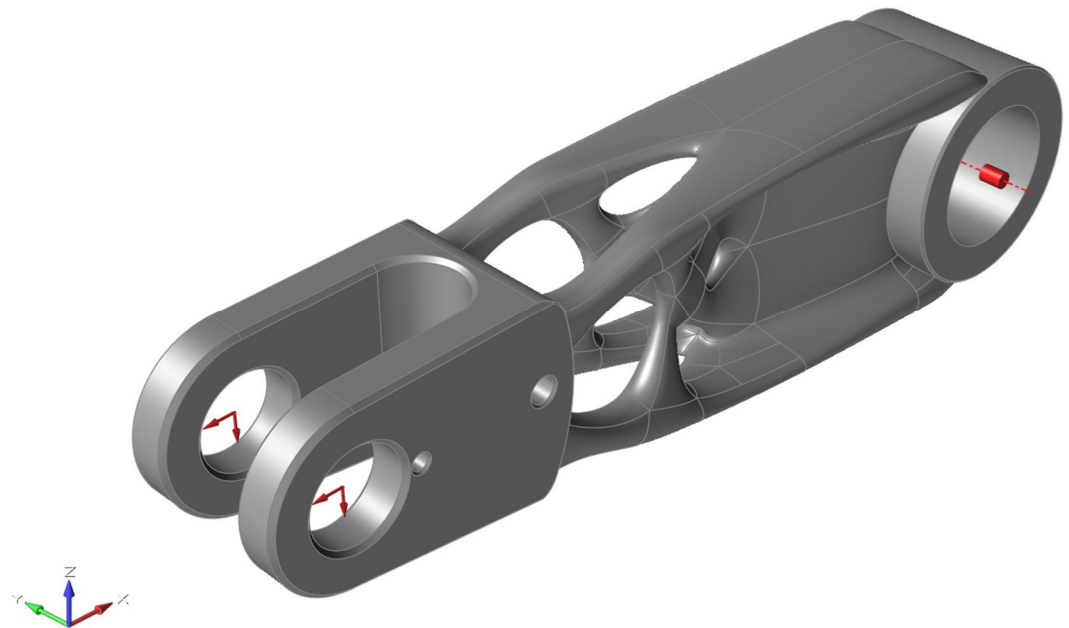


Figure 51. The result of surface modelled topology optimization.

6.2.5.2.2 Von Mises Stress

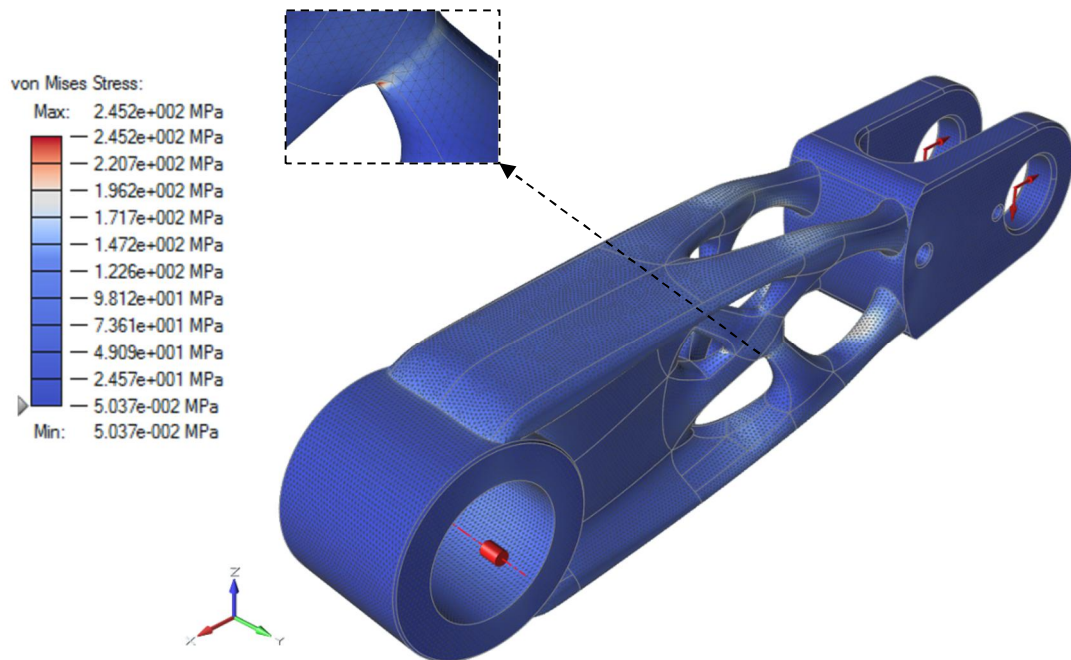


Figure 52. A maximum Von Mises stress of 245.23 MPa is observed as highlighted.

$$\text{Factor of safety: } FOS = \frac{355}{245.23} = 1.45 \approx 1.4 ; \text{Within Range} \quad (42)$$

6.2.5.2.3 Deformation

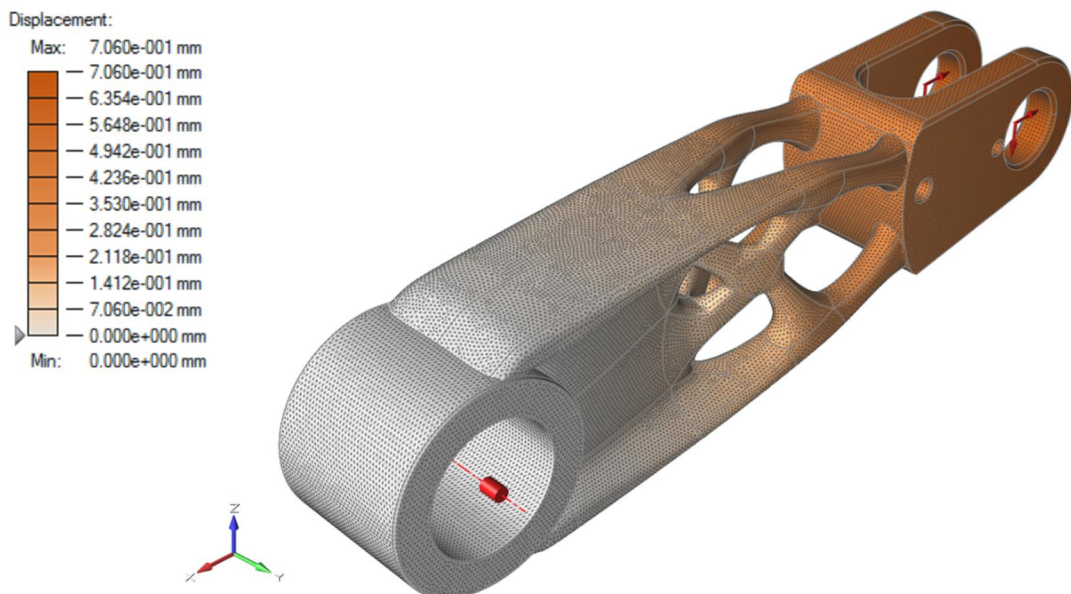


Figure 53. A maximum deformation of 0.7060mm is observed at right edge of the part.

$$0.7060 \text{ [mm]} < \text{Deformation}_{\text{allowable}} ; \text{Within Range} \quad (43)$$

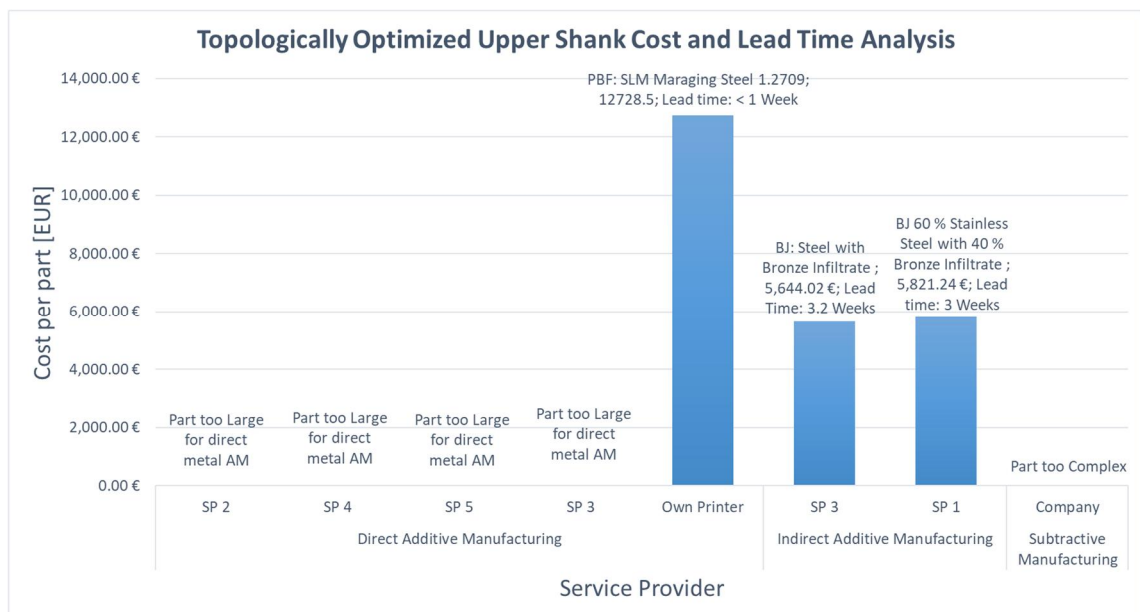
Table 38. Upper Shank properties of preliminary iteration.

Upper Shank Properties						
Iteration [No.]	Volume [mm³]	Mass [Kg]	Weight [N]	Max. Von Mises Stress [MPa]	Max. Displacement [mm]	Factor of Safety
Original	2.74e + 06	21.53	211.21	188.11	0.569	1.9
1	1.45e + 06	11.39	111.74	245.23	0.706	1.4

According to Table 38, the mass of the iterated design for AM is reduced to approximately 47% with an increase in Von Mises stress of 23.29%. Since the material is experiencing higher stress levels, the Max. Deformation is increased by approximately 19.40% and the factor of safety is decreased by nearly 26% however, these parameters are still within the defined range of stability.

6.2.6 Preliminary Cost and Lead Time Analysis

After inserting the standardized keyways of 8x62x68 DIN 5462 to the final model and converting the final CAD data to the AM compatible STL format, the cost effectiveness and its associated lead-time are evaluated based on comparison of quotations received from AM service providers to that of the original model presented in Section 5.2.2. The cost and lead time analyses of the original model are described in Section 5.2.2.1. According to Section 5.2.2.1 analyses, the lead time of direct and indirect AM is remarkably fast and the price is ridiculously high since the part is made for design for assembly and design for manufacturing rather than for design of AM. On the other hand, the topologically optimized model of this component presented in Section 6.2.5 is designed for AM.

**Graph 33. Upper Shank AM quotations and lead times.**

According to Graph 33, the optimized component size is too large for direct metal printing from four major AM service providers and its design is too complex for conventional subtractive manufacturing. The cost and lead time of own printer are evaluated using Aalto University's AM calculator using SLM Solutions 500 HL machine, consisting of 4 lasers with a power of 700W each. In this case, the cost per part is remarkably high however, the lead-time is remarkably fast since the component can be manufactured within just few days. It is also noted that this optimized model is approximately 7% cheaper than

the original model shown in Graph 13 with a relatively similar lead time when manufactured through the same printer. This is because the percentage of support structures required for direct metal PBF is increased from approximately 3% to 11% due to the geometric complexity even though the mass is reduced by approximately 47%. The indirect method of the optimized component offers a better approach with respect to cost as it can be up to approximately 56% cheaper in contrast to the direct metal PBF of the optimized part and up to approximately 47% cheaper in contrast to indirect metal BJ of the original part. Furthermore, the part can be delivered to its destination within 3.2 weeks according to SP3 quotation and within 3 weeks in accordance with SP1 quotation.

6.2.6.1 Preliminary Prototype

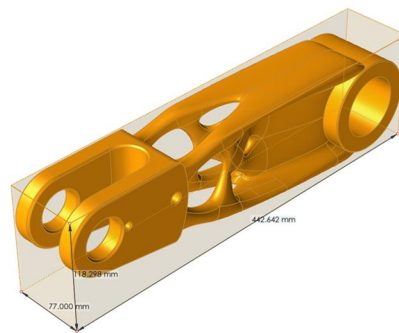
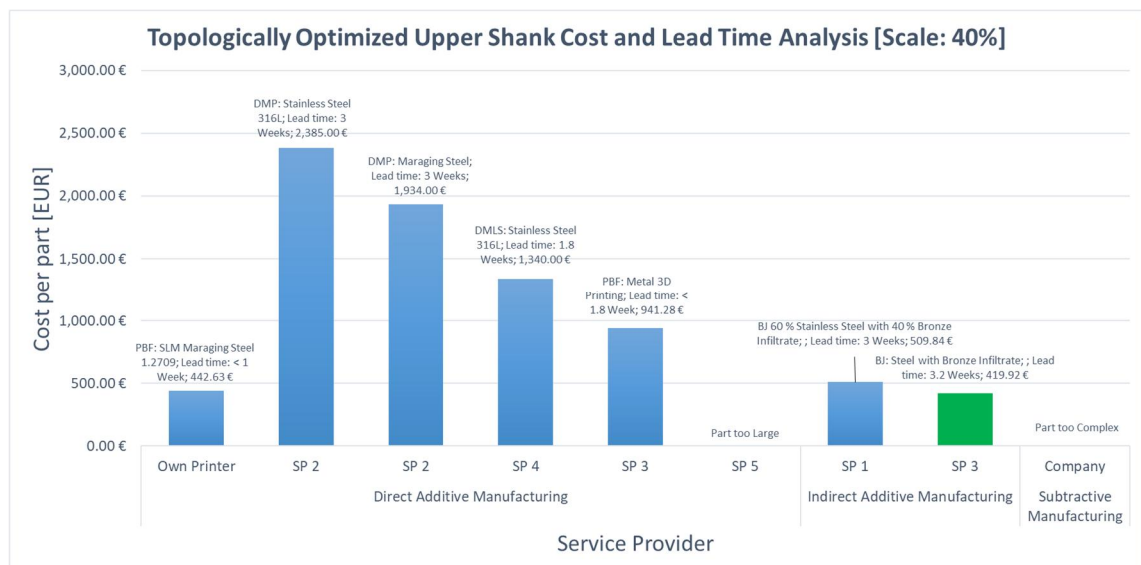


Figure 54. Optimized Upper Shank with original dimensions of 442.6mm x 77mm x 118.3mm.

A scale of 40% was selected in order to evaluate the comparison of costs and lead times between direct and indirect metal AM methods. Another reason for selecting this specific scale was the fact that it fulfilled the selected budget for eventually printing a prototype of the model. Figure 54 shows the dimensions of the original model. Graph 34 shows the cost and lead time analysis of the rescaled model. It can be observed that Metal 3D Printing from SP3 offers approximately the same cost per part as of the original fully scaled model made from subtractive manufacturing method at the benefit of 55 % faster lead-time. According to this analysis, it can be deduced that the indirect AM method from SP3 shows the most economic method in terms of cost with a lead time of 3.2 weeks represented by green colour in Graph 34.



Graph 34. Upper Shank quotations and lead times with a scale of 40%.

6.2.7 Static Analysis: Final Baseline

As a result of the preliminary iteration process, indirect BJ process for metals from SP3 proved to be the most economical choice in terms of cost for manufacturing the 40% rescaled model of the topologically optimized design. In order to go ahead with manufacturing a prototype of the rescaled model, an advanced topology optimization was performed in which ASTM E8 tested material properties of Stainless Steel infiltrated with Bronze were used according to the published data sheet from SP3.

6.2.7.1 Material Properties

Upper Shank was assigned ASTM E8 tested material properties of SP3 stainless steel as shown in the following table. According to the data sheet, the material did not exhibit anisotropic properties. This is due to the high intensity of heat treatment process through which isotropic properties are achieved.

Table 39. Material Properties of SP3 Stainless Steel.

SP3 Stainless Steel infiltrated with Bronze	
Density	7860 [Kg/m ³]
Young's Modulus	147000 [MPa]
Poisson's Ratio	—
Coefficient of Thermal Expansion	1.34×10^{-5} [/K]
Tensile Yield Stress (0.2% offset)	455 [MPa]

6.2.7.2 Loading and Boundary Conditions

An axial and vertical force of 1025.875 N and 981 N respectively, are applied to each pinhole of the shank represented by red arrows. The standard keyways of 8x62x68 DIN 5462 are removed and a cylindrical hole is created at a radius of 65mm, equivalent to the mid-value of the outer and inner diameter of the keyways for simplicity and mass conservation. A rigid support is applied represented by a red cylindrical constraint in Figure 55.

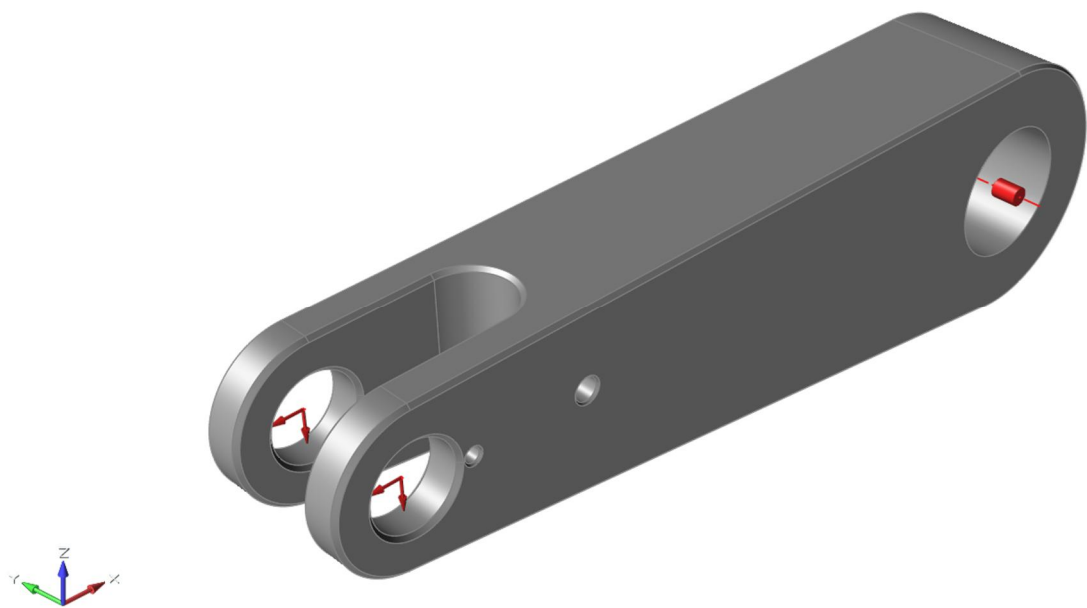


Figure 55. Loading and Boundary Conditions of the original design.

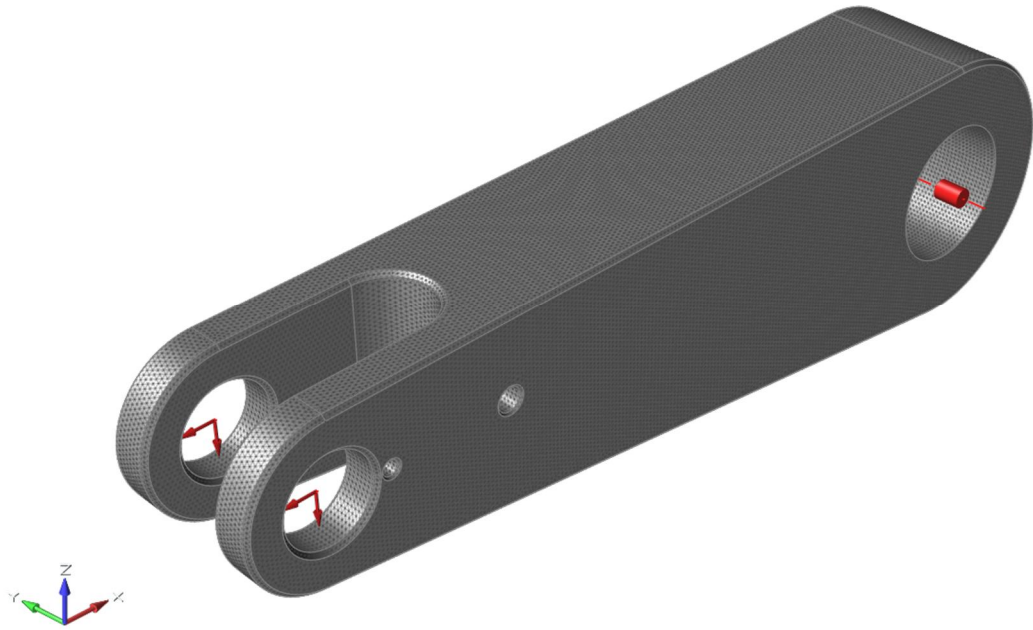


Figure 56. Upper Shank with a mesh size of 2 mm.

6.2.7.3 Results

6.2.7.3.1 Von Mises Stress

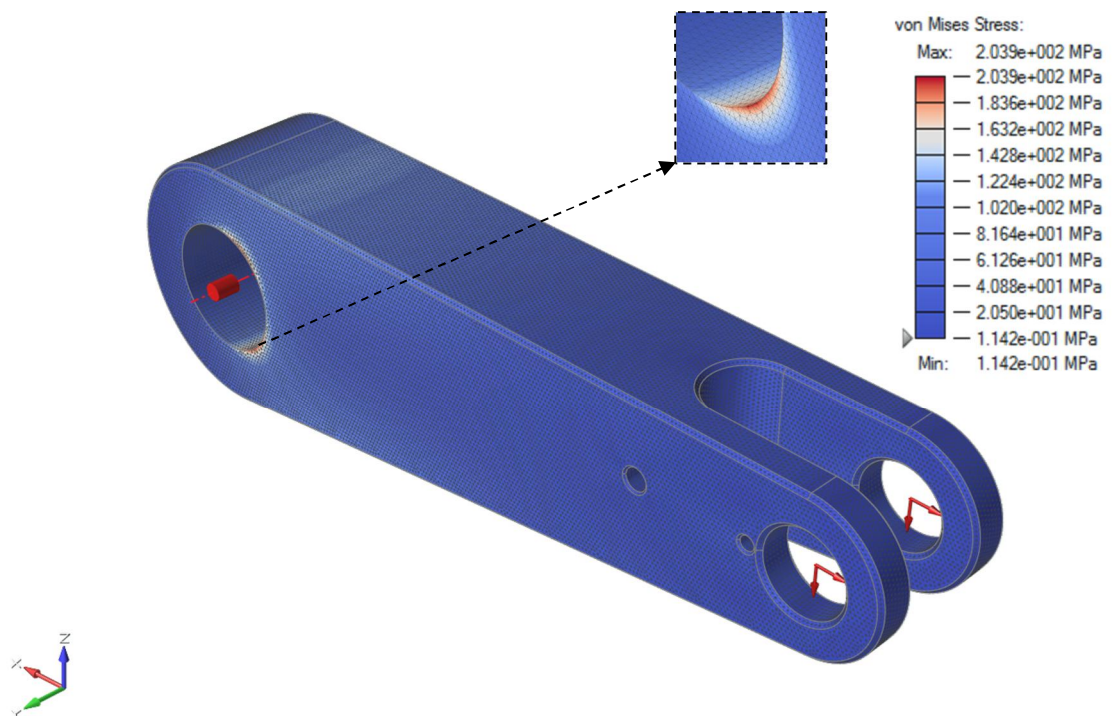


Figure 57. A maximum Von Mises stress of 203.93 MPa is observed in the vicinity of the cylindrical support.

$$\text{Factor of safety: } FOS = \frac{455}{203.93} = 2.23 \approx 2.2 \quad (44)$$

As observed from above Figure 57 and the factor of safety, the blue region occupies a non-existence level of stress which can be used as an opportunity for enhancing the performance of the part through topology optimization.

6.2.7.3.2 Deformation

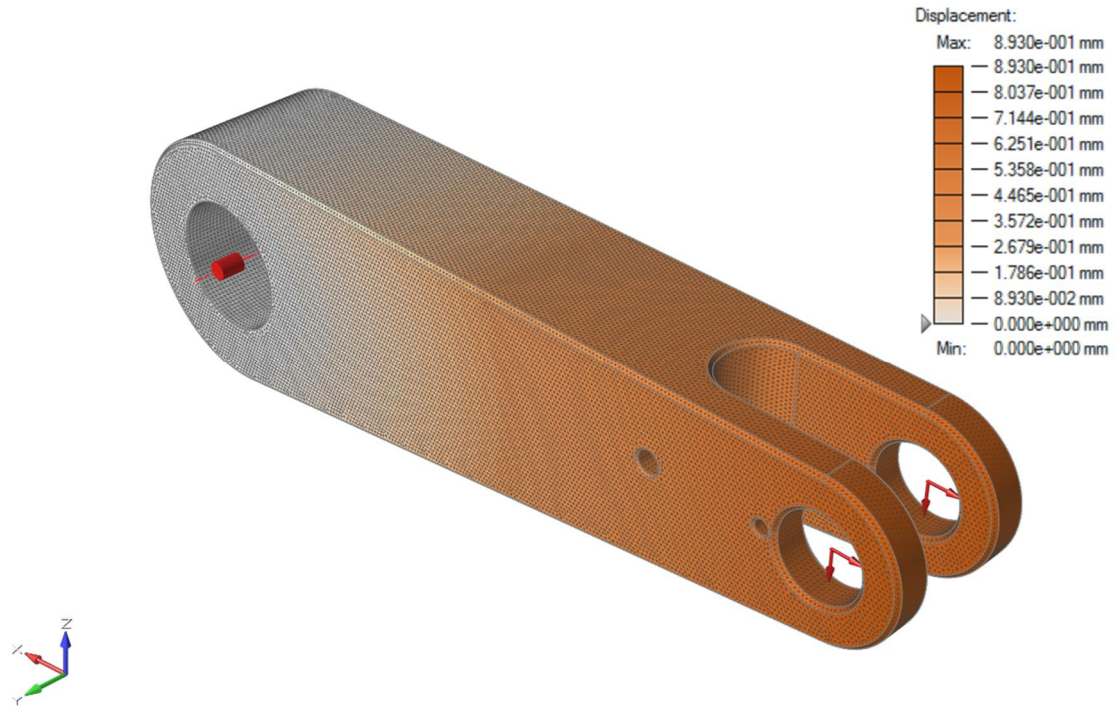


Figure 58. A maximum deformation of 0.8930 mm is observed at the edge of the part near the loads.

$$0.8930 \text{ [mm]} < Deformation_{allowable} ; \text{Within Range} \quad (45)$$

Table 40. Upper Shank Original Properties

Upper Shank Properties							
Iteration [No.]	Material [Prop.]	Volume [mm³]	Mass [Kg]	Weight [N]	Max. Von Mises Stress [MPa]	Max. Displacement [mm]	Factor of Safety
Original_0	Inspire Steel	2.74e+06	21.53	211.21	188.11	0.569	1.9
1	Inspire Steel	1.45e+06	11.39	111.74	245.23	0.706	1.4
Original_1	SP3 Steel	2.74e+06	23.75	232.99	203.93	0.8930	2.2

6.2.8 Topology Optimization Final Iteration

In order to enhance the performance as well as cost effectiveness of upper shank for the selected AM method, an advanced design space was determined for topology optimization, which incorporated higher volume of the component. The optimization process and its results are explained in the subsequent text.

6.2.8.1 Loading and Boundary Conditions

An axial and vertical force of 1025.875 N and 981 N respectively, are applied to each pinhole of the shank represented by red arrows. The standard keyways of 8x62x68 DIN

5462 are removed and a cylindrical hole is created at a radius of 65mm, equivalent to the mid-value of the outer and inner diameter of the keyways for simplicity and mass conservation. A rigid support is applied represented by a red cylindrical constraint in Figure 59. The brown region illustrates the design space of the optimization presented in Figure 60.

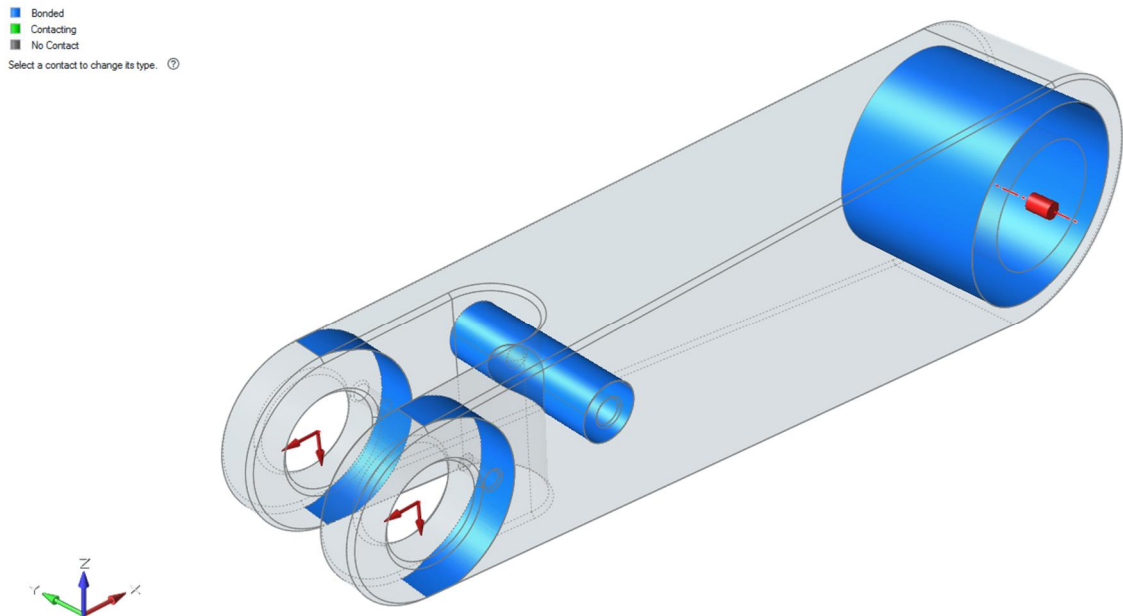


Figure 59. Upper Shank contact surfaces with respect to loading conditions, boundary conditions and design space.

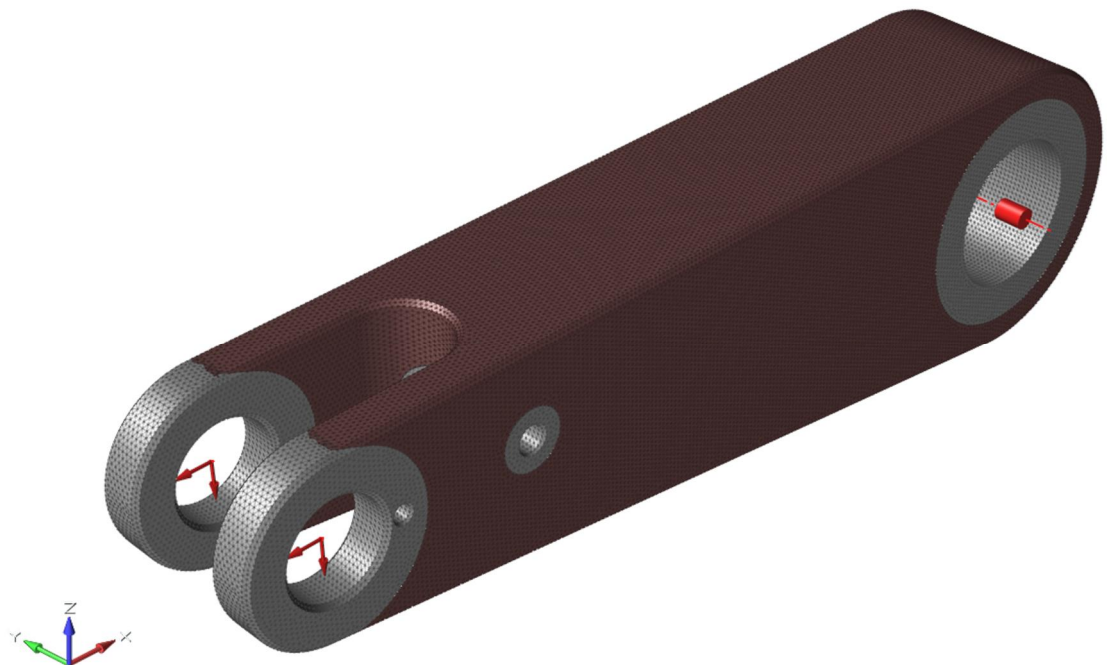


Figure 60. Upper Shank with a mesh size of 2mm and design space represented by brown region.

6.2.8.2 Results

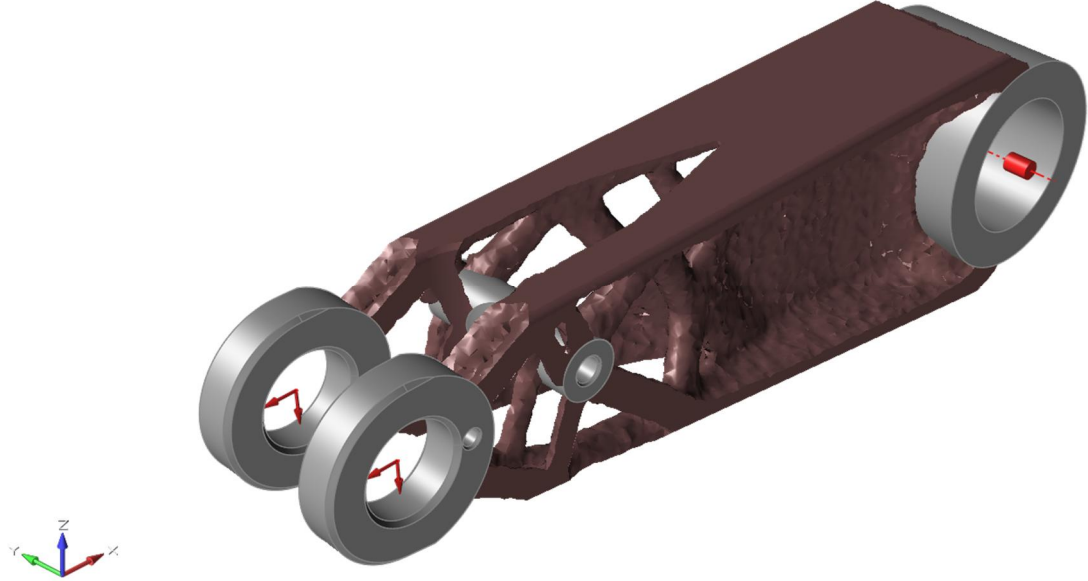


Figure 61. The result of raw topology optimization.

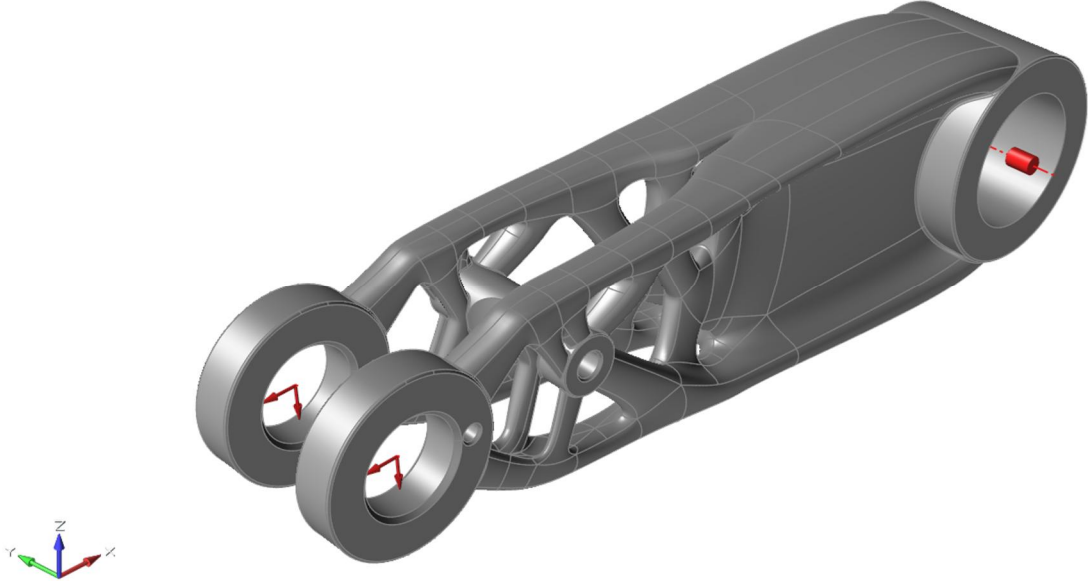


Figure 62. The result of surface modelled topology optimization.

6.2.8.2.1 Von Mises Stress

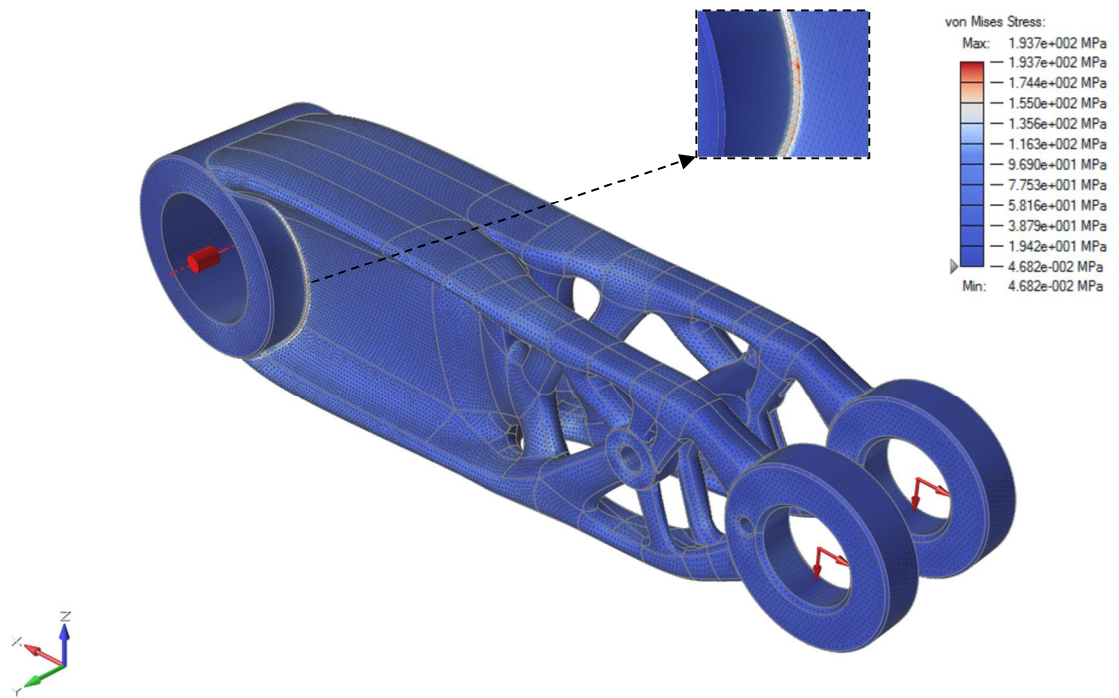


Figure 63. Upper Shank illustrating a maximum Von Mises Stress of 193.75 MPa.

$$\text{Factor of safety: } FOS = \frac{455}{193.75} = 2.35 \approx 2.3 ; \text{Within Range} \quad (46)$$

6.2.8.2.2 Deformation

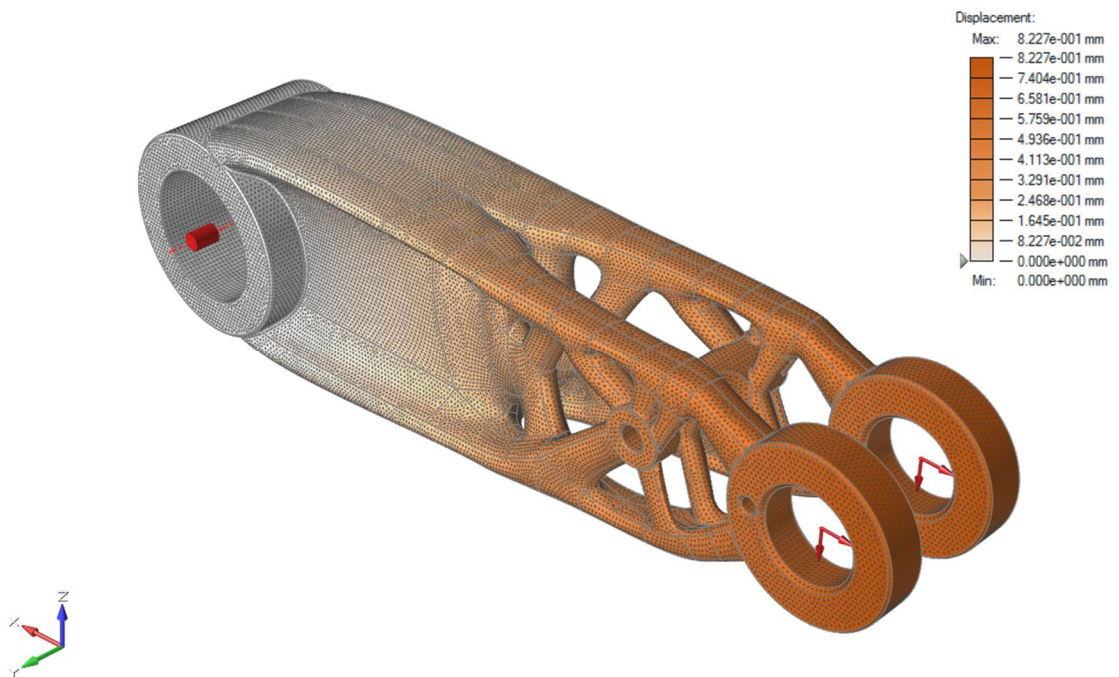


Figure 64. Upper Shank illustrating a maximum deformation of 0.8227 mm.

$$0.8227 \text{ [mm]} < \text{Deformation}_{\text{allowable}} ; \text{Within Range} \quad (47)$$

Table 41. Upper Shank Properties of Final Iteration

Upper Shank Properties							
Iteration [No.]	Material [Prop.]	Volume [mm³]	Mass [Kg]	Weight [N]	Max. Von Mises Stress [MPa]	Max. Displacement [mm]	Factor of Safety
Original_0	Inspire Steel	2.74e+06	21.53	211.21	188.11	0.569	1.9
1	Inspire Steel	1.45e+06	11.39	111.74	245.23	0.706	1.4
Original_1	SP3 Steel	2.74e+06	23.75	232.99	203.93	0.8930	2.2
2	SP3 Steel	1.48e+06	12.81	125.67	193.75	0.8227	2.3

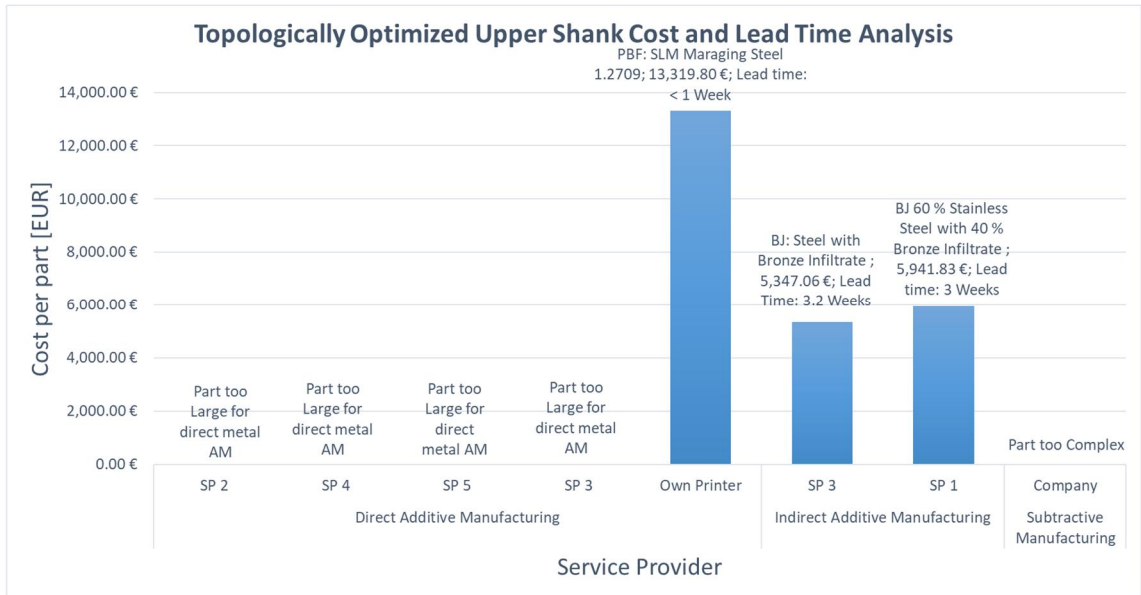
6.2.9 Conclusion

As seen from Upper Shank properties of the final iteration from Table 41, the performance of the component has been enhanced with respect to the material, mass, weight, volume, maximum stress, maximum displacement and factor of safety. The yield of the material is increased by 21.98% with a value of 100 MPa. This is due to the fact that the metal AM via BJ process undergoes excessive heat treatment during debinding, sintering and infiltration after the green-part has been additively manufactured. The mass and weight is reduced by 40.50 % and the volume of the component is decreased by 45.99% compared to the Original_0 model. The maximum Von Mises stress is decreased by approximately 5% compared to Original_1 model and increased by roughly 3 % compared to Original_0 model. The decrease in Von Mises stress of the final iterated model compared to Original_1 can be explained due to the truss based design of the iterated model which has greater tendency to be loaded in tension and compression throughout the truss members rather than having pure bending at the constrained hinge. Finally, the factor of safety is increased approximately 17.39 % in contrast to Original_0 model.

6.2.10 Final Cost and Lead Time Analysis

After re-inserting the standardized keyways of 8x62x68 DIN 5462 and converting the 3D data of the final iterated model to STL, the cost per part and its associated lead time are calculated for indirect and direct metal AM as shown in Graph 35. According to the results, the size of optimized component is still too large for direct metal printing from four major AM service providers and its design is too complex for conventional subtractive manufacturing.

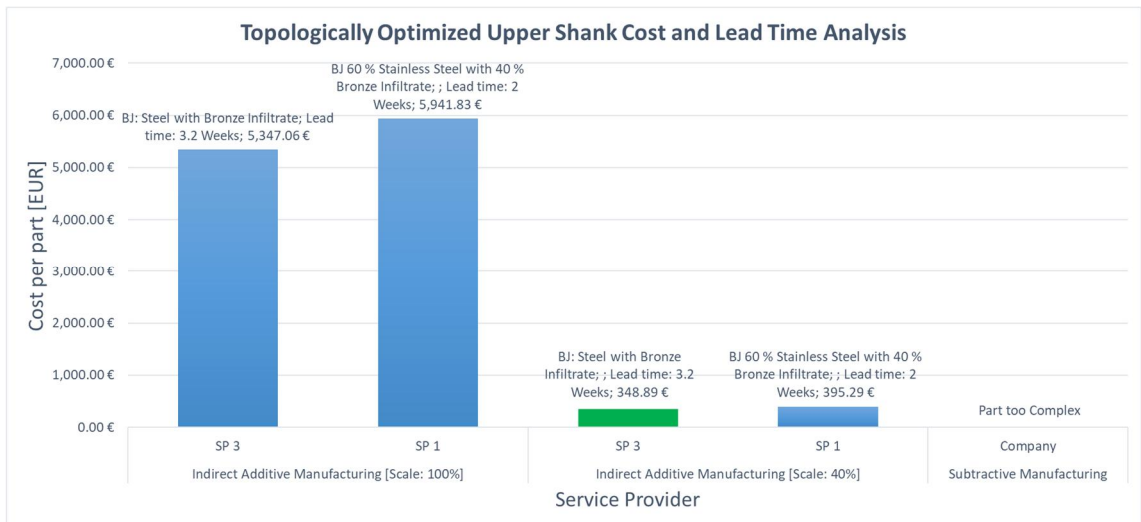
In contrast to the direct metal AM of original design presented in Section 5.2.2, the cost per part of direct metal AM of the optimized model is decreased by approximately 3% with relatively similar lead time of less than 1 week. Even though there is a mass reduction of approximately 41%, such a small percentage of cost reduction can be explained by the fact that metal support structures are always required for direct metal AM and the percentage of supports is increased from approximately 3% for the original model to 12% for the optimized model due to higher level of design complexity. Furthermore, the cost per part of indirect AM is decreased up to 46% with relatively the same lead time of 3 weeks. This is because no support structures are required for indirect metal AM via BJ as the part is supported by the powder bed. Since BJ method for metals requires a secondary process involving debinding, sintering and infiltration, the difference in lead time is negligible.



Graph 35. Cost and lead time analysis of topologically optimized Upper Shank.

6.2.10.1 Final Prototype

In accordance to the results of the preliminary prototype analysis explained in Section 6.2.6.1, indirect metal AM offers the most economical method for additively manufacturing the topologically optimized Upper Shank. Hence, Graph 36 illustrates the cost and lead time analysis of the original and scaled models for indirect metal AM through BJ.



Graph 36. Upper Shank quotations and lead times for the original and scaled model.

As a result of this analysis, a 40% scaled model is additively manufactured for prototyping purposes after geometrical preparation according to the design specifications of the indirect metal AM through BJ from SP3. The model was slightly reconfigured to take into account the minimum wall thickness of 1mm in the vicinity of the rescaled M8 holes. The final version of the rendered model and the metallic prototype can be seen in Figure 65.



Figure 65. A Rendered Image of CAD model (Left) and metallic prototype (Right) of the final optimized model of Upper Shank.

7 Verification

The operational environment of the spare parts analysed in this study differentiates from variable levels of mechanical stress and variable intensities of corrosion. Stress is generally defined as the force distributed over an area (Collins, 2003). While corrosion may have multiple forms, it is generally defined as a process created by the interaction or reaction between material such as a metal or an alloy and its environment that results in deterioration or degradation of that material and its properties (S. Covino Jr. & Cramer, 2008).

For the purpose of verifying the ultimate tensile strength and corrosion resistance of the additively manufactured metal spare parts, two metals that are Stainless Steel and Titanium were selected and their specimens were printed in accordance to the tensile and corrosion testing. Stainless Steel is the most common among spare parts and Titanium is also typically used in the industry and offers relatively higher strength and corrosion properties. Since directly and additively manufactured metal parts through PBF consist of different material properties, surface roughness and possible build errors in different directions, the specimens were printed in horizontal orientation as well as vertical orientation. Figure 66 and Figure 67 illustrate an example specimen of Stainless Steel 316L and Titanium Ti64 with rounded dimensions, respectively. Table 42 presents a summary of the printed specimens. In addition, corrosion test specimens of bulk material of Titanium and Stainless Steel are also prepared in order to correlate the difference in corrosion behaviour of printed and bulk materials. In case of Stainless Steel, two bulk materials are used with European standard of 1.4404 and 1.4432 which mainly differ in their composition of Molybdenum content. The European standard of 1.4404 consists of 2.50% of molybdenum whereas, EN 1.4432 contains 3.00% of Molybdenum. The reason for using two bulk materials was due to the fact that the printed stainless steel 316L had a variable composition of Molybdenum ranging from 2.25% to 3.00%. The supports of the horizontally printed specimens were removed using electron discharge machining and supports of the vertically printed specimens were removed by means of grinding. The subsequent text presents the results accumulated according to the behaviour of the specimens from corrosion tests conducted at Outotec Research Centre and tensile tests conducted at Aalto University.



Figure 66. A specimen of additively manufactured Stainless Steel 316L with dimensions of 60mm x 10mm x 5mm.



Figure 67. A specimen of additively manufactured Titanium Ti64 with dimensions of 60mm x 10mm x 3mm.

Table 42. Summary of the printed specimens.

Summary of the Additively Manufactured Metal Specimens			
Specimen	Additive Manufacturing Orientation		Total [No.]
	Horizontal	Vertical	
Stainless Steel 316L [No.]	18	18	36
Titanium Ti64 [No.]	18	18	36
Total [No.]	36	36	72

7.1 Corrosion Testing

While corrosion may have many forms, additively manufactured or printed specimens are evaluated with respect to the resistance against typical uniform and localized corrosion. According to Phull, (2008), uniform corrosion is defined as an attack on an exposed surface of a metal that leads to homogenous loss of thickness and according to S. Covino Jr. & Cramer (2008), localized corrosion is defined as corrosion that takes place at discrete locations on a material. Table 43 presents the summary of the nomenclature for the laboratory testing in a controlled test environment. The variables of the environment include dissolved gases, temperature, volume and flow of the solution and exposure time (Phull, 2008). The corrosion resistance of Titanium is evaluated through 3 independent test environments or solutions and the corrosion resistance of Stainless Steel is evaluated through 4 independent test environments as illustrated in Table 43. The test environments or solution types include acidified chloride, sulfuric acid, oxidizers and chlorides. The acidity refers to the hydrogen ion concentration and oxidizers refer to the oxidizing power or electrochemical potential which have an impact on oxidation of the surface of an alloy leading to corrosion mechanism. Chlorides refer to chloride content which has been reported to act as an accelerator for corrosion rate and to promote localized corrosion (S. Covino Jr. & Cramer, 2008). The difference between solution number 2 and 3 for Titanium and 4 to 6 for Stainless Steel is the concentration of oxidizers and chloride content, respectively. The duration of 1 week refers to uniform corrosion testing and the duration of 4 weeks refers to localized corrosion testing as listed in Table 43. The dependent variables of the tests are mass loss and presence of localized corrosion. The mass loss is evaluated by subtracting the mass of the tested/exposed specimen from the mass of that original/unexposed specimen. The presence of localized corrosion is verified by visual observation.

Table 43. Corrosion test summary.

Corrosion Laboratory Test Nomenclature Summary					
Specimen Material	Specimen Coupons [Code]		Test Environment / Solution Type	Solution Number [No.]	Duration [Weeks]
	AM Orientation				
	H:Horizontal	V:Vertical			
Titanium	1-4	1-4	Acidified Chloride	1	4
Titanium	5-8	5-8	Sulfuric Acid + oxidizers	2	1
Titanium	9-12	9-12	Sulfuric Acid + oxidizers	3	1
Stainless Steel	1-3	1-3	Sulfuric Acid + chlorides	4	4
Stainless Steel	4-6	4-6	Sulfuric Acid + chlorides	5	4
Stainless Steel	7-9	7-9	Sulfuric Acid + chlorides	6	4
Stainless Steel	10-12	10-12	Sulfuric Acid	7	1

7.1.1 Uniform Corrosion

Uniform corrosion, also known as general corrosion is measured as loss of metal thickness per unit time in a controlled test environment. The uniformity of the mass loss is observed visually and the corrosion rate is calculated according to Equation 48 as per Phull, 2008.

$$Corrosion_{Rate} = \frac{(K \times W)}{(A \times t \times \rho)} \quad (48)$$

Where $Corrosion_{Rate}$ is the corrosion rate [mm/y]
 K is a unit conversion constant, in this case, it is 8.76×10^4
 W is mass loss [g]
 A is the exposed specimen area [cm²]
 t is time [hours]
 ρ is the density of the material [g/cm³]

The results of the uniform corrosion of the test environment or solution number 2, 3 and 7 are presented in Figure 68 as a, b and c, respectively in accordance to the ranking of corrosion rate presented in Table 44. A detailed analysis is presented in Appendix 3A.

Table 44. Ranking criteria of uniform corrosion rate. (Outokumpu Stainless AB, 2009)

Legend		
Rank	Corrosion rate	Description
	<0.1 mm/y	Material is corrosion resistant.
	0.1-1.0 mm/y	Material is not corrosion resistant but useful in certain cases.
	>1.0 mm/y	Serious corrosion: Material is not usable.

Titanium			Titanium			SS 316L		
Solution nr.	Sample code	Corrosion rate [mm/y]	Solution nr.	Sample code	Corrosion rate [mm/y]	Solution nr.	Sample code	Corrosion rate [mm/y]
2	5V	2.41E-02	3	9V	*	7	10V	4.27E-01
	6V	2.31E-02		10V	2.01E-02		11V	4.08E-01
	7V	2.11E-02		11V	*		12V	1.60E-02
	8V	2.31E-02		12V	1.61E-02	7	10H	1.54E+00
2	5H	2.10E-02		3	9H		2.10E-02	11H
	6H	1.91E-02	10H		1.63E-02		12H	7.82E-01
	7H	1.91E-02	11H		2.01E-02	7	1.4404	3.99E-03
	8H	1.82E-02	12H		1.72E-02	7	1.4432	1.36E-03
2	Bulk	2.23E-03	3		Bulk	3.26E-03		

*Signifies mass gain due to deposition

Figure 68. Results of the uniform corrosion according to the material, test environment and specimen. (Results modified with permission: Courtesy of Outotec Research Centre)

According to the results, it can be deduced that Titanium specimens, additively manufactured through PBF process are corrosion resistant regardless of their printing orientation being horizontal or vertical since their corrosion rate is well below 0.1 mm per year threshold for being uniformly corrosion resistant. In addition, the difference between the printed specimens and bulk specimen is negligible. This can be due to the fact that the test environments were not aggressive enough to deteriorate the material of the specimens. The test environments of the Titanium specimens were devised based on the results of Titanium Grade 2. A higher corrosion rate may be achieved if the Titanium specimen are tested based on results of higher Titanium grade. For instance, direct metal AM via PBF of Grade 5 Ti-6Al-4V exhibits inferior corrosion resistance compared to that of rolled sample according to Yang, et al. (2017). No corrosion rate is calculated for two specimens as seen in Figure 68b because the mass of the specimens was increased due to deposition which cannot solely be removed by cleaning the specimens.

Furthermore, high levels of uniform corrosion are detected for printed Stainless Steel 316L specimens according to Figure 68c while both bulk materials have not been affected. The orientation of the printed samples also has an impact on the rate of corrosion. It is observed that horizontally printed specimens are more prone to corrosion than vertically printed specimens. By recalling the principle of direct metal AM through PBF, the cause of this behaviour can be interpreted. PBF process involves fusion of powder bed region on a layer by layer basis by using thermal energy. The depth of this impinging thermal energy exceeds that of the layer thickness in order to re-melt portion of the existing solidified layer to form a fully bonded solid structure. This leads to the notion that the last layer of the top face of the specimen consists of the least heat treated region and the first layer of the specimen other than the support structures consists of the second least heat treated region. Now, when the specimen is printed vertically, it has the least amount of bottom, back and top, face print surface area whereas, when the specimen is printed horizontally, the bottom and top print surfaces contain the highest amount of surface area. Since less heat treated region exhibits different morphology of the microstructure of the material, this can lead to smaller microstructures and corrosion mechanism. Corrosion rate is observed to decrease over increasing annealing time according to Fritz (2008). As

a result, additively manufactured Stainless Steel 316L is not corrosion resistant as wrought stainless steel EN 1.4404 and EN 1.4432 in very aggressive environments however, it can be useful in certain cases if the printing orientation of the specimen is vertical leading to smaller surface area of the face and back print.

7.1.2 Localized Corrosion

Localized corrosion in this case is identified through visual examination for pitting corrosion and the extent of pitting is measured through mass loss. The results of Titanium specimens can be seen in Figure 69 and the results of stainless steel can be seen in Figure 70 according to the ranking criteria presented in Table 45. The detailed analysis including the extent of pitting identified through mass loss is attached in Appendix 3B.

Table 45. Ranking criteria of localized corrosion based on visual inspection. (Outokumpu Stainless AB, 2009)

Legend	
Rank	Description
	No localized corrosion
	Localized corrosion with increasing intensity

Titanium		
Solution nr.	Sample code	Rank
1	1V	
	2V	
	3V	
	4V	
1	1H	
	2H	
	3H	
	4H	
1	Bulk	

Figure 69. Result of localized corrosion of Titanium with respect to test environment and specimen. (Results: Courtesy of Outotec Research Centre)

SS 316L			SS 316L			SS 316L		
Solution nr.	Sample code	Rank	Solution nr.	Sample code	Rank	Solution nr.	Sample code	Rank
4	1V		5	4V		6	7V	
	2V							
	3V							
4	1H			4H				
	2H							
	3H							
4	1.4404		5	1.4404		6	1.4404	
4	1.4432		5	1.4432		6	1.4432	

Figure 70. Result of localized corrosion of Stainless Steel with respect to test environment and specimen. (Results: Courtesy of Outotec Research Centre)

As per the results of Titanium specimens shown in Figure 69, no localized corrosion is observed regardless of the orientation of the print direction. The causes of the results are

in line to those presented for uniform corrosion of Titanium specimens explained in Section 7.1.1.

According to the results of Stainless Steel, SS specimens, printed specimens regardless of print orientation as well as EN 1.4404 Stainless Steel specimens with low Molybdenum content are affected by localized corrosion in all test environments whereas, EN 1.4432 Stainless Steel specimens with higher Molybdenum content did not show signs of localized corrosion in all test environments. The most severely affected specimens of localized corrosion can be seen in Figure 71. The difference between the SS 1.4404 and printed SS 316L is the morphology of the localized damage. SS 1.4404 illustrated widespread pits in terms of quantity and had a higher mass loss whereas, the printed SS 316L had substantially deeper corrosion pits. The occurrence of localized corrosion presented a scatter that is inherent to it. According to the setup, the chloride content of the test environment is increased from solution 4 to 6 presented in Figure 70 a to c, respectively. It can be observed that the chloride content had an impact on initiation of localized corrosion because the intensity of localized corrosion is higher in Figure 70 b and c than a. The intensity of localized corrosion in Figure 70 c is observed to be less than the one presented in Figure 70 b. Since the intensity of localized corrosion is not directly proportional to the higher chloride content, it can be deduced that the chloride content did not have an effect on the propagation of localized corrosion. A similar conclusion can be reached by observing the extent of localized corrosion through mass loss presented in Appendix 3B because the mass loss is not directly proportional to the increase in chloride content of the test environments. As a result, additively manufactured Stainless Steel 316L and conventionally manufactured EN 1.4404 Stainless Steel are more prone to localized corrosion compared to EN 1.4432 Stainless Steel.

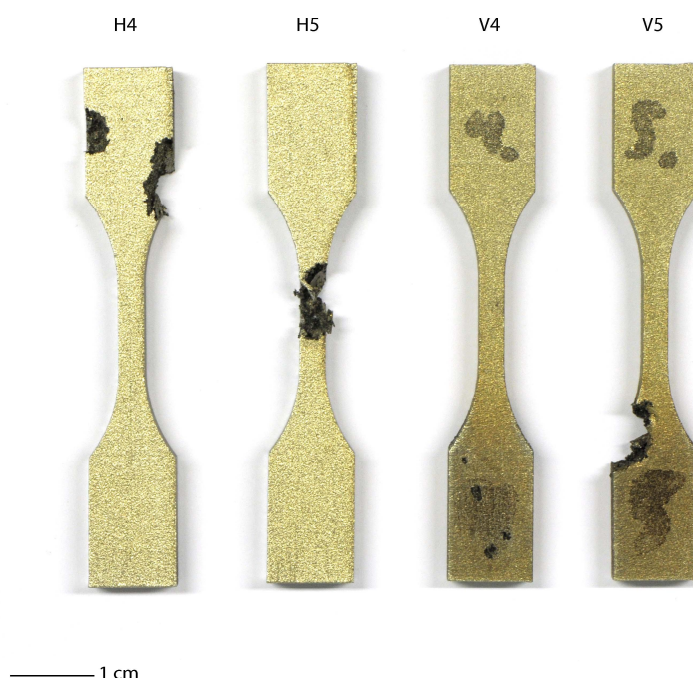


Figure 71. Result of the most severe localized corrosion of additively manufactured Stainless Steel 316L obtained from test environment/solution number 5 as presented in Figure 70 b. (Results: Courtesy of Outotec Research Centre)

7.2 Tensile Testing

A uniaxial tensile testing is performed to evaluate the ultimate tensile strength of additively manufactured Titanium and Stainless Steel specimens including the specimens which had undergone corrosion testing. As per Holt, 2000, a tensile test simply involves gripping the opposite ends of a test specimen and applying tensile force within the load frame of a test machine until gradual elongation fractures the test specimen. The test machine used for this analysis is MTS 858 Material Testing System. The independent variable of the test is the speed of testing which is calculated to be 0.75 mm/min according to the specimen geometry and the SFS EN ISO 6892 standard. The dependent variable of the test is the axial force measured in kilonewtons required to maintain the speed of testing until fracture of the specimen. Subsequently, the axial displacement and the axial force for each specimen is recorded and the engineering stress and strain are calculated. The averaged longitudinal engineering stress is measured by the following Equation 49 as per Dieter (2000).

$$s = \frac{P}{A_0} \quad (49)$$

Where s is the engineering stress [MPa]
 P is the applied load [kN]
 A_0 is the original cross-sectional area of the specimen [mm²]

Furthermore, the ultimate tensile strength is defined as follows according to Equation 50 (Dieter, 2000):

$$s_u = \frac{P_{max}}{A_0} \quad (50)$$

Where s_u is the ultimate tensile strength [MPa]
 P_{max} is the maximum load that is applied [kN]
 A_0 is the original cross-sectional area of the specimen [mm²]

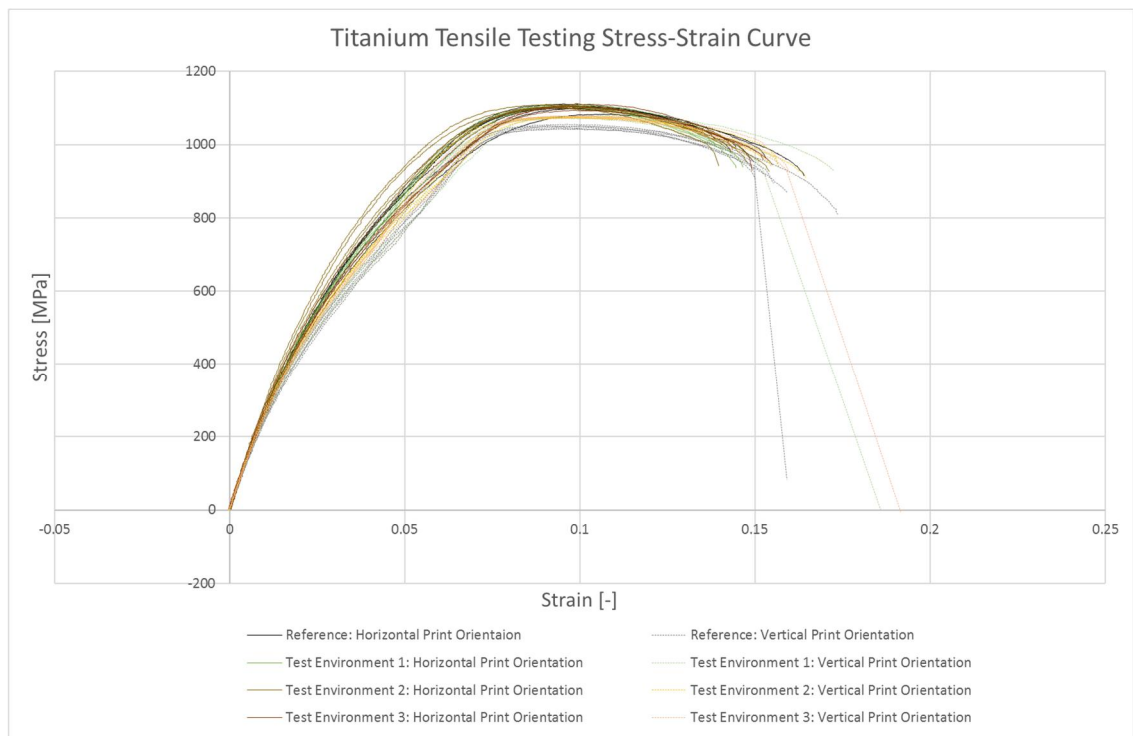
The average linear engineering strain is calculated by the following Equation 51 as per Dieter (2000).

$$e = \frac{\delta}{L_0} = \frac{\Delta L}{L_0} = \frac{L - L_0}{L_0} \quad (51)$$

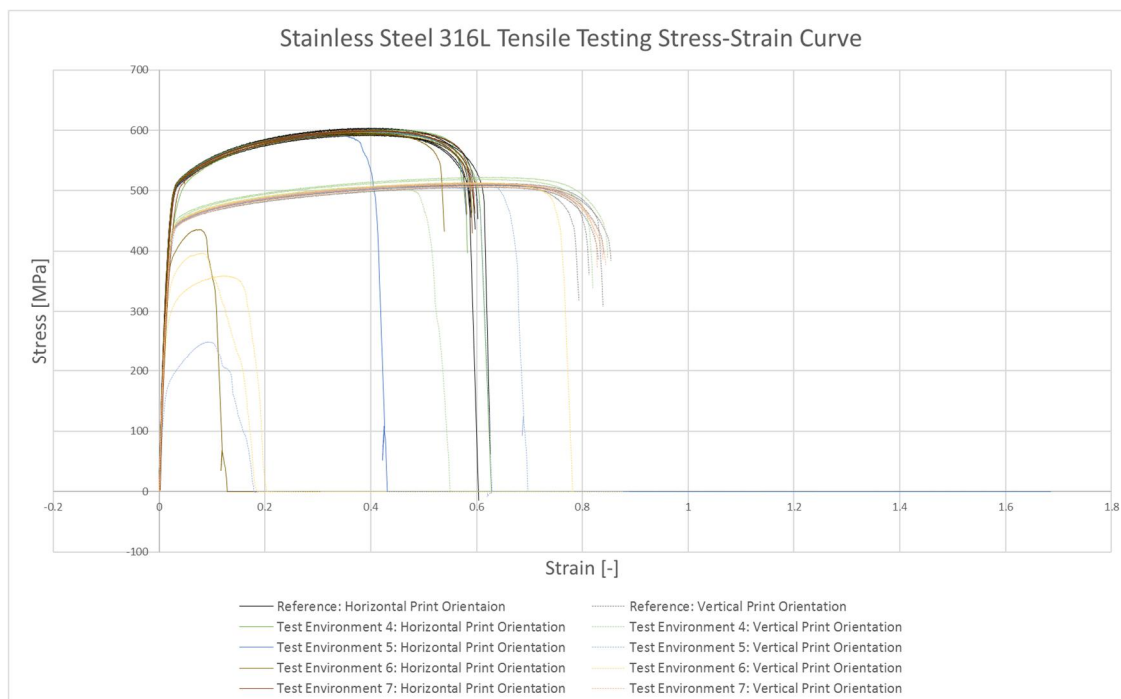
Where e is the engineering strain [-]
 δ is the elongation of the gauge length of the specimen [mm]
 L is the final gauge length of the specimen [mm]
 L_0 is the original gauge length of the specimen [mm]

The acquired and processed data is eventually plotted by means of Stress-Strain curves to evaluate the ultimate tensile stress of the specimens. The Stress-Strain curves for printed Titanium specimens are shown in Graph 37 and the Stress-Strain curves for Stainless Steel are shown in Graph 38. The solid curves represent horizontally printed specimens and the dashed lines represent the vertically printed specimens.

Based on the data presented in Graph 37, it can be observed that the ultimate tensile strength of additively and horizontally manufactured Titanium specimens is approximately 1100 MPa for all test environments including the reference specimens. This is due to the fact that no signs of corrosion were observed in all test environments. On the other hand, the ultimate tensile strength of additively and vertically manufactured Titanium specimens is approximately 1050 MPa for the reference specimens and 1075 MPa for all test environments. This slight increase of approximately 2 % in ultimate tensile strength of the corrosion tested specimens can be explained by the fact that the specimens were held at elevated temperature for considerably long corrosion test duration. As a result, the anisotropy of Titanium printed specimen can be estimated to be 5% with higher strength in horizontal build orientation.



Graph 37. The Stress-Strain behaviour of additively manufactured Titanium specimens by means of reference and corrosion test environments.



Graph 38. The Stress-Strain behaviour of additively manufactured Stainless Steel specimens by means of reference and corrosion test environments.

Based on the data presented in Graph 38, it can be observed that the ultimate tensile strength of additively and horizontally manufactured Stainless Steel specimens is approximately 595 MPa for the reference specimens and the specimens which had undergone corrosion testing. On the other hand, the ultimate tensile strength of additively and vertically manufactured Stainless Steel specimens is approximately 520 MPa for the reference specimens and the specimens which had relatively survived corrosion testing. The intensity of corrosion is observed to be inversely proportional to the ultimate tensile strength of the specimens. This is due to the fact that mass loss due to uniform or localized corrosion decreased the cross-sectional area of the specimen over which the force is distributed. As a result, the anisotropy of the printed Stainless Steel is approximately 13% in favour of the horizontal print orientation. The trailing values of some specimens are recorded since the machine was unable to automatically detect fracture of the specimens. Only one horizontally printed specimen, H5 was not tested due to extreme severity of localized corrosion that it had sustained. Two vertically printed specimens, V5 and V7 did not fracture within the gauge area due to localized corrosion on the fillet of the specimens. These specimens are represented by the two smallest curves with lowest ultimate tensile strength in Graph 38. In addition, vertically printed Stainless Steel specimens exhibited approximately 33% more strain than that of the horizontally printed specimens. This behaviour can be explained by the layer by layer build nature of the AM process which is most sensitive to variation in vertical direction as observed from lower ultimate tensile strength. Hence, metallic bonds between the layers are more prone to stretching and dislocating than the metallic bonds of the layers.

8 Discussion

8.1 Results

As the patented restrictions imposed by major key players of AM are coming to an end, the technology in AM industry is developing on a continuous scale with introduction of game-changing startups and services. This has induced considerable amount of competition that is changing the dynamics of AM industry. This master's thesis has provided the current affairs with respect to cost effective implementation of AM by means of an industrial spare part service. When delivering the product to the customer as soon as possible is of crucial importance due to exponential setbacks of costs originating from the downtime of equipment, AM is the key because it has provided faster lead times for all cases analysed in this study. Applications that are satisfied by polymer components should be utilized for good advantage since AM has made moulds of IM obsolete and as a result proved to be economical up to considerable amount in case of IM components and SM components evaluated in this study. To date, Metal AM remains expensive to manufacture according to all 8 metal AM spare parts that were analysed in this study. Indirect metal AM was economical compared to direct metal AM in all cases. Spare parts that are considerably larger for indirect (762mm x 393mm x 393mm) and direct (400mm x 400mm x 400mm) metal AM should not be overlooked as 22% of the spare parts that were considered for AM rapid tooling to assist casting proved to be economical to manufacture when lead time was not as important. However, optimization methods can be opted to decrease costs further and increase the performance of not only the spare part itself but also the equipment that it operates. In this study, the cost of a lifting component, Upper Shank was decreased by 46% in case of indirect metal AM and at the same time, its performance was increased by 17% in terms of yielding of the material and by 40% in terms of mass reduction. All in all, a considerable amount of 53% of all spare parts analysed in this study proved to be economical and faster to manufacture through AM. This serves as a proof of concept that AM can be used to save costs when it comes to low volume production, short lead time and higher performance. The verifications and validations conducted in this study prove that directly and additively manufactured Stainless Steel spare parts can be used in mild corrosion environments in hydrometallurgical industry whereas directly and additively manufactured Titanium spare parts can be functional in extreme corrosion environments in hydrometallurgical industry. The tensile tests performed in this study compliment those of the published literature where anisotropic nature of the direct metal AM is observed by horizontal and vertical print orientations. The performance of these spare parts can be maximized by ensuring that the maximum loads are projected onto the horizontal build orientation of the part.

8.2 Challenges

The accessibility of data was challenging with regards to receiving quotations from selected service providers and with regards to receiving loading and boundary conditions of industrial components. In case of polymer materials, the quotations including the lead times were rather easily obtained through the online quotation algorithms of the service providers up to an extent after which the algorithms failed to calculate the lead time and/or cost of the component(s). Hence, small series production cost and lead time analyses were performed by extensively contacting each service provider. The service providers also faced difficulties in providing such data since their production capacity, current and pending orders effected the lead time as well as the cost especially in case of expedited scenario. In case of metallic materials, the level of difficulty for obtaining the data varied by

means of indirect metal AM and direct metal AM. Indirect metal AM quotations were easily received from the online calculators of respective service providers whereas, the quotation for direct metal AM could only be obtained by contacting the personnel of respective service providers. The data of loading and boundary conditions of most industrial components was non-existent hence, it had to be evaluated on a case by case scenario with a varying level of engineering approximation due to complexity of the equipment and time limitations. The size of the tensile test specimens was selected to keep corrosion testing in mind and as a result it was relatively small compared to typical tensile testing specimens. Hence, extra care and stoppers were needed to place each specimen into the gripper of the Material Testing System. This relatively smaller size also restricted the use of available extensometer because it was not within the operational range.

The evaluation of data was challenging with respect to limitations of software and hardware that are used for this study. The iterations of shape optimization lasted up to 8 hours per iteration. Furthermore, certain geometrical features of the Inspire Solidthinking software that was used for topology optimization contained serious bugs through which the software consistently crashed. These restrictions were overcome by performing the geometrical tasks in another software and importing the geometry back to Inspire.

Last but not least, this study involved the analysis of industrial components hence, an administrative process had to be iterated on a case by case scenario in order to release the data to third parties.

8.3 Future Development

The additive manufacturing integrated screening and design process developed in this study can fundamentally be applied to any finite number of parts. The AM screening algorithm can be deployed using any programming language and specifications of any number or type of AM machine(s) for a desired user interface. While contacting the selected AM service providers for quotations including the lead times of the spare parts analysed in this study, it was discovered that the cost and lead time parameters were negotiable to an extent. As dynamics of competition in AM industry are growing more than ever before, the costs and lead times can be anticipated to decrease. Hence, these should be re-evaluated over a certain interval of time. Furthermore, an additional service provider to those that are analysed in this study was also considered for additively manufacturing certain spare parts. Upon negotiations of possible long-term contracts, this undisclosed service provider offered relatively lower costs at a reasonable lead time. The values of this analysis however, are not disclosed in this study due to a non-disclosure agreement. When considering CAD modelling, this study illustrates the power of parametric modelling with user guided interface of only one but the most complex spare part that is the DOP Turbine. This programmable approach can be applied to the rest of the spare parts as well for ease of use for modification purposes. The design intent of all 15 spare parts which are received and analysed in this study is based on design for manufacturing and/or design for assembly. Due to time limitations, only two of these spare parts are further analysed in detail by evaluating the loading and boundary conditions in order to apply and assess design for additive manufacturing. In case direct metal AM is selected to manufacture the component(s), a redesign should be opted to minimize the required support structures. A varying level of engineering approximation is used to analyse the rest of the 13 parts. For future development, the loading and boundary conditions of the rest of the 13 spare parts can also be analysed in detail for performance efficiency with respect to design for additive manufacturing. Furthermore, measurement instruments can be used to

evaluate the loading and boundary conditions with higher levels of accuracy. In addition to the displacement and stress analyses, fatigue and modal analyses can also be performed in the future to predict the behaviour of cyclic loading and vibrations induced in the structures.

In case of future developments of verification and validation methods used in this study, corrosion testing of Titanium specimens can be performed in more aggressive test environments to observe the behaviour of printed specimens in contrast to those of the bulk material. Additionally, tensile testing can be performed using a specimen relative extensometer or strain gauges in order to calculate the yield or offset yield of the metal alloys in addition to the ultimate tensile strength measured in this study. The percentage elongation of the specimens can also be evaluated by measuring the gauge length before and after the fracture of the specimens.

9 Conclusion

As described earlier, the evolution of manufacturing has progressed throughout the centuries starting from craftsmanship, to industrialization, to mass production, to mass customization and finally to the era of eManufacturing. E-Manufacturing combines the most challenging market demands including variable volume, consistent quality, statistical process control, compatibility and complete customization incorporating lean manufacturing and agile manufacturing. To this end, the development of new technologies pushes existing technologies to adapt to such demands to keep up with the dynamics of growing competition. The purpose of this study was to define digital unique component manufacturing through direct and indirect additive manufacturing to meet such challenging demands.

This study has systematically explained the working principles of ISO/ASTM approved AM methods, their variants and their correlation with indirect and direct additive manufacturing including rapid tooling. A classification of metal AM is adopted for direct and indirect AM from literature based on ISO/ASTM method, material feed stock, energy source, bonding mechanism and manufacturer. The benefits of design for additive manufacturing are described in detail leading to various business potentials with ever-growing economy of AM industry through agile and lean manufacturing. The implementation of AM is also discussed and applied with various examples in contrast to formative and subtractive manufacturing methodologies.

In order to conduct this study, a screening algorithm is developed to evaluate the eligibility of any finite number of spare parts. Consequently, 16 individual components and 7 assemblies were reduced to 9 individual components and 6 assemblies. The exclusion scenarios included cheap to manufacture via SM, short lead time via SM, too long and narrow for AM, and too big for AM with respect to technical specifications. Ultimately, 5 individual components and 6 assemblies are three dimensionally modelled including one parametric model due to lack of 3D data. In addition, 7 moulds are three dimensionally modelled for the selected components to evaluate AM rapid tooling.

As a result of two formative or injection moulded parts of polymer, it is discovered that direct polymer AM is beneficial in terms of cost and lead time of small series production to an extent which needs to be calculated on a case by case scenario. Production volumes of up to 51 pieces are recorded for economical and shorter lead times when considering AM.

As a result of thirteen subtractive manufacturing parts, it is discovered that indirect and/or direct polymer and/or metal AM including rapid tooling has provided shorter lead times for all spare parts analysed in this study. The results of direct polymer AM proved to be economical in all cases. On the other hand, the results of indirect and direct metal AM proved to be expensive to manufacture in all cases. Furthermore, indirect metal AM proved to be economical compared to direct metal AM. However, in case AM rapid tooling is considered to cast the metallic component, approximately 22% of considered components proved to be economical at the cost of longer lead times. Since the cost of AM rapid tooling depends on volume, complexity and lead time, the economical spare parts define a probable range before and after which AM rapid tooling is defined expensive to manufacture in case lead time is not crucial.

As a result of optimization studies through design for additive manufacturing, it can be deduced that the performance of components can be increased by 17% when considering the factor of safety even after reducing the mass or weight of the component by up to

40%. Such mass reductions led to cost reductions of up to 46% in case of indirect metal AM and up to 3% in case of direct metal AM due to nature of required support structures. The difference in lead time is observed to be negligible due to the nature of AM processes.

Finally, as a result of verification and validation methods, it is deduced that directly and additively manufactured Titanium is corrosion resistant with regards to its bulk material with an ultimate tensile strength of approximately 1100 MPa containing 5% anisotropy in favour of horizontal print orientation. Whereas, directly and additively manufactured Stainless Steel 316L is not as corrosion resistant compared to stainless steel with European standards of EN 1.4404 and EN 1.4432 in highly aggressive environments and it has an ultimate tensile strength of approximately 595 MPa with 13% anisotropy in favour of horizontal print orientation.

10 References

1. 3D Systems Inc., 2017. *3D Systems: Home*. [Online]
Available at: <https://www.3dsystems.com/>
[Accessed 05 04 2017].
2. Additively Ltd. , 2017. *Binder Jetting*. [Online]
Available at: <https://www.additively.com/en/learn-about/binder-jetting>
[Accessed 10 09 2017].
3. Additively Ltd., 2017. *Fused Deposition Modeling*. [Online]
Available at: <https://www.additively.com/en/learn-about/fused-deposition-modeling>
[Accessed 10 09 2017].
4. Additively Ltd., 2017. *Material Jetting*. [Online]
Available at: <https://www.additively.com/en/learn-about/material-jetting>
[Accessed 10 09 2017].
5. Additively Ltd., 2017. *Selective Laser Melting*. [Online]
Available at: <https://www.additively.com/en/learn-about/laser-melting>
[Accessed 10 09 2017].
6. Additively Ltd., 2017. *Stereolithography*. [Online]
Available at: <https://www.additively.com/en/learn-about/stereolithography>
[Accessed 10 09 2017].
7. Align Technology Inc., 2017. *The Invisalign System*. [Online]
Available at: <http://www.aligntech.com/solutions/invisalign>
[Accessed 13 07 2017].
8. ASTM International, 2013. *Standard Terminology for Additive Manufacturing Technologies*, West Conshohocken: ASTM International.
9. Atzeni, E., Iuliano, . L., Minetola, P. & Salmi, A., 2010. Redesign and cost estimation of rapid manufactured plastic parts. *Rapid Prototyping Journal*, 16(5), pp. 308-317.
10. Atzeni, E. & Salmi, A., 2012. Economics of additive manufacturing for end-usable metal parts. *The International Journal of Advanced Manufacturing Technology*, 62(9), pp. 1147-1155.
11. Autodesk Inc., 2017. *Reimagining the Future of Air Travel*. [Online]
Available at: <https://www.autodesk.com/customer-stories/airbus>
[Accessed 13 07 2017].
12. Brevini UK Ltd., 2017. *Industrial Series*. [Online]
Available at: http://www.brevini.co.uk/pdf/brevini/B_IndustrialSeries.pdf
[Accessed 09 05 2017].
13. Campbell, J., 2001. *Castings*. Oxford: Elsevier.
14. Caterpillar, 2017. *3D Printing*. [Online]
Available at: <http://www.caterpillar.com/en/company/innovation/customer-solutions/technology/additive-manufacturing.html>
[Accessed 07 07 2017].
15. Collins, J. A., 2003. *Mechanical Design of Machine Elements and Machines*. New York: John Wiley & Sons Inc..
16. CustomPartNet., 2017. *Laminated Object Manufacturing*. [Online]
Available at: <http://www.custompartnet.com/wu/laminated-object-manufacturing>
[Accessed 10 09 2017].
17. Dieter, G. E., 2000. Mechanical Behaviour Under Tensile and Compressive Loads. In: A. I. H. Committee, ed. *ASM Handbook Volume 8: Mechanical Testing and Evaluation*. Ohio: ASM International.

18. DM3D Technology LLC, 2017. *DM3D: Home*. [Online]
Available at: <http://www.pomgroup.com/>
[Accessed 05 04 2017].
19. Eberhard, A. & Kniepkamp, M., 2015. Analysis and optimisation of vertical surface roughness in micro selective laser melting. *Surface Topography: Metrology and Properties*, Volume 3, p. 8.
20. EnvisionTEC, 2017. *Envisiontec: Home*. [Online]
Available at: <https://envisiontec.com/>
[Accessed 08 07 2017].
21. EOS GmbH, 2017. *EOS e-Manufacturing Solutions*. [Online]
Available at: <https://www.eos.info/en>
[Accessed 26 05 2017].
22. EOS GmbH, 2017. *Industry: Wittmann Group - EOS additive manufactured lightweight grip system with integrated functionality*. [Online]
Available at: https://www.eos.info/press/customer_case_studies/gripper
[Accessed 06 09 2017].
23. ExOne GmbH, 2017. *ExOne: Digital Part Materialization*. [Online]
Available at: <http://www.exone.com/>
[Accessed 05 04 2017].
24. Formlabs, 2017. *Formlabs: Home*. [Online]
Available at: <https://formlabs.com/>
[Accessed 08 07 2017].
25. Frazier, W. E., 2014. Metal Additive Manufacturing: A Review. *Journal of Materials Engineering and Performance*, 23(6), pp. 1917-1928.
26. Fritz, J. D., 2008. Effects of Metallurgical Variables on the Corrosion of Stainless Steels. In: A. I. H. Committee, ed. *ASM Handbook Volume 13A Corrosion: Fundamentals, Testing and Protection*. 4 ed. Ohio: ASM International.
27. Gardner Business Media, Inc., 2015. *How Is Caterpillar Moving Forward with AM?*. [Online]
Available at: <http://www.additivemanufacturing.media/blog/post/how-is-caterpillar-moving-forward-with-am>
[Accessed 07 07 2017].
28. Gibson, I., Rosen, D. & Stucker, B., 2015. *Additive Manufacturing Technologies*. New York: Springer.
29. Granta Design Limited, 2017. *CES EduPack 2017*, Cambridge: s.n.
30. Gu, D., 2015. *Laser Additive Manufacturing of High-Performance Materials*. 1 ed. Nanjing: Springer.
31. Gu, D. D., Meiners, W., Wissenbach, K. & Poprawe, R., 2012. Laser additive manufacturing of metallic components: materials, processes and mechanisms. *International Materials Reviews*, 57(3), pp. 133-164.
32. Guo, N. & Leu, M. C., 2013. Additive manufacturing: technology, applications and research needs. *Frontiers of Mechanical Engineering*, 8(3), pp. 215-243.
33. Herderick, E., 2011. *Additive Manufacturing of Metals: A Review*. Columbus, ASM International.
34. Herzog, D. S. V. W. E. E. C., 2016. Additive Manufacturing of Metals. *Acta Materialia*, Volume 117, pp. 371-392.
35. Hofmeister, W., Griffith, M., Ensz, M. & Smugeresky, J., 2001. Solidification in Direct Metal Deposition by LENS Processing. *The Journal of The Minerals, Metals & Materials Society*, 53(9), p. 30.34.

36. Holmström, J., Partanen, J., Tuomi, J. & Walter, M., 2009. Rapid manufacturing in the spare parts supply chain: Alternative approaches to capacity deployment. *Journal of Manufacturing Technology Management*, 21(6), pp. 687-697.
37. Holt, J. M. (., 2000. Uniaxial Tension Testing. In: A. I. H. Committee, ed. *ASM Handbook Volume 8: Mechanical Testing and Evaluation*. Ohio: ASM International.
38. Horn, T. J. & Harrysson, O. L. A., 2012. Overview of current additive manufacturing technologies and selected applications. *Science Progress*, 95(3), pp. 255-282.
39. Hue, P. L., 1998. Progress and Trends in Ink-jet Printing Technology. *Journal of Imaging Science and Technology*, 42(1), pp. 49-62.
40. ISO/TC 261, 2015. *ISO/ASTM 52900:2015(en) Additive Manufacturing - General principles - Terminology*. s.l.:ISO/ASTM International 2015.
41. Ituarte, I. F. et al., 2015. Post-processing opportunities of professional and consumer grade 3D printing equipment: a comparative study. *International Journal of Rapid Manufacturing*, 5(1), pp. 58-75.
42. Jelaska, D. T., 2012. *Gears and Gear Drives*. 1 ed. New York: John Wiley & Sons, Incorporated.
43. Joh. Winklhofer Beteiligungs GmbH & Co. KG, 2016. *Chain Engineering IWIS*. [Online]
Available at:
http://www.iwis.de/uploads/tx_sbdownloader/KettenHandbuch_E.pdf
[Accessed 09 05 2017].
44. K.P. Karunakaran, A. B. S. S. L. D. G. T., 2012. Rapid manufacturing of metallic objects. *Rapid Prototyping Journal*, 18(4), pp. 264-280.
45. Koch, J. & Mazumder, J., 2000. *Apparatus and methods for monitoring and controlling multi-layer laser cladding*. US, Patent No. 6122564.
46. Liao, Y. S. C. Y. Y., 2001. Adaptive crosshatch approach for the laminated object manufacturing (LOM) process. *International Journal of Production Research*, 39(15), pp. 3479- 3490.
47. M+S Hydraulics Plc., 2015. *B/MR*. [Online]
Available at: <http://www.ms-hydraulic.com/en/component/k2/item/86-b-mr.html>
[Accessed 09 05 2017].
48. Martikka, H., Niemi, E. & Verho, A., 1985. *Koneenosien Suunnittelu 2*. Porvoo, Helsinki, Juva: Werner Söderström Osakeyhtiö.
49. Mcor Technologies Ltd., 2015. *Mcor*. [Online]
Available at: <http://mcor technologies.com/>
[Accessed 04 07 2017].
50. Nycz, A., Adediran, A. I., Noakes, M. W. & Love, L. J., 2016. *Large Scale Metal Additive Techniques Review*. Tennessee, The Department of Energy, US.
51. Optomec Inc., 2017. *Optomec: Production-Grade 3D Printing*. [Online]
Available at: <https://www.optomec.com/>
[Accessed 05 04 2017].
52. Outokumpu Stainless AB, 2009. *Corrosion Handbook*. 10 ed. s.l.:s.n.
53. Phull, B., 2008. Evaluating Uniform Corrosion. In: A. I. H. Committee, ed. *ASM Handbook Volume 13A Corrosion: Fundamentals, Testing and Protection*. Ohio: ASM International.
54. Piili, H. et al., 2015. Cost Estimation of Laser Additive Manufacturing of Stainless Steel. *Physics Procedia*, Volume 78, pp. 388-396.

55. S. Covino Jr., B. & Cramer, S. D., 2008. Introduction to Forms of Corrosion. In: A. H. Committee, ed. *ASM Handbook Volume 13A Corrosion: Fundamentals, Testing and Protection*. New York: ASM International .
56. Salmi, M., 2013. *Medical applications of additive manufacturing in surgery and dental care*. Helsinki: Aalto University publication series: Doctoral Dissertations.
57. Salmi, M., 2016. Possibilities of preoperative medical models made by 3D printing or additive manufacturing. *Journal of Medical Engineering*, Volume 2016, p. 6.
58. Salmi, M., Huuki, J. & Ituarte, I. F., 2017. The ultrasonic burnishing of cobalt-chrome and stainless steel. *Progress in Additive Manufacturing*, 2(1-2), pp. 31-41.
59. Salmi, M., Ituarte, I. F., Chekurov, S. & Huotilainen, E., 2016. Effect of build orientation in 3D printing production for material extrusion, material jetting, binder jetting, sheet object lamination, vat photopolymerisation, and powder bed fusion. *International Journal of Collaborative Enterprise* , 5(3/4).
60. Salmi, M. et al., 2013. A digital process for additive manufacturing of occlusal splints: a clinical pilot study. *Journal of the Royal Society Interface*, 10(84).
61. Senvol LLC, 2017. *Additive Manufacturing*. [Online] Available at: <http://senvol.com/additive-manufacturing/> [Accessed 27 07 2017].
62. Senvol LLC, 2017. *Senvol Database*. [Online] Available at: <http://senvol.com/database/> [Accessed 27 07 2017].
63. Siemens AG, 2017. *Siemens Hearing Aid*. [Online] Available at: <https://usa.bestsoundtechnology.com/> [Accessed 13 07 2017].
64. Stratasys Direct, Inc., 2017. *Direct Metal Laser Sintering (DMLS)*. [Online] Available at: <https://www.stratasysdirect.com/resources/direct-metal-laser-sintering-dmls/> [Accessed 21 04 2017].
65. Stratasys Direct, Inc., 2017. *Direct Metal Laser Sintering Materials*. [Online] Available at: <https://www.stratasysdirect.com/materials/direct-metal-laser-sintering/> [Accessed 11 07 2017].
66. Stratasys Ltd., 2017. *PolyJet Technology*. [Online] Available at: <http://www.stratasys.com/3d-printers/technologies/polyjet-technology> [Accessed 13 04 2017].
67. Stratasys Ltd., 2017. *Stratasys: Home*. [Online] Available at: <http://www.stratasys.com/> [Accessed 05 04 2017].
68. Vaezi, M., Chianrabutra, S., Mellor, B. & Yang, S., 2013. Multiple material additive manufacturing – Part 1: a review. *Virtual and Physical Prototyping*, 8(1), pp. 19-50.
69. Vayre, B., Vignat, . F. & Villeneuve , F., 2012. METALLIC ADDITIVE MANUFACTURING: STATE-OF-THE-ART REVIEW AND PROSPECTS. *Mechanics and Industry*, 13(2), pp. 89-96.
70. Voxeljet AG, 2017. *3D Printing Systems: Profitability Included*. [Online] Available at: <http://www.voxeljet.com/> [Accessed 05 04 2017].

71. Voxeljet AG, 2017. *VX4000 - The World's biggest Industrial 3D Printer*. [Online]
Available at: <http://www.voxeljet.com/3d-printing-systems/vx4000/>
[Accessed 05 04 2017].
72. Wang, L. & Koh, S. L., 2010. *Enterprise Networks and Logistics for Agile Manufacturing*. London: Springer.
73. Wimpenny, D. I., Bryden, B. & Pashby, I. R., 2003. Rapid laminated tooling. *Journal of Materials Processing Technology*, 138(1-3), pp. 214-218.
74. Wohlers Associates Inc., 2017. *Wohlers Report*, Colorado: Wohlers Associates Inc..
75. Wuhan Binhu Mechanical & Electrical Co. Ltd., 2014. *Selective Laser Sintering*. [Online]
Available at: <http://www.binhurp.com/en/>
[Accessed 04 07 2017].
76. XJET Ltd., 2016. *XJET: Home*. [Online]
Available at: <https://xjet3d.com/>
[Accessed 10 07 2017].
77. Yang, J. et al., 2017. Corrosion Behavior of Additive Manufactured Ti-6Al-4V Alloy in NaCl Solution. *Metallurgical and Materials Transactions A*, 48(7), p. 3583–3593.
78. Zelinski, P., 2017. *Video: Additive Manufacturing Advances at Caterpillar* [Interview] (13 01 2017).

Appendices

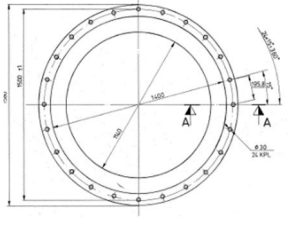
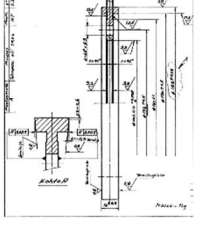
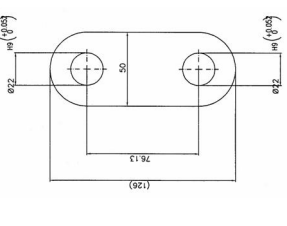
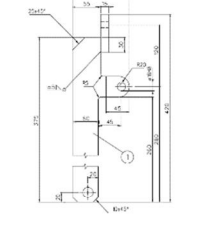
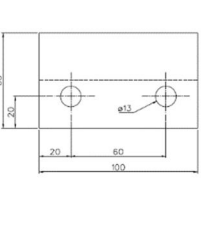
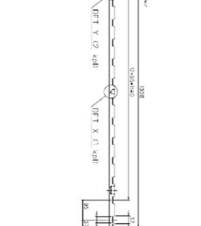
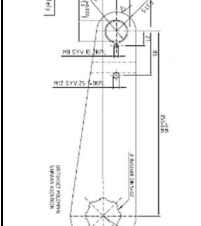
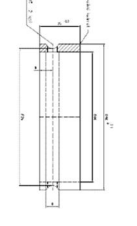
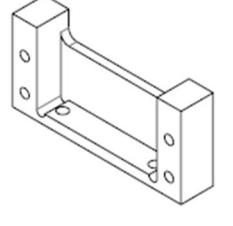
Appendix 1. Spare Parts Screening Process. 11 pages.

Appendix 2. Spare Parts Further Analysis. 15 pages.

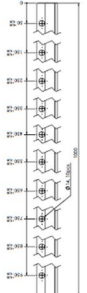
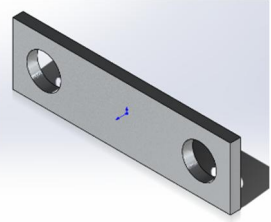
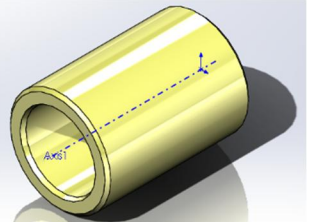
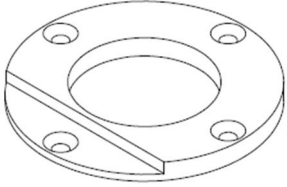
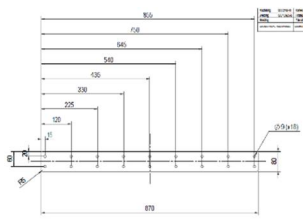

Appendix 3A. Uniform Corrosion Testing Results. 2 pages.

Appendix 3B. Localized Corrosion Testing Results. 3 pages.

Appendix 1. Spare Parts Screening Process

Spare parts Screening										
Part No.	###	###	###	###	###	###	###	###	###	
Preview										
Year Designed	1978	1976	1993	1997	1997	2000	2006	2006	2010	
Format	2D Drawing	2D Drawing	2D Drawing	2D Drawing	2D Drawing	2D Drawing	2D Drawing	2D Drawing	2D Drawing	
Purpose	Valupöydän Runko Jarrulaippa	Terä Korvaliuskaleikkuri	Tuki (Levy)	Rullatuki (Assembly)	Kisko Kiinnike Kiskoon	Jaotintanko	Upper Bar	Bush	Guide Frame	
Material	???	Stainless steel (50- 55 HRC) Böhler No Antinit KW80	Steel (SS1312/RSt37)	???	???	???	???	???	Steel EN 10025-2- S355J2	
Dimensions (L x W x H) [mm]	1580 x 1580 x 35	183 x 183 x 16	126 x 50 x 20	420 x 110 x 40	100 x 60 x 20	1308 x 30 x 25	455 x 125 x 77	90 x 90 x 25	40 x 100 x 210	
Tolerance (tightest) [mm]	-1	+0.035	+0.052	-0.2	±0.144	-0.2	+0.039	-0.1	+0.2	
Overall tolerance [mm]	Machining: ±1.2 Without Machining: ±6.0	Machining: ±0.5 Without Machining: ±2.5	±0.78 (*GTT provided)	±2.52 (According to previous GTT)	±0.9 (According to previous GTT)	±3.924 (According to previous GTT)	±0.05	-0.2	±0.5 (GTT provided)	
Surface Roughness (Smoothest) [µm]	1.6	0.8	-	6.3	-	-	3.2	-	6.3	
Parallelism [mm]	-	0.005	-	-	-	-	0.1	-	-	
Perpendicularity [mm]	-	-	-	-	-	-	0.1	-	-	
Possible Conventional Manufacturing Methods	Primary:	Rolling	Casting	Extrusion/casting	Casting	Extrusion/casting	Rolling	Casting	Extrusion/ casting	Casting
	Machining:	Cutting (Plasma?) + forming+ welding + turning + drilling	Sawing + Boring + drilling	Sawing + milling + grinding + drilling	Sawing + milling + drilling	Sawing + milling + drilling	Sawing + milling + drilling	Sawing + milling + grinding + drilling	Sawing + drilling + boring + turning	Sawing + milling + drilling
Eligibility [Included for further review or Excluded]	Included	Included	Excluded	Included	Included	Excluded	Included	Included	Included	
Reasoning	Too big for direct AM but can be sand casted through AM molds	Direct printing via EBM and/or AM pattern for Investment casting	Consists of a relatively simple design and requires workshop processing due to drilling even after AM	Part Consolidation and AM patterns for investment casting	AM molds for casting	Part is too long for direct AM and such straightness and flatness can be hard to manufacture through AM assisted casting due to such narrowness	AM molds for casting	FDM if it can be made out of a polymer	Direct AM (PBF) and/or AM patterns for Investment casting	

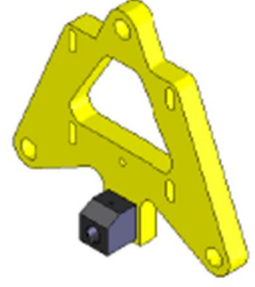
*GTT = General Tolerance Table

Spare parts Screening							
Part No.	###	###	###	###	###	###	
Preview							
Year Designed	2010	2010	2010	2006	2008	2011	
Format	2D Drawing	3D Model [Solidworks]	3D Model [Solidworks]	2D Drawing	2D Drawing	2D Drawing	
Purpose	Support Bar	Crane Grab Plate	Sliding Bush	Crane Grab Cover	Crane Grab Comb Plate	Hollow Bar Roll	
Material	Steel EN 10025-2-S355J2	Steel EN 10025-2-S355J2	???	???	Stainless Steel EN 1.4432	Stainless Steel EN 10088-2 - 1.4462	
Dimensions (L x W x H) [mm]	45 x 50 x 1000	210 x 60 x 10	70 x 70 x 100	100 x 100 x 8	870 x 80 x 5	90 x 90 x 30	
Tolerance (tightest) [mm]	+0.2	±0.2	±0.2	±0.1	±0.1	+0.2	
Overall tolerance [mm]	±0.8 (GTT provided)	±0.5 (According to previous GTT)	±0.35 (According to previous GTT)	±0.3 (GTT provided)	±0.8 (GTT provided)	±0.3 (According to previous GTT)	
Surface Roughness (Smoothest) [μm]	6.3	-	-	-	-	3.2	
Parallelism	-	-	-	-	-	-	
Perpendicularity	-	-	6.3	-	-	-	
Possible Conventional Manufacturing Methods	Primary:	Extrusion /casting	Rolling	Extrusion/casting	Rolling	Rolling	Extrusion/casting
	Machining:	Sawing + milling + drilling	Cutting (laser/water-Jet)	Sawing + drilling + boring + turning	Cutting (laser) + milling + drilling	Cutting (laser) + Drilling	Sawing + drilling + boring + turning
Eligibility [Included for further review or Excluded]	Excluded	Excluded	Included	Excluded	Excluded	Excluded	
Reasoning	Part is too long for direct AM and such straightness and flatness can be hard to manufacture through AM assisted casting	Consists of a relatively simple design which can easily be manufactured with the above mentioned conventional machining process relatively fast and through standard sheets available in the market	Possible via Direct and Indirect AM	Consists of a relatively simple design which can easily be manufactured with the above mentioned conventional machining process relatively fast and through standard sheets available in the market. In addition, would require workshop processing due to drilling even after AM.	Part is too long for direct AM and such straightness and flatness can be hard to manufacture through AM assisted casting due to such narrowness	Consists of a relatively simple design which can easily be manufactured with the above mentioned conventional machining process relatively fast and through standard bars available in the market	

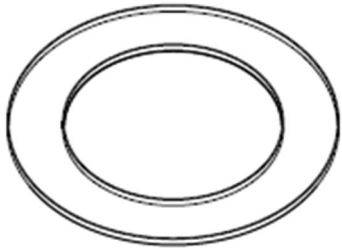
Spare parts Screening						
DOP Turbine 200 CW						
Part No.	###					
Preview						
Year Designed	2012					
Format	2D Drawing					
Purpose	Blade (1)	Top plate (2)	Bottom Plate (3)	Shaft Round Bar (4)	Flange Steel (5)	
Material	Steel EN 10088-2- 1.4404	Steel EN 10088-2- 1.4404	Steel EN 10088-2- 1.4404	Steel EN 10088-2- 1.4404	Steel EN 10088-2- 1.4404	
Dimensions (L x W x H) [mm]	200 x 200 x 48	200 x 200 x 4	200 x 200 x 4	40 x 40 x 881.5	115 x 155 x 26	
Tolerance (tightest) [mm]	±0.1	±0.1	±0.1	±0.2	+0.02	
Overall tolerance [mm]	±0.5 (GTT provided)	±0.5 (GTT provided)	±0.5 (GTT provided)	±0.8 (GTT provided)	±0.3 (GTT provided)	
Surface Roughness (Smoothest) [µm]	-	-	-	-	3.2	
Parallelism	-	-	-	-	-	
Perpendicularity	-	-	0.5	-	0.2	
Possible Conventional Manufacturing Methods	Primary:	Casting	Rolling	Rolling	Extrusion/casting	Extrusion/casting
	Machining:	Sawing + turning + milling	Cutting (laser)	Cutting (laser)	Sawing + turning + milling	Sawing + turning + milling
Eligibility [Included for further review or Excluded]	Included					
Reasoning	AM Molds for sand casting can be used for part consolidation of top plate, bottom plate and blade. Possible via Direct AM part consolidation of bottom plate and the turbine					

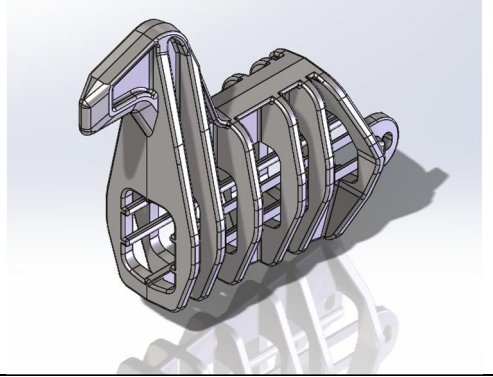
Spare parts Screening		
Chain Wheel		
Part No.	###	
Preview		
Year Designed	2005	
Format	2D Drawing	
Purpose	Steel Plate (1)	Round Bar (2)
Material	Steel EN 10025 S235JRG2	Steel EN 10025 S355J2G3
Dimensions (L x W x H) [mm]	345 x 345 x 20	150 x 150 x 120
Tolerance (tightest) [mm]	±0.026	±0.05
Overall tolerance [mm]	±0.5 (According to previous GTT)	±0.5 (According to previous GTT)
Surface Roughness (Smoothest) [μm]	3.2	-
Parallelism	-	-
Perpendicularity	-	-
Runout	0.2	-
Possible Conventional Manufacturing Methods	Primary: Casting Machining: Sawing + turning + milling + drilling + boring + form cutting	Casting Sawing + turning + drilling + boring
Eligibility [Included for further review or Excluded]	Included	
Reasoning	Part Consolidation AM molds for sand casting Possibility of Optimization	

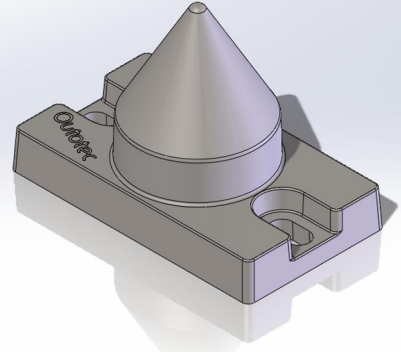
Spare parts Screening			
Fork Bar			
Part No.	###		
Preview			
Year Designed	2010		
Format	2D Drawing		
Purpose	Hollow Section (1)	Steel Plate (2)	Square Bar (3)
Material	Steel EN 10088-3 -1.4401	Steel EN 10088-2 -1.4436	Steel EN 10088-3 – 1.4436
Dimensions (L x W x H) [mm]	50 x 50 x 230	50 x 50 x 20	50 x 50 x 75
Tolerance (tightest) [mm]	±0.1	±0.2	±0.025
Overall tolerance [mm]	±0.5 (GTT provided)	±0.3 (GTT provided)	±0.3 (GTT provided)
Surface Roughness (Smoothest) [µm]	-	6.3	3.2
Parallelism	-	-	-
Perpendicularity	-	-	-
Runout	-	-	-
Possible Conventional Manufacturing Methods	Primary:	Rolling	Extrusion/Casting
	Machining:	Cutting + forming + welding	Sawing + Milling + drilling
Eligibility [Included for further review or Excluded]	Included		
Reasoning	Possibility of using AM Part Consolidation Possibility of Topology Optimization		

Spare parts Screening			
Adjustable Mounting Plate: Drawing No. ###			
Part No.	###	###	###
Preview			
Year Designed	2012		
Format	2D Drawing		
Purpose	Adjustable Mounting Plate	Plate	
Material	Steel EN 10025 S235JRG2	Steel EN 10025 S235JRG2	
Dimensions (L x W x H) [mm]	476 x 424 x 40	65 x 60 x 63	
Tolerance (tightest) [mm]	±0.2, ± 0°30'	±0.1	
Overall tolerance [mm]	±0.8 (According to previous GTT)	±0.3 (According to previous GTT)	
Surface Roughness (Smoothest) [µm]	6.3	-	
Parallelism	-	-	
Perpendicularity	-	-	
Runout	-	-	
Possible Conventional Manufacturing Methods	Primary:	Rolling	Casting/Extrusion
	Machining:	Cutting (flame or plasma?)	Sawing + milling
Eligibility [Included for further review or Excluded]	Included		
Reasoning	AM molds for casting Part Consolidation Possibility of Optimization		

Spare parts Screening				
Stopper Flange Assembly: Drawing No. ###				
Part No.	###	###	###	
Preview	<p>The diagram shows an exploded view of a stopper flange assembly. It consists of three main components: a sliding ring (1), a flange (2), and a stopper flange (3). The stopper flange (3) has six screws (4) that pass through it and the flange (2) into the sliding ring (1). The flange (2) has six holes (5) for the screws. The sliding ring (1) has six holes (6) for the screws. The assembly is shown in a perspective view.</p>			
Year Designed	2010			
Format	2D Drawing			
Purpose	Stopper Flange (1)	Flange (2)	Sliding Ring (3)	
Material	Steel EN 10025 S235JRG2	Steel EN 10025 S235JRG2	EN 10029 Plastic – PE Rigid	
Dimensions (L x W x H) [mm]	236 x 236 x 45	236 x 236 x 40	180 x 180 x 40	
Tolerance (tightest) [mm]	±0.2	±0.2	±0.3	
Overall tolerance [mm]	±0.5 (GTT provided)	±0.5 (GTT provided)	±0.5 (GTT provided)	
Surface Roughness (Smoothest) [µm]	-	-	-	
Parallelism	-	-	-	
Perpendicularity	-	-	-	
Runout	-	-	-	
Possible Conventional Manufacturing Methods	Primary:	Casting/Extrusion	Casting /Extrusion	Rolling
	Machining:	Sawing + drilling + boring + turning	Sawing + drilling + boring + turning	cutting + forming + welding + sawing + boring + turning
Eligibility [Included for further review or Excluded]	Included			
Reasoning	Part Consolidation Possibility of the whole part being polymer through AM			

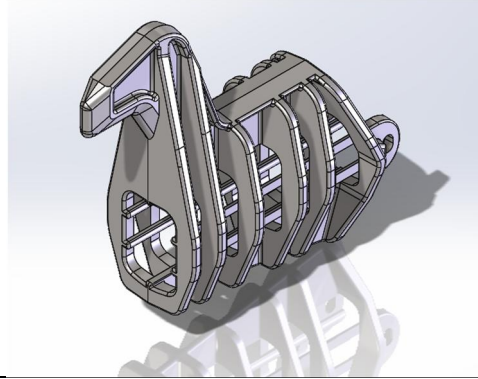
Spare parts Screening			
VSF DOP-SPIROK SYSTEM, DOP Pump Adjustment Ring: Drawing No. ###			
Part No.	###	###	###
Preview			
Year Designed	2003		
Format	2D Drawing		
Purpose	Adjustment top plate	Adjustment outer ring	Adjustment inner ring
Material	Stainless Steel AISI 316L	Stainless Steel AISI 316L	Stainless Steel AISI 316L
Dimensions (L x W x H) [mm]	1674 x 1674 x 6	1680 x 1680 x 40	1118 x 1118 x 40
Tolerance (tightest) [mm]	±0.1	±0.1	±0.1
Overall tolerance [mm]	±1.2 (GTT provided)	±1.2 (GTT provided)	±1.2 (GTT provided)
Surface Roughness (Smoothest) [µm]	12.5	-	-
Parallelism	-	-	-
Perpendicularity	-	-	-
Runout	-	-	-
Flatness	0.5	-	-
Possible Conventional Manufacturing Methods	Primary:	Rolling	Rolling
	Machining:	Cutting (laser)	Cutting + forming + welding + grinding
Eligibility [Included for further review or Excluded]	Excluded		
Reasoning	Parts are too big for direct AM and consist of a relatively simple design which can easily be manufactured with the above mentioned conventional machining process relatively fast and through standard sheets available in the market.		

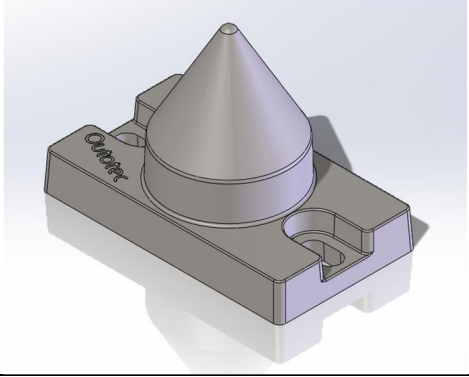
Spare parts Screening		
DWG No.	###	
SAP-Code	###	
Preview		
Year Designed	2011	
Format	2D + 3D Drawing	
Purpose	Anode Hangerbar	
Material	Polymer: suitable for copper electrolysis	
Equipment	Anode Top Insulator	
Dimensions (L x W x H) [mm]	210 x 200 x 66	
Tolerance (tightest) [mm]	+2	
Overall tolerance [mm]	±0.5	
Surface Roughness (Smoothest) [µm]	-	
Parallelism [mm]	-	
Perpendicularity [mm]	-	
Possible Conventional Manufacturing Methods	Primary:	Polymerisation/Polycondensation
	OT Machining:	Injection Moulding Only
Eligibility [Included for further review or Excluded]	Included	
Reasoning	Direct AM via PBF: SLS	


Spare parts Screening		
DWG No.	###	
SAP-Code	###	
Preview		
Year Designed	2012	
Format	2D + 3D Drawing	
Purpose	Positioning Cone	
Material	Polymer: PP	
Equipment	ANODE CATHODE CRANE & GRAB	
Dimensions (L x W x H) [mm]	200 x 115 x 141	
Tolerance (tightest) [mm]	±0.2	
Overall tolerance [mm]	±0.5	
Surface Roughness (Smoothest) [µm]	-	
Parallelism [mm]	-	
Perpendicularity [mm]	-	
Possible Conventional Manufacturing Methods	Primary:	Polymerisation/Polycondensation
	OT Machining:	Injection Moulding Only
Eligibility [Included for further review or Excluded]	Included	
Reasoning	Direct AM via PBF: SLS	


Spare Parts Screening Summary 1st Iteration			
Description	Included	Excluded	Total
No. of Individual Parts	9	7	16
No. of Assemblies	6	1	7
No. of Total Parts	26	10	36

Appendix 2. Spare Parts Further Analysis

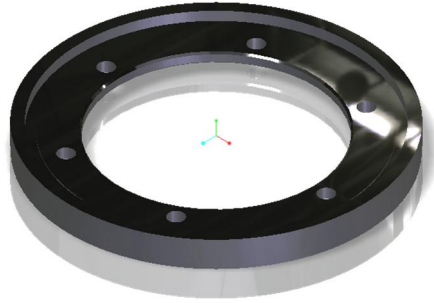
Spare parts Screening		
DWG No.	###	
SAP-Code	###	
Preview		
Year Designed	2011	
Format	2D + 3D Drawing	
Purpose	Anode Hangerbar	
Material	Polymer: suitable for copper electrolysis	
Equipment	Anode Top Insulator	
Dimensions (L x W x H) [mm]	210 x 200 x 66	
Tolerance (tightest) [mm]	+2	
Overall tolerance [mm]	±0.5	
Surface Roughness (Smoothest) [µm]	-	
Parallelism [mm]	-	
Perpendicularity [mm]	-	
Possible Conventional Manufacturing Methods	Primary:	Polymerisation/Polycondensation
	Machining:	Injection Moulding Only
Additive Manufacturing Eligibility	<ul style="list-style-type: none"> • Direct printing PBF: SLS 	
Downtime	No	
FCA Lead Time [Weeks]	2-3 however, 4-8 for new configuration	
Cost [€]	Part	$(200 \text{ euro} + 1,5 \text{ euro/pc} * x(\text{pc})) : x(\text{pc}) = y \text{ euro}$
	Tooling	20000
Loading Type	Variable loading	

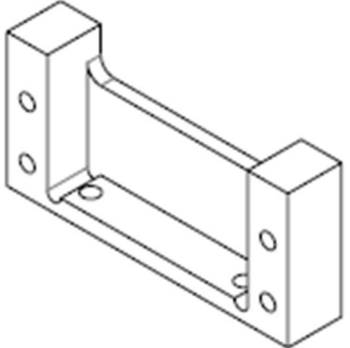
Spare parts Screening		
DWG No.	###	
SAP-Code	###	
Preview		
Year Designed	2012	
Format	2D + 3D Drawing	
Purpose	Positioning Cone	
Material	Polymer: PP	
Equipment	ANODE CATHODE CRANE & GRAB	
Dimensions (L x W x H) [mm]	200 x 115 x 141	
Tolerance (tightest) [mm]	±0.2	
Overall tolerance [mm]	±0.5	
Surface Roughness (Smoothest) [µm]	-	
Parallelism [mm]	-	
Perpendicularity [mm]	-	
Possible Conventional Manufacturing Methods	Primary:	Polymerisation/Polycondensation
	Machining:	Injection Moulding Only
Additive Manufacturing Eligibility	<ul style="list-style-type: none"> Direct printing PBF: SLS 	
Downtime	No	
FCA Lead Time [Weeks]	2-3 however, 20 for new mould	
Cost [€]	Part	$(200 \text{ euro} + 3,4 \text{ euro/pc} * x(\text{pc})) : x(\text{pc}) = y \text{ euro}$
	Tooling	15000
Loading Type	Shock and variable loading	

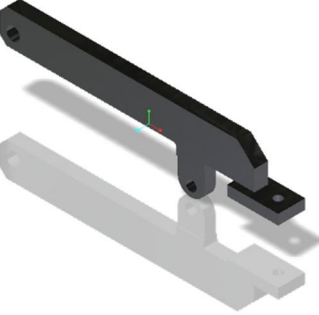
Spare parts Screening					
DOP Turbine 200 CW					
DWG No.	###				
SAP-Code	###				
Preview					
Year Designed	2012				
Format	2D Drawing + 3D Model				
Purpose	Blade (1)	Top plate (2)	Bottom Plate (3)	Shaft Round Bar (4)	Flange Steel (5)
Equipment	MIXER				
Material	Steel EN 10088-2- 1.4404	Steel EN 10088-2- 1.4404	Steel EN 10088-2- 1.4404	Steel EN 10088-2- 1.4404	Steel EN 10088-2- 1.4404
Dimensions (L x W x H) [mm]	200 x 200 x 48	200 x 200 x 4	200 x 200 x 4	40 x 40 x 881.5	115 x 155 x 26
Tolerance (tightest) [mm]	±0.1	±0.1	±0.1	±0.2	+0.02
Overall tolerance [mm]	±0.5 (GTT provided)	±0.5 (GTT provided)	±0.5 (GTT provided)	±0.8 (GTT provided)	±0.3 (GTT provided)
Surface Roughness (Smoothest) [µm]	-	-	-	-	3.2
Parallelism	-	-	-	-	-
Perpendicularity	-	-	0.5	-	0.2
Possible Conventional Manufacturing Methods	Primary:	Casting	Rolling	Rolling	Extrusion/casting
	Machining:	Cutting, drilling, milling, welding			
Additive Manufacturing Eligibility	<ul style="list-style-type: none"> AM Moulds for sand casting can be used for part consolidation of top plate, bottom plate and blade. Possible via Direct AM part consolidation of bottom plate and the turbine 				
Downtime	Yes: Usually have one spare, can be welded in some cases when damaged				
FCA Lead Time [Weeks]	4				
Cost [€]	3000				
Loading Type	Variable Load				

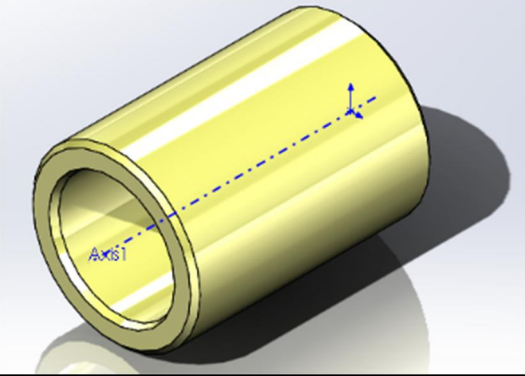
Spare parts Screening		
DWG No.	###	
SAP-Code	###	
Preview		
Year Designed	2006	
Format	2D Drawing	
Purpose	Upper Bar/Upper Shank	
Equipment	(APM-LINE) LIFTER ASSEMBLY	
Material	S355K2G3 EN 10025	
Dimensions (L x W x H) [mm]	455 x 125 x 77	
Tolerance (tightest) [mm]	+0.039	
Overall tolerance [mm]	±0.05	
Surface Roughness (Smoothest) [µm]	3.2	
Parallelism [mm]	0.1	
Perpendicularity [mm]	0.1	
Possible Conventional Manufacturing Methods	Primary:	Casting
	Machining:	Flame cutting, milling, drilling, pull groves, grinding, surface
Additive Manufacturing Eligibility	<ul style="list-style-type: none"> AM moulds for casting 	
Downtime	Yes: takes months to get a new one, may not be repaired if grooves are damaged	
FCA Lead Time [Weeks]	4	
Cost [€]	910	
Loading Type	Variable Loading (1milj. per/y)	

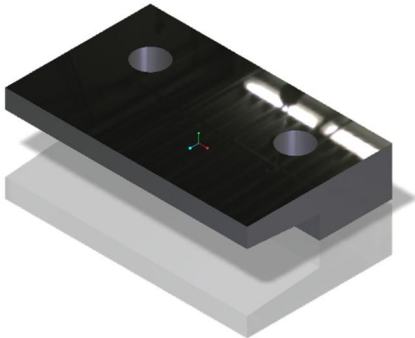
Spare parts Screening	
Chain Wheel	
DWG No.	###
SAP-Code	###
Preview	
Year Designed	2005
Format	2D Drawing
Purpose	Steel Plate (1) Round Bar (2)
Equipment	(APM-LINE) LIFT TRANSFER DEVICE / CONVEYOR
Material	Steel EN 10025 S235JRG2 Steel EN 10025 S355J2G3
Dimensions (L x W x H) [mm]	345 x 345 x 20 150 x 150 x 120
Tolerance (tightest) [mm]	±0.026 ±0.05
Overall tolerance [mm]	±0.5 (According to previous GTT) ±0.5 (According to previous GTT)
Surface Roughness (Smoothest) [µm]	3.2 -
Parallelism	- -
Perpendicularity	- -
Runout	0.2 -
Possible Conventional Manufacturing Methods	Primary: Casting Casting
	Machining: Flame cutting, cutting, milling, facing, drilling, pull grove, welding
Additive Manufacturing Eligibility	<ul style="list-style-type: none"> • Part Consolidation • AM moulds for sand casting • Possibility of Optimization
Downtime	Yes
FCA Lead Time [Weeks]	6
Cost [€]	445: Steel plate costs about 70-80% of the total price
Loading Type	Static, shock load

Spare parts Screening		
DWG No.	###	
SAP-Code	###	
Preview		
Year Designed	1976	
Format	2D Drawing	
Purpose	Terä Korvaliuskaleikkuri/Cutting Blade	
Equipment	LUG STRIP CUTTING MACHINE	
Material	Stainless steel (50-55 HRC) Böhler No Antinit KW80	
Dimensions (L x W x H) [mm]	183 x 183 x 16	
Tolerance (tightest) [mm]	+0.035	
Overall tolerance [mm]	Machining:	±0.5
	Without Machining:	±2.5
Surface Roughness (Smoothest) [μm]	0.8	
Parallelism [mm]	0.005	
Perpendicularity [mm]	-	
Possible Conventional Manufacturing Methods	Primary:	Casting
	Machining:	Cutting, facing, grinding, hardened
Additive Manufacturing Eligibility	<ul style="list-style-type: none"> • Direct printing (EBM) • AM pattern for Investment casting 	
Downtime	Yes: Cannot be repaired, customer has to have a spare	
FCA Lead Time [Weeks]	4	
Cost [€]	390	
Loading Type	Variable load, shock load	

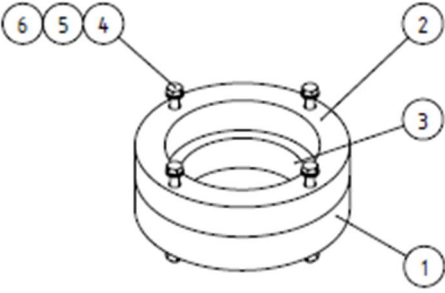
Spare parts Screening		
DWG No.	###	
SAP-Code	###	
Preview		
Year Designed	2010	
Format	2D Drawing + 3D Model	
Purpose	Guide Frame	
Material	Steel EN 10025-2-S355J2	
Equipment	(ANODE CATHODE CRANE & GRAB) BALE ASSEMBLY: supports a moving PP shaft	
Dimensions (L x W x H) [mm]	40 x 100 x 210	
Tolerance (tightest) [mm]	+0.2	
Overall tolerance [mm]	±0.5 (GTT provided)	
Surface Roughness (Smoothest) [μm]	6.3	
Parallelism [mm]	-	
Perpendicularity [mm]	-	
Possible Conventional Manufacturing Methods	Primary:	Casting
	Machining:	Flame cutting, milling, drilling
Additive Manufacturing Eligibility	<ul style="list-style-type: none"> • Direct AM (PBF) • AM patterns for Investment casting 	
Downtime	No	
FCA Lead Time [Weeks]	4	
Cost [€]	272	
Loading Type	Static Loading	

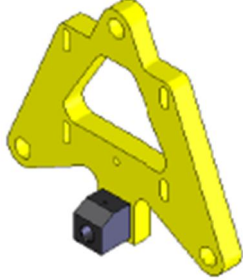
Spare parts Screening		
DWG No.	###	
SAP-Code	###	
Preview		
Year Designed	1997	
Format	2D Drawing	
Purpose	Rullatuki (Assembly)/Roll Support	
Equipment	(APM-LINE MILLING UNIT) ANODE HOLDER	
Material	ST52-3 DIN / EN 10025	
Dimensions (L x W x H) [mm]	420 x 110 x 40	
Tolerance (tightest) [mm]	-0.2	
Overall tolerance [mm]	±2.52 (According to previous GTT)	
Surface Roughness (Smoothest) [μm]	6.3	
Parallelism [mm]	-	
Perpendicularity [mm]	-	
Possible Conventional Manufacturing Methods	Primary:	Casting
	Machining:	Flame cutting, welding, drilling, milling
Additive Manufacturing Eligibility	<ul style="list-style-type: none"> • Part Consolidation • AM patterns for investment casting 	
Downtime	Yes: but can be repaired on site completely, repairs take dew days and repaired by mainly welding	
FCA Lead Time [Weeks]	4	
Cost [€]	205	
Loading Type	Shock Load	

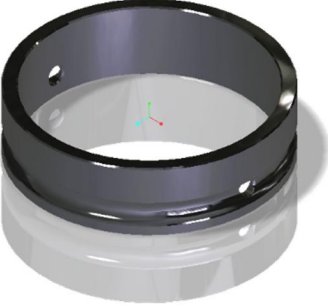
Spare parts Screening		
DWG No.	###	
SAP-Code	###	
Preview		
Year Designed	2010	
Format	2D Drawing + 3D Model [Solidworks]	
Purpose	Sliding Bush	
Equipment	(ANODE CATHODE CRANE & GRAB) BALE ASSEMBLY	
Material	JM1-15 Cu85 Sn5 Pb5 Zn5 (BRASS / BRONZE / RED METAL)	
Dimensions (L x W x H) [mm]	70 x 70 x 100	
Tolerance (tightest) [mm]	±0.2	
Overall tolerance [mm]	±0.35 (According to previous GTT)	
Surface Roughness (Smoothest) [μm]	-	
Parallelism	-	
Perpendicularity	6.3	
Possible Conventional Manufacturing Methods	Primary:	Extrusion/casting
	Machining:	Casting, milling
Additive Manufacturing Eligibility	<ul style="list-style-type: none"> Possible via Direct and Indirect AM 	
Downtime	No	
FCA Lead Time [Weeks]	4	
Cost [€]	108	
Loading Type	Variable Load	

Spare parts Screening		
DWG No.	###	
SAP-Code	###	
Preview		
Year Designed	1997	
Format	2D Drawing	
Purpose	Kisko Kiinnike Kiskoon/Rail Fastener	
Material	FE 510 C	
Equipment	(APM-LINE) ANODE STORAGE BEAM	
Dimensions (L x W x H) [mm]	100 x 60 x 20	
Tolerance (tightest) [mm]	±0.144	
Overall tolerance [mm]	±0.9 (According to previous GTT)	
Surface Roughness (Smoothest) [µm]	-	
Parallelism [mm]	-	
Perpendicularity [mm]	-	
Possible Conventional Manufacturing Methods	Primary:	Extrusion/casting
	Machining:	Flame cutting, milling, drilling
Additive Manufacturing Eligibility	<ul style="list-style-type: none"> • AM moulds for casting 	
Downtime	No	
FCA Lead Time [Weeks]	4	
Cost [€]	95	
Loading Type	Static Load	

Spare parts Screening	
Fork Bar	
DWG No.	Drawing No. ###
SAP-Code	###
Preview	
Year Designed	2010
Format	2D Drawing + 3D Model
Purpose	Hollow Section (1) Steel Plate (2) Square Bar (3)
Equipment	(ANODE CATHODE CRANE & GRAB) ALIGNING COMB ASSEMBLY
Material	Steel EN 10088-3 -1.4401 Steel EN 10088-2 -1.4436 Steel EN 10088-3 – 1.4436
Dimensions (L x W x H) [mm]	50 x 50 x 230 50 x 50 x 20 50 x 50 x 75
Tolerance (tightest) [mm]	±0.1 ±0.2 ±0.025
Overall tolerance [mm]	±0.5 (GTT provided) ±0.3 (GTT provided) ±0.3 (GTT provided)
Surface Roughness (Smoothest) [µm]	- 6.3 3.2
Parallelism	- - -
Perpendicularity	- - -
Runout	- - -
Possible Conventional Manufacturing Methods	Primary: Rolling Extrusion/Casting Extrusion/casting Machining: Flame cutting, cutting, milling, facing, drilling, welding
Additive Manufacturing Eligibility	<ul style="list-style-type: none"> • Possibility of using AM • Part Consolidation • Possibility of Topology Optimization
Downtime	No
FCA Lead Time [Weeks]	5
Cost [€]	223
Loading Type	Variable load

Spare parts Screening			
Stopper Flange Assembly: Drawing No. ###			
DWG No.	###	###	###
SAP-Code	###		
Preview			
Year Designed	2010		
Format	2D Drawing + 3D Model		
Purpose	Stopper Flange (1)	Flange (2)	Sliding Ring (3)
Equipment	(ANODE CATHODE CRANE & GRAB) ANTI SWAY FRAME ASSEMBLY		
Material	Steel EN 10025 S235JRG2	Steel EN 10025 S235JRG2	EN 10029 Plastic – PE Rigid
Dimensions (L x W x H) [mm]	236 x 236 x 45	236 x 236 x 40	180 x 180 x 40
Tolerance (tightest) [mm]	±0.2	±0.2	±0.3
Overall tolerance [mm]	±0.5 (GTT provided)	±0.5 (GTT provided)	±0.5 (GTT provided)
Surface Roughness (Smoothest) [µm]	-	-	-
Parallelism	-	-	-
Perpendicularity	-	-	-
Runout	-	-	-
Possible Conventional Manufacturing Methods	Primary:	Casting/Extrusion	Casting /Extrusion
	Machining:	Cutting, milling, drilling	
Additive Manufacturing Eligibility	<ul style="list-style-type: none"> Part Consolidation Possibility of the whole part being polymer 		
Downtime	No		
FCA Lead Time [Weeks]	5		
Cost [€]	451		
Loading Type	Variable load, shock load		

Spare parts Screening			
Adjustable Mounting Plate: Drawing No. ###			
DWG No.	###	###	
SAP-Code	###		
Preview			
Year Designed	2012		
Format	2D Drawing + 3D Model		
Purpose	Adjustable Mounting Plate	Plate	
Equipment	(CASTING SHOP) TAKE-OFF DEVICE / LIFTING DEVICE		
Material	Steel EN 10025 S235JRG2	Steel EN 10025 S235JRG2	
Dimensions (L x W x H) [mm]	476 x 424 x 40	65 x 60 x 63	
Tolerance (tightest) [mm]	±0.2, ± 0°30'	±0.1	
Overall tolerance [mm]	±0.8 (According to previous GTT)	±0.3 (According to previous GTT)	
Surface Roughness (Smoothest) [µm]	6.3	-	
Parallelism	-	-	
Perpendicularity	-	-	
Runout	-	-	
Possible Conventional Manufacturing Methods	Primary:	Rolling	Casting/Extrusion
	Machining:	Flame cutting, milling, facing, welding	
Additive Manufacturing Eligibility	<ul style="list-style-type: none"> • AM moulds for casting • Part Consolidation • Possibility of Optimization 		
Downtime	Yes		
FCA Lead Time [Weeks]	5		
Cost [€]	626		
Loading Type	Variable load		

Spare parts Screening		
DWG No.	###	
SAP-Code	###	
Preview		
Year Designed	2006	
Format	2D Drawing	
Purpose	Bush	
Material	S355J2G3 EN 10025	
Equipment	(APM-LINE LUG PRESS) TRANSFER DEVICE	
Dimensions (L x W x H) [mm]	90 x 90 x 25	
Tolerance (tightest) [mm]	-0.1	
Overall tolerance [mm]	-0.2	
Surface Roughness (Smoothest) [μm]	-	
Parallelism [mm]	-	
Perpendicularity [mm]	-	
Possible Conventional Manufacturing Methods	Primary:	Extrusion/ casting
	Machining:	Cutting, milling, drilling
Additive Manufacturing Eligibility	<ul style="list-style-type: none"> FDM if it can be made out of a polymer 	
Downtime	Yes	
FCA Lead Time [Weeks]	4	
Cost [€]	48	
Loading Type	Static Loading	

Spare parts Screening		
DWG No.	###	
SAP-Code	###	
Preview		
Year Designed	1978	
Format	2D Drawing	
Purpose	Valupöydän Runko Jarrulaippa/Brake Flange	
Equipment	(CASTING SHOP) CASTING WHEEL / CASTING TABLE	
Material	S355J2G3 (TAI VALU GGG 70 DIN 1693)	
Dimensions (L x W x H) [mm]	1580 x 1580 x 35	
Tolerance (tightest) [mm]	-1	
Overall tolerance [mm]	Machining:	±1.2
	Without Machining:	±6.0
Surface Roughness (Smoothest) [µm]	1.6	
Parallelism [mm]	-	
Perpendicularity [mm]	-	
Conventional Manufacturing Methods	Primary:	Rolling
	Machining:	Flame cutting, milling, drilling
Additive Manufacturing Eligibility	<ul style="list-style-type: none"> • Too big for direct AM • Can be sand casted through AM sand moulds 	
Downtime Impact	Yes	
FCA Lead Time [Weeks]	5	
Cost [€]	3755	
Loading Type	Variable Load	

Appendix 3A. Uniform Corrosion Testing Results

UNIFORM CORROSION

(Outokumpu Stainless AB, 2009)

Legend		
Rank	Corrosion rate	Description
	<0.1 mm/y	Material is corrosion resistant.
	0.1-1.0 mm/y	Material is not corrosion resistant but useful in certain cases.
	>1.0 mm/y	Serious corrosion: Material is not usable.

Titanium		Sample weight						Corrosion rate [mm/y]
Solution nr.	Sample code	Before [g]	After [g]	Change [g]	Surface area [cm ²]	Density [g/cm ³]	Test duration [h]	
2	5V	5.0166	5.0142	-0.0024	12.9865	4.00	168	2.41E-02
	6V	5.0046	5.0023	-0.0023	12.9865	4.00	168	2.31E-02
	7V	5.0052	5.0031	-0.0021	12.9865	4.00	168	2.11E-02
	8V	4.9929	4.9906	-0.0023	12.9865	4.00	168	2.31E-02
2	5H	5.3988	5.3966	-0.0022	12.9865	4.20	168	2.10E-02
	6H	5.3704	5.3684	-0.0020	12.9865	4.20	168	1.91E-02
	7H	5.3741	5.3721	-0.0020	12.9865	4.20	168	1.91E-02
	8H	5.4041	5.4022	-0.0019	12.9865	4.20	168	1.82E-02
2	Bulk	8.0753	8.0751	-0.0002	10.5475	4.43	168	2.23E-03

Titanium		Sample weight						Corrosion rate [mm/y]
Solution nr.	Sample code	Before [g]	After [g]	Change [g]	Surface area [cm ²]	Density [g/cm ³]	Test duration [h]	
3	9V	4.9875	5.0128	0.0253	12.9865	4.00	168	*
	10V	4.9944	4.9924	-0.0020	12.9865	4.00	168	2.01E-02
	11V	4.9748	4.9863	0.0115	12.9865	4.00	168	*
	12V	4.9765	4.9749	-0.0016	12.9865	4.00	168	1.61E-02
3	9H	5.4073	5.4051	-0.0022	12.9865	4.20	168	2.10E-02
	10H	5.3552	5.3535	-0.0017	12.9865	4.20	168	1.63E-02
	11H	5.3440	5.3419	-0.0021	12.9865	4.20	168	2.01E-02
	12H	5.3203	5.3185	-0.0018	12.9865	4.20	168	1.72E-02
3	Bulk	8.5273	8.5276	0.0003	10.8156	4.43	168	3.26E-03

*Signifies mass increase due to deposition

UNIFORM CORROSION

(Outokumpu Stainless AB, 2009)

Legend		
Rank	Corrosion rate	Description
	<0.1 mm/y	Material is corrosion resistant.
	0.1-1.0 mm/y	Material is not corrosion resistant but useful in certain cases.
	>1.0 mm/y	Serious corrosion: Material is not usable.

SS 316L		Sample weight			Change [g]	Surface area [cm ²]	Density [g/cm ³]	Test duration [h]	Corrosion rate [mm/y]
Solution nr.	Sample code	Before [g]	After [g]						
7	10V	16.7288	16.6276	-0.1012	15.8504	7.80	168	4.27E-01	
	11V	16.7890	16.6922	-0.0968	15.8504	7.80	168	4.08E-01	
	12V	16.7959	16.7921	-0.0038	15.8504	7.80	168	1.60E-02	
7	10H	16.9785	16.6276	-0.3509	15.8504	7.50	168	1.54E+00	
	11H	16.9848	16.6922	-0.2926	15.8504	7.50	168	1.28E+00	
	12H	16.9703	16.7921	-0.1782	15.8504	7.50	168	7.82E-01	
7	1.4404	15.4252	15.4242	-0.0010	16.5555	7.90	168	3.99E-03	
7	1.4432	22.7156	22.7161	0.0005	23.9904	8.00	168	1.36E-03	

Appendix 3B. Localized Corrosion Testing Results

LOCALIZED CORROSION

The occurrence and intensity of localized corrosion based on visual observations

(Outokumpu Stainless AB, 2009)

Legend	
Rank	Description
	No localized corrosion
	Localized corrosion with increasing intensity

Titanium

Solution nr.	Sample code	Rank
1	1V	
	2V	
	3V	
	4V	
1	1H	
	2H	
	3H	
	4H	
1	Bulk	

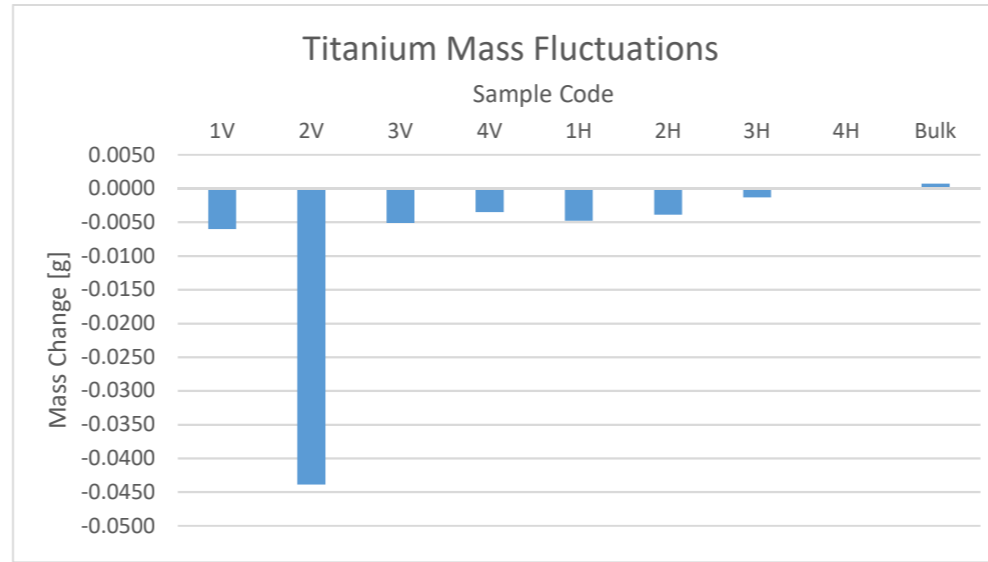
SS 316L

Solution nr.	Sample code	Rank	Solution nr.	Sample code	Rank	Solution nr.	Sample code	Rank
4	1V		5	4V		6	7V	
	2V							
	3V							
4	1H		5	4H		6	7H	
	2H							
	3H							
4	1.4404		5	1.4404		6	1.4404	
4	1.4432		5	1.4432		6	1.4432	

LOCALIZED CORROSION

Mass Fluctuations

Titanium		Sample weight		
Solution nr.	Sample code	Before [g]	After [g]	Change [g]
1	1V	5.0284	5.0224	-0.0060
	2V	5.0144	4.9705	-0.0439
	3V	5.0160	5.0109	-0.0051
	4V	4.9596	4.9561	-0.0035
1	1H	5.3744	5.3696	-0.0048
	2H	5.3762	5.3723	-0.0039
	3H	5.3844	5.3831	-0.0013
	4H	5.3990	5.3989	-0.0001
1	Bulk	8.4288	8.4295	0.0007



LOCALIZED CORROSION

Mass Fluctuations

SS 316L		Sample weight			
Solution nr.	Sample Serial nr.	Sample code	Before [g]	After [g]	Change [g]
4	1	1V	16.6723	16.5981	-0.0742
	2	2V	16.6822	16.5994	-0.0828
	3	3V	16.7015	16.6845	-0.0170
4	4	1H	17.0035	16.1089	-0.8946
	5	2H	16.9659	16.9598	-0.0061
	6	3H	16.9972	16.9880	-0.0092
4	7	1.4404	13.4476	11.5360	-1.9116
4	8	1.4432	22.8477	22.8659	0.0182

SS 316L		Sample weight			
Solution nr.	Sample Serial nr.	Sample code	Before [g]	After [g]	Change [g]
5	1	4V	16.7045	16.2667	-0.4378
	2	5V	16.6644	15.4070	-1.2574
	3	6V	16.7019	16.5750	-0.1269
5	4	4H	16.9997	15.8838	-1.1159
	5	5H	16.9710	16.1019	-0.8691
	6	6H	16.9789	16.5536	-0.4253
5	7	1.4404	12.9312	11.4340	-1.4972
5	8	1.4432	22.8255	22.8230	-0.0025

SS 316L		Sample weight			
Solution nr.	Sample Serial nr.	Sample code	Before [g]	After [g]	Change [g]
6	1	7V	16.7224	15.9718	-0.7506
	2	8V	16.7114	16.2234	-0.4880
	3	9V	16.7457	16.3715	-0.3742
6	4	7H	16.9839	16.4130	-0.5709
	5	8H	16.9901	16.4702	-0.5199
	6	9H	16.9438	16.3198	-0.6240
6	7	1.4404	16.1473	14.7111	-1.4362
6	8	1.4432	22.8188	22.7927	-0.0261

